THEORETICAL INVESTIGATION OF SELF-ASSEMBLED PEPTIDE NANOSTRUCTURES FOR BIOTECHNOLOGICAL AND BIOMEDICAL APPLICATIONS

A Dissertation

by

JENNIFER ANDREA CARVAJAL DIAZ

Submitted to the Office of Graduate Studies of
Texas A&M University
in partial fulfillment of the requirements for the degree of

DOCTOR OF PHILOSOPHY

May 2011

Major Subject: Chemical Engineering

THEORETICAL INVESTIGATION OF SELF-ASSEMBLED PEPTIDE NANOSTRUCTURES FOR BIOTECHNOLOGICAL AND BIOMEDICAL APPLICATIONS

A Dissertation

by

JENNIFER ANDREA CARVAJAL DIAZ

Submitted to the Office of Graduate Studies of
Texas A&M University
in partial fulfillment of the requirements for the degree of

DOCTOR OF PHILOSOPHY

Approved by:

Chair of Committee,	Tahir Cagin
Committee Members,	Arul Jayaraman
	Victor Ugaz
	Wonmuk Hwang
Head of Department,	Michael Pishko

May 2011

Major Subject: Chemical Engineering

ABSTRACT

Theoretical Investigation of Self-Assembled Peptide Nanostructures for Biotechnological and Biomedical Applications.

(May 2011)

Jennifer Andrea Carvajal Diaz, B.S., Universidad Industrial de Santander

Chair of Advisory Committee: Dr. Tahir Cagin

In this dissertation, molecular simulation techniques are used for the theoretical prediction of nanoscale properties for peptide-based materials. This work is focused on two particular systems: peptide nanotubes formed by cyclic-D,L peptide units and peptide nanotubes formed by phenylalanine dipeptides [-Phe-Phe-].

Mechanical characterization of cyclic peptide nanotubes is a challenging problem due the anisotropy resulting from the nature of their molecular interactions. To address rigorously the thermo-mechanical stability of cyclic peptide nanotubes (CPNTs), a homogeneous deformation method combined with the generalized elasticity theory and molecular dynamics simulations (MD) were used for the calculation of second order anisotropic elastic constants. The results for anisotropic elastic constants, yield behavior and engineering Young's modulus show remarkable mechanical stability for these materials supporting experiments for the development of their applications. Furthermore, the heat capacity, thermal expansion coefficient and isothermal compressibility were predicted using numerical difference methods and molecular dynamics.

In order to understand the transport properties of confined water in cyclic peptide nanotubes, the influence of nanotube diameter was studied and self-diffusion coefficient, dipole correlation functions and hydrogen bond probabilities were calculated via molecular dynamics and statistical mechanics. Enhanced transport and higher diffusion rates for water were obtained in cyclic peptide nanotubes (CPNTs) compared with

commonly used biomedical channels like carbon nanotubes (CNTs). The greater transport efficiency in CPNTs is attributed to the hydrophilic character and high hydrogen bonding presence along their tubular structure, versus the hydrophobic core of CNTs.

One of the most important opportunities for cyclic peptide nanotubes is their utilization as artificial ion channels in antibacterial applications. Here, molecular dynamics methods were used to investigate the effect of confinement on the transport properties of Na+ and K+ ions under the influence of electric field; the ion mobility, selectivity, radial distribution function, coordination number and effect of temperature were studied and results from simulations proved their ability to transport ions.

Additionally, the molecular organization of phenylalanine dipeptides into ordered peptide nanotubes was investigated, a model for the molecular structure of these nanotubes was proposed and optimized through molecular simulations; a helical pattern was found and characterized. Thermal stability results show that phenylalanine dipeptide nanotubes are stable up to about 400K; above this temperature, a significant decrease in hydrogen bonding was observed and the perfect pattern was altered.

Findings from this work open new opportunities for research in the area of peptide based materials and provide tools and methods to study these systems efficiently at nanoscale.

DEDICATION

This dissertation is especially dedicated to my mother, Edda Diaz, for her encouragement, guidance and unconditional love.

To my younger brother, Mauricio Carvajal-Diaz, for his support, patience and for making me proud and happy with his academic successes and excellent personality.

To my dear husband, Diego Cristancho, for his valuable advices, constant love and motivation throughout my Ph.D. studies.

To Juan Diego for sharing his happiness and love at all times.

To our families.

ACKNOWLEDGEMENTS

I would like to thank my committee chair, Dr. Tahir Cagin, for his support, valuable knowledge and encouragement to always achieve a deep understanding of the methods and problems. Also I would like to thank my committee members, Dr. Arul Jayaraman, Dr. Victor Ugaz and Dr. Wonmuk Hwang for their time and support throughout the course of this research.

My gratitude also goes to all the members of my research group; I have been fortunate to share good times and discussions with such great people. Also I thank Dr. Lijun Liu for his contributions and suggestions in the initial stages of this research.

I am very thankful to Dr. Kenneth Hall for his support and professional recommendations and to Dr. Yin Qin Gao for serving on my committee before leaving Texas A&M University.

I would like to thank the Theoretical and Computational Biophysics Group at the University of Illinois for kindly providing excellent open-source documentation and training information in computational biophysics topics through their web site.

The greatest appreciation is reserved for my dear friend and mother, Edda Diaz; I am grateful for her sacrifices and for always expecting the best personal and professional achievements from me, while supporting my life with constant motivation. Her encouragement has been essential to be perseverant in pursuing my dreams and goals.

Equally, I am grateful to my brother for his love and for always being responsible and caring. His intelligence and character make me proud and happy every day.

Special thanks to my beloved best friend and husband, Diego Cristancho, for his unconditional support, patience and understanding. I find myself fortunate to have him in my life, his love and affection have been source of inspiration, strength and happiness.

Finally, thanks to our families, friends, colleagues and the department faculty and staff for making my time at Texas A&M University a great experience. The doctoral program has been a rewarding experience in my professional and personal development.

NOMENCLATURE

CPNT	Cyclic Peptide Nanotubes
CN	Carbon Nanotubes
MD	Molecular Dynamics
MSD	Mean Square Deviation
RMSD	Root Mean Square Deviation
FF	di-Phenylalanine
CHARMM	Chemistry at HARvard Macromolecular Mechanics
NAMD	Non-Another Molecular Dynamics (MD code)
VMD	Visual Molecular Dynamics
NPT	Isothermal-Isobaric Ensemble
NVT	Isothermal-Isocoric Ensemble
Ala	Alanine
Gln	Glutamine
Glu	Glutamic Acid
Phe	Phenylalanine

TABLE OF CONTENTS

CHAPTER Page

CHAPTER Page

LIST OF FIGURES

FIGURE Page

FIGURE Page

FIGURE Page

LIST OF TABLES

CHAPTER I
INTRODUCTION

Complex three-dimensional structures are formed by nature through spontaneous association of molecules, termed molecular self-assembly[1]. In this study we will focus on a theoretical investigation of synthetic peptide based self-assembled nanostructures that have recently reported potential applications in nanotechnology and biomedicine.

Peptides constitute useful building blocks with excellent chemical-physical stability and diversity[1,2]. Also, inexpensive large scale production methods are becoming available for peptides, making feasible the fabrication of novel materials from these monomeric units. They can form materials whose structures and functionalities can be controlled to perform a variety of functions in both biological systems and nanotech devices[1]. Peptide based materials can be found in different morphologies, like fibrils, nanospheres and nanotubes, these materials present adjustability and functional capabilities that direct their wide range of applications, from biomedicine[2] to molecular electronics, tissue engineering[3] and drug delivery[1]. Recently, interest in the mechanical stability of peptide nanostructured materials has increased due to their potential applications and also because of connections with peptide aggregates resulting from the mis-folding of proteins[4], these aggregates can be toxic if formed in the human body and are linked to a high number of human diseases like Alzheimer's, Parkinson's and Huntingston[5]. Nano-structured peptide materials have also been reported as efficient chemotherapeutic agents used to destroy cancer cells[6]. These findings have illustrated the potential of peptide materials for nano-scale and biomedical applications[3]. However, understanding the effect of molecular scale organization in the macroscopic behavior of these materials still remains in the earlier stages. Therefore, further experimental and theoretical studies have an important role contributing to the rational design of new functional peptide nanostructures.

This dissertation follows the style of *Nature Materials*.

Self-assembled peptide structures were first synthesized in laboratories during the 1990s[4]. Nowadays, large-scale production of peptide nanostructures is promising due to the availability of inexpensive methods such as a simple solution-phase for their synthesis[2]. Challenges in the context of these novel nanostructures are to obtain a full rational control and understanding of the thermo-mechanical, transport properties and the final molecular organization patterns as well as the conditions of the peptides self-assembly process. This knowledge will allow a rational design of novel materials and development of new applications for peptide nanostructures; also it will contribute in the treatment of human diseases caused by analogous molecular processes of peptide aggregation.

Molecular dynamics (MD) is a valuable computational tool in the study of the thermodynamics, mechanical and transport properties for materials[7-9] providing a complementary component to experimental studies. A general scheme of the potential uses of peptide nanostructures and theoretical methods available for their study is shown in Fig.1.1.

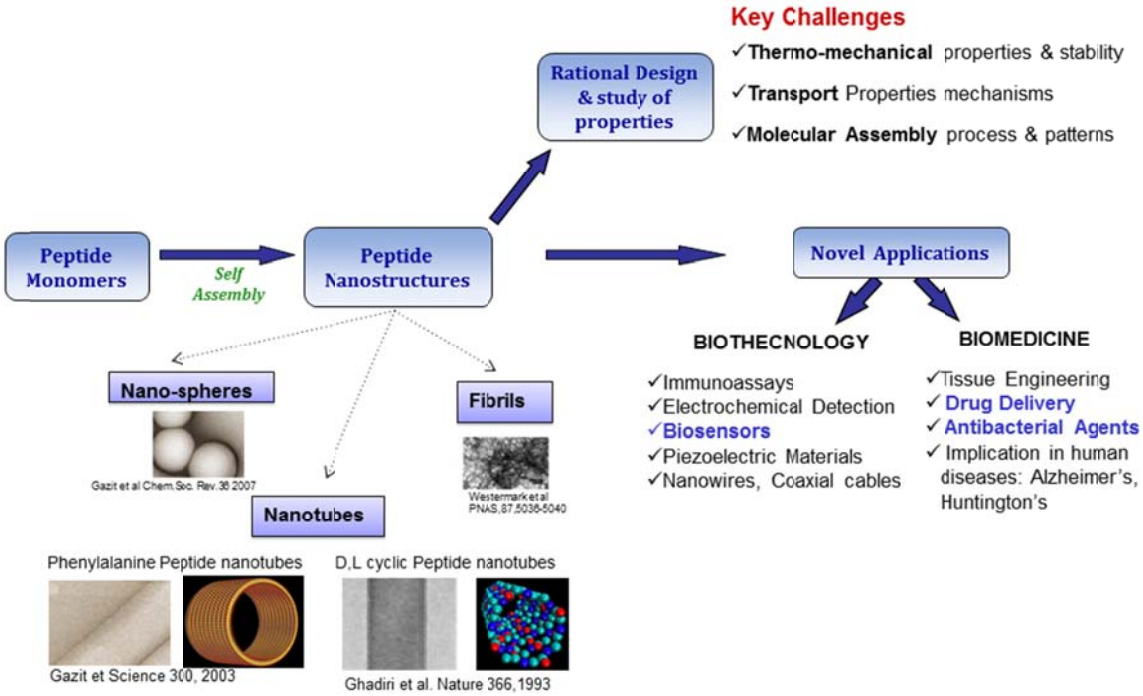

Figure 1.1. Opportunities for Theoretical Investigations of Peptide Nanostructures

Molecular Processes under nanoscale confinement conditions are not fully understood and explored yet; it is because the material properties are significantly different from those in the bulk phase: thermal, mechanical, structural and transport properties such as fluid viscosity are drastically influenced[10,11]. Particularly, in order to explore potential applications of self-assembled polypeptide materials, it is important to understand these properties under nanoscale confinement conditions. With these objectives in mind, the scope of research for this work is shown in Fig. 1.2.

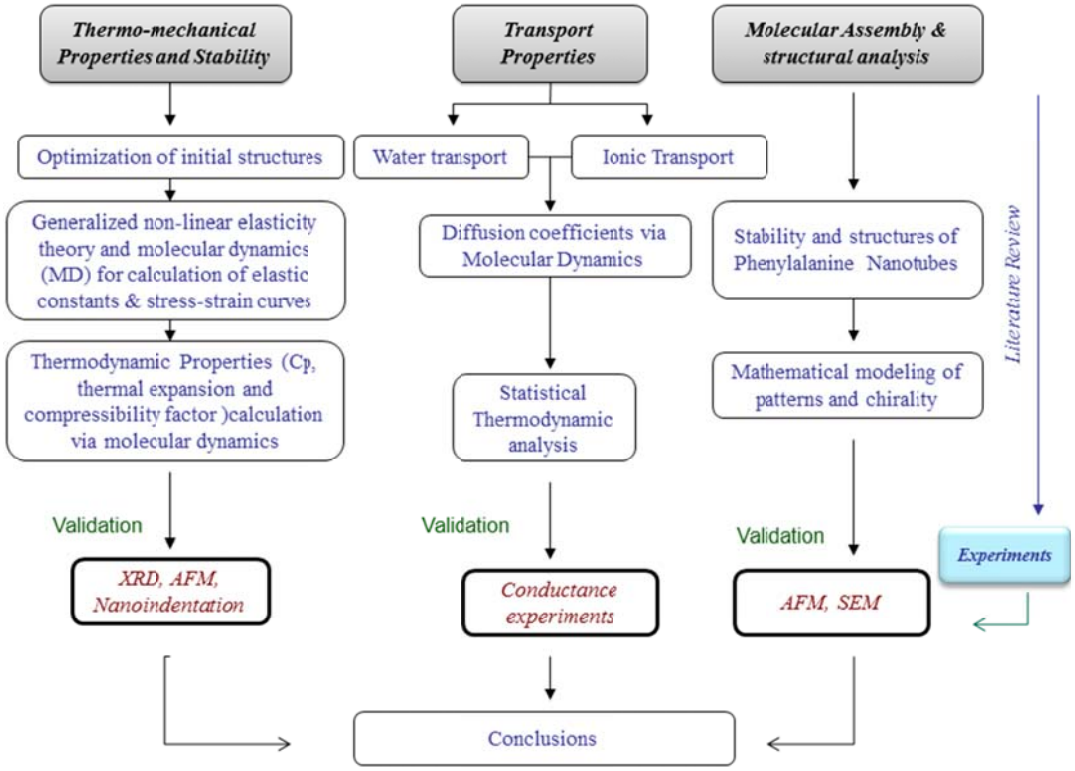

Figure 1.2. Plan Of Research: Three Main Problems are Addressed, Mechanical Characterization, Transport Properties for Water and Ions and Molecular Organization Analysis for Peptide Nanostructures. Computational results are Validated through Comparison with Experiments to Formulate Conclusions.

The main goal of this work is to develop an understanding of peptide-based nanomaterials and support their future technological applications. Peptide nanotubes are taken as model for peptide nanostructures; in Chapter III, their molecular detail structure, mechanical stability and strength are presented; a homogeneous deformation

method combined with molecular dynamics is used to calculate anisotropic elastic constants, and molecular dynamics is used for the determination of their thermodynamic properties.

In Chapter IV, the dynamics of water within cyclic peptide nanotube (CPNT) systems is presented, and their transport properties are compared with those obtained from equivalent diameter single wall carbon nanotubes (CNTs); findings from this work play an important role understanding the influence of channel-water on diffusion properties and for future applications of these systems as artificial ion channels, drug delivery and nano-fluidics devices.

In Chapter V, results of ion (Na+ and K+) transport dynamics under the effect of electric field are presented for the CPNTs; these results provide basic key information for the design of applications where CPNTs could perform as antibacterial agents and artificial ion channels.

In Chapter VI, the stability and molecular organization of diphenylalanine (FF) peptides forming stable nanotubes are reported; conclusions from this investigation have implications in the understanding of molecular forces stabilizing these structures after self-assembling processes.

Finally, Chapter VII draws conclusions from the work presented in this dissertation and lists recommendations for future work.

CHAPTER II
BACKGROUND

2.1. Recent Developments of Peptide-based Nanostructures

2.1.1. Peptide Nanotubes

In 1974 De Santis et. al discovered the conformational possibilities of D,L peptides sequences to form cyclic and tubular structures[12]. It took 20 years to realize this potential and only until 1993 Ghadiri and coworkers[13] demonstrated, for the first time, that nanotubes can be self-assembled by a process based upon β-sheet like interactions between macrocyclic D, L-peptides. These cyclic peptides were designed with an alternating even number of D- and L- amino acids, which interact through hydrogen bonding to form nanotubes, and the hydrophobic side chains interact to form arrays of self-assembled associated nanotubes. The internal diameter of the nanotubes can be manipulated by changing the number of amino acids per ring, and the surface characteristics can be controlled by selecting the appropriated amino acid depending on the desired functionality for the side chain groups in the cyclic peptide sequence[14].

One of the first applications of peptide nanotubes was based on their membrane function. As the cyclic peptide nanotubes (CPNTs) were toxic to bacteria, they were demonstrated to serve as novel antibiotic agents[15]. Several investigations have revealed that peptide nanotubes may act as highly selective and efficient transmembrane channels as well. These structures are shown to be large enough to serve as a channel for water[16], as size-selective ion channels[17] and as the medium for the transport of biologically relevant molecules[16]. Peptide nanotubes have been observed to form 2-D crystals of tubes[18], and can be found as embedded tubes in lipid membranes[15,19], as branched network tubes in solution[20], or as isolated nanotubes in solution[21]. Manipulation of electronic and optical properties of CPNTs have been investigated by side chain modification to allow charge transfer; these results provide important basis for

applications in molecular electronics[22]. Different peptide sequences have been investigated to form cyclic peptide units that can self-assemble into tubular structures through hydrogen bonding between the C=O and the N-H groups located in the backbone of the planar ring structure. In similar studies Clark et al. reported the synthesis of β^3-cyclic peptides forming nanotubes with applications as artificial ion channels[23]. Lorenzi and Sun, investigated the tubular formations through self-assembly of Cyclo(-D-Leu-L-MeLeu-D-Leu-L-MeLeu-D-Leu-L-MeLeu-) polypeptides[24]. Seebach et. al reported the structure and tubular stacking of cyclic tetramers of 3-aminobutanoic acid[25]. Gauthier and coworkers studied cyclic peptide nanotubes forming highly anisotropic crystalline structures formed by cyclo-$[\beta\text{-Ala}]_3$ subunits. Amorin et. al, explored nanotubular segments out of cyclic α,γ-tetrapeptide dimers[26] and recently Granja et. al. synthetized peptide nanotubes from cyclic-α-γ-peptides[27].

On the other hand, a different type of nanotube based on Lanreotide-acetate and formed by self-assembly of aliphatic and aromatic residues was also reported[28,29]. These Lanreotide peptide nanotubes present beta-sheet configurations and hydrogen bond networks like the cyclic peptide nanotubes. The self-assembly pathway for the formation of the Lanreotide nanotubes was recently investigated via molecular dynamics (MD) simulations[30]. Scanlon et al. reviewed advances in peptide nanotubes science, from simple to complex morphologies; applications and future perspectives are also discussed in a recent review[31]. Schematic of the Lanreotide peptide nanotubes is shown in Fig. 2.1.

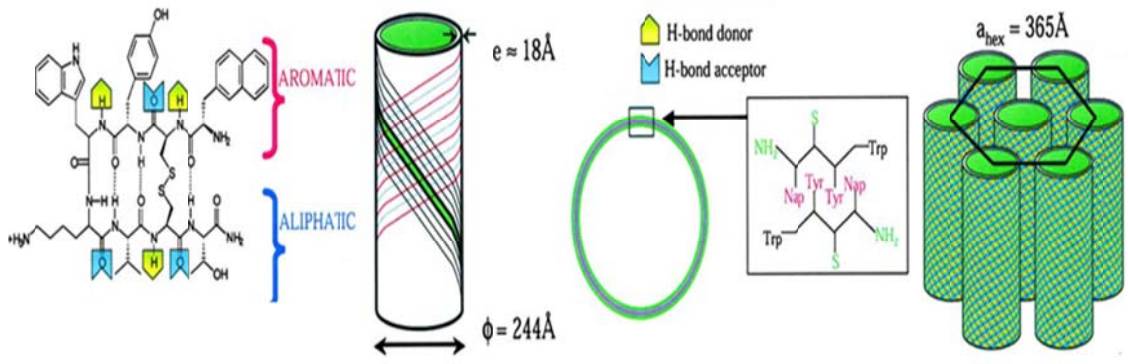

Figure 2.1. Lanreotide Peptide Nanotubes. Image taken from Ref[29]

Self-assembly of poly-glutamine into nanotube was recently reported and their structure was studied via molecular dynamic simuations[32]. Temperature effects were explored, and all monomers showed similar structural changes at the same temperature from alpha-helical structure to random coil. Antiparallel beta-sheets, triangular and circular beta-sheet structures from dimer units were formed.

An interesting type of peptide nanotubes self-assembled from diphenylalanine (F) dipeptides were discovered in 2003[21]; these nanotubes present remarkable mechanical properties[33], and good thermal and chemical stability[34]. Their piezoelectric properties have also been recently studied[35]. Fig. 2.2. shows experimental and a theoretical models for the molecular organization of FF peptides into nanotubes.

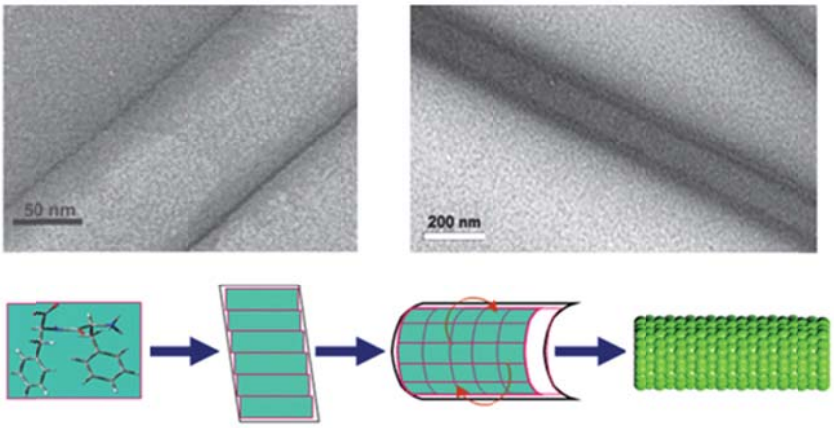

Figure 2.2. Diphenylalanine Peptide Nanotubes. Image taken from Ref. [36]

Phenylalanine dipeptide (FF) nanotubes have been used in recent applications; they have improved electrochemical parameters and performance of graphite electrodes[37] with implications in future electro analytical devices. In the fabrication of nanowires[21], as shown in Fig.2.3., FF nanotubes were used as tubular envelopes for silver metal ions as well as templates for coaxial cables[38]. Recently, Diphenylalanine/Cobalt Oxide composite nanotubes are reported to work as ultra-capacitors for energy storage applications[39].

Figure 2.3. Nanowires Fabrication. Image taken from Ref. [21]

#

Recently a hydrogen peroxide biosensor was developed by combining the known properties of microperoxidase-11 as an oxidation catalyst with di-phenylalanine peptide nanotubes (FF-PNTs) as a supporting matrix to allow a good bio-electro-chemical interface for a biosensor[40].

Vapor deposition techniques have been proposed for the production of FF-PNTs and recent "bottom-up" nanotechnology methods for patterning of these nanotubes have been reported [41,42]. Nanotubes can also be derived from a cationic dipeptide (H-Phe-Phe-NH_2·HCl); the conditions for the transition between vesicles and nanotubes are reported in the literature[36,43,44]. These peptide nanotubes are formed by hydrophobic residues (-Phe-Phe-); their crystallographic characteristics are being explored, but are not fully understood yet[45-48].

2.1.2. DNA-based Materials

Nanostructured materials based on DNA provide basis for applications such as scaffolds, supramolecular arrays and nanodevices. The possibility of rational design of these DNA materials through nucletide and sequence manipulations has increased interest in the scientific community[49]. DNA monomers present higher thermal stability compared to proteins; however, they present high sensitivity to enzymatic degradation. The formation and melting of DNA nanotubes were experimentally investigated for understanding the factors that influence the assembly process of DNA nanostructures[50] . Challenges in DNA nanotechnology suggest the use of periodic arrays, for example, recent progresses report the ability of pattern manipulation and cavity design from 2D-DNA arrays. Advances in structural DNA nanotechnology have been reviewed in the literature[51,52]. In Fig. 2.4 DNA nanotubes with different diameters are shown.

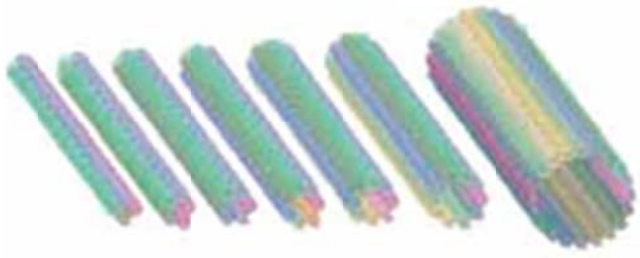

Figure 2.4. DNA Tubes with Programed Circumferences. Image taken from Ref. [53]

2.1.3. Surfactant-like Peptides

Peptides formed by hydrophobic aminoacids and containing one or two charged amino acids as the polar head and a tail were reported to self-assemble to give nanotubes and vesicles[20,54]. The peptides interact and form closed rings that self-assemble into nanotubes. Three nanotubes can be connected to each other through a three-way junction. These peptide nanostructures were formed by V6D (Valine-6-Aspartic Acid) peptides, each building block is 2 nm, and the diameter of the nanotube is 50 nm, as shown in the Fig.2.5. below.

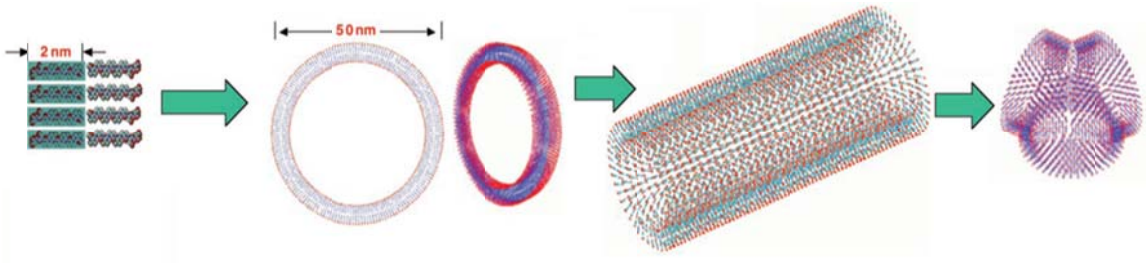

Figure 2.5. Potential Pathway of V6D Peptide Nanotube Formation (Red= hydrophilic head; blue=hydrophobic tail). Image taken from Ref. [20]

Nanostructures formed by short peptide amphiphiles and lipopeptides show promising applications in biotechnology and nanotechnology. Nanotubes can be formed from COOH-I3K-NH2 (I: Isoleucine, K: Lysine) monomers by a self-assembly process with potential use as templates for silicification. A wide range of amphiphile peptides forming nanorods, nanovesicles, nanotubes, nanofibers, micelles and core-shell

nanopartices have been reported for use as antimicrobial agents, gene/drug delivery and scaffolds, among other applications[55].

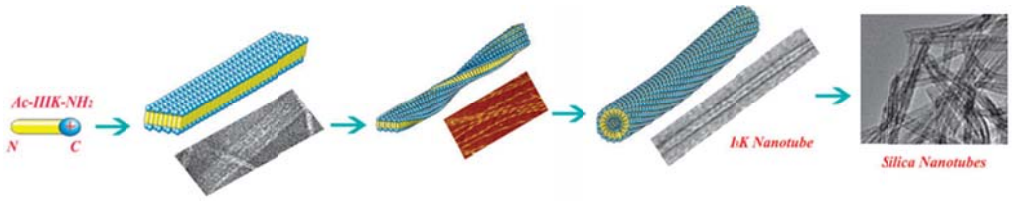

Figure 2.6. I3K Nanotube Image taken from Ref. [55]

In these materials, the shape and molecular organization can be affected by the peptide chain length, the solution pH, the ionic strength, the size of hydrophobic amino acid and the number of charge groups in the head. In Fig. 2.6., nanotubes formed out of peptide amphiphiles are shown. Additional self-assembly studies of peptide amphiphiles into nanofibers and nanotubes were also reported recently[56-58].

2.1.4. Hydrogels from Peptides

By co-assembling two aromatic short peptide derivatives, Fmoc-FF (Fluorenylmethoxycarbonyl-di-phenylalanine) and Fmoc-RGD (arginine-glycine-aspartic acid)], Orbach et.al. reported fibers that self-assemble into β-sheets interlocked by π–π stacking of the Fmoc groups. Also RGD (arginine-glycine-aspartic acid) peptide hydrogels may be used as scaffolds for 3D-culture cells[59]. Different FMoc-peptides monomers with natural and synthetic amino acids have been reported for the fabrication of hydrogels for applications in tissue engineering [60]. A schematic of these hydrogels is shown in Fig. 2.7.

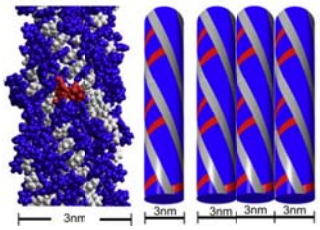

Figure 2.7. Peptide-based Hydrogels. Gray= Fmoc, Blue= FF and Red= RGD. Image taken from Ref. [59]

2.1.5. Peptide Nanospheres

Nanoshperes may self-assemble out of diphenyl-glycine peptides, see monomer in Fig.2.8. These peptide nanosheres were synthesized and characterized by Reches et.al.[61]. Their remarkable stability is attributed to π- π staking interactions and hydrogen bonds as in the FF peptide nanotubes. Up to date, molecular studies for stability or mechanical properties via molecular simulation have not been reported for these materials.

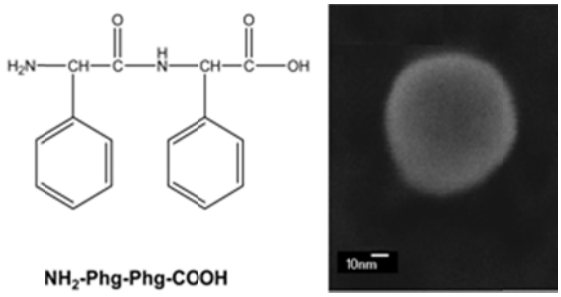

Figure 2.8. Phg-based Nanospheres. Image taken from Ref. [61]

Beta-sheet-forming poly-peptides of FKFEFKFE (F: Phenylalanine, K: Lysine, E: Glutamic acid) were also able to self-assemble into nanospheres[62]. Recently, 3D colloidal spheres containing diphenylalanine, peptides were fabricated in aqueous phase with diameters of about 150 nm [36,43,63].

2.1.6. Peptide-based Porous Solids

Peptide based porous solids were recently reviewed[64]. The ability to control opening and closure of the pores by manipulation of external conditions and molecular transitions, attributed to peptides, represent a good alternative to design gated porous materials, see Fig.2.9.. Rabone *et al*. synthesized a metal-organic framework formed by zinc ions and glycyl-alanine dipeptides. The pores in the framework open to absorb the gas molecules at a critical pressure of carbon dioxide. The opening results from torsional motions of the glycylalanine linkers[65].

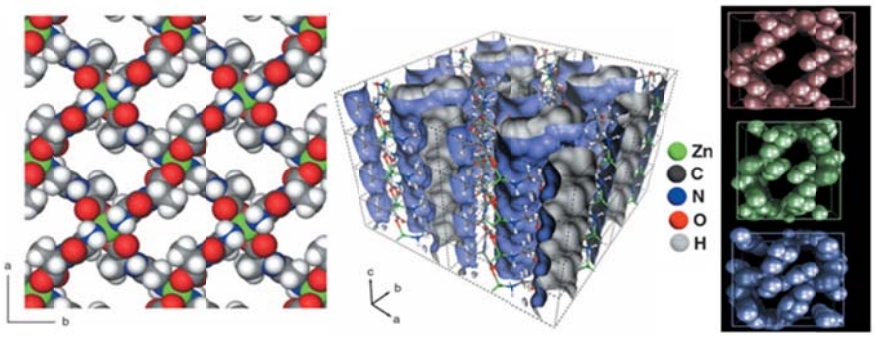

Figure 2.9. Left & Middle: Molecular Model for Peptide-MOF; Right: Transition from Open (pink) to Close (blue) State for Peptide-based Metal Organic Frameworks Images taken from Ref. [65]

2.2. Review of Relevant Computational Characterization Approaches for Peptide Nanostructures

2.2.1. Mechanical Properties

A key challenge in the context of these novel nanostructures is to obtain a full rational control of the final spatial organization as well as their mechanical stability. The knowledge of these conditions will allow new applications of the peptide nanostructures and manipulation of sizes and sequences for desired applications. Polypeptide chains forming beta-sheet rich structures have revealed remarkable structural stability and mechanical resistance. This mechanical stability is achieved by weak intermolecular forces like hydrogen bonds and hydrophobic interactions. Peptide-based materials reported to have modulus measuring up to 40GPa[66].

In the field of molecular modeling of mechanical properties, few studies have been reported for engineered peptide materials, one of the most common approaches is to perform steered molecular dynamics (SMD) simulations combined with classical elasticity theory. SMD approaches have been used for the calculation of elastic modulus; however, many simulations should be performed in order to correctly perform statistical analysis and to ensure that results are not dependent of the pulling forces and represent bulk properties. In this work, an alternative method consisting in non-linear elasticity theories combined with molecular dynamics is used for the first time for the calculation

of elastic properties of peptide nanostructures. Below, state of the art for theoretical methods used in calculation of mechanical properties for some peptide nanostructures are listed in Table 2.1.

Table 2.1. State of the Art: Computational Approaches for Mechanical Properties of Biomaterials

Nanostructure	Contribution	Methods	Ref(Year)
Beta-sheet-rich proteins	Mechanical energy transfer and energy dissipation studies.	Steered molecular dynamics	[66,67](2010)
Helical Peptides and Proteins	Evaluation of different AMBER Potentials for Molecular Mechanics simulations.	Explicit solvent molecular dynamics simulations	[68] (2010)
Coiled Protein Filaments	Results indicate that α-β transitions may increase energy dissipation capacity, stiffness and strength in proteins filaments	All atomistic steered molecular dynamics	[69] (2010)
Spider Silk Fibrils	Molecular Mechanisms of Deformation, Strength and Toughness of Spider Silk Fibrils are explained in terms of confinement of beta-sheet nanocrystals, and extensible semiamorphous domains	Coarse Grain molecular dynamics	[70] (2010)
Alpha-helical proteins	Development of a coarse grain mesoscale model fro alpha helical proteins.	Atomistic and CG steered molecular dynamics	[71] (2010)
Collagen	Mechanical Properties, Young Modulus.	Steered molecular dynamics	[72](2008) [73](2006)
Microtubules	Anisotropic Elastic constants	Mathematical modeling of elasticity	[74] (2005)
Cyclic peptide nanotubes	Anisotropic Elastic constants and thermodynamic properties	MD simulations and non-linear elasticity theory.	[75] (2010)
Bio-materials	Review of bio-mechanical characterization methods	Experimental and Theoretical	[76] (2003)

2.2.2. Transport Properties

In order to use the self-assembled polypeptide materials in the design of better nano-fluidic devices and to understand biological function of cell membranes, it is important to investigate the change in structure and transport of fluids under nanoscale confinement conditions.

Studies with molecular detail under confinement are quite new and in particular behavior for peptide channels is not fully explored yet. Most of the molecular simulation studies have focused the attention in natural process such as ion transport and cellular transport phenomena; however similar techniques can be used to explore transport properties of engineered peptide channels. Below, in Table 2.2., recent studies of transport within peptide materials are briefly reviewed. Also in Chapters IV and V the state of the art for water and ion transport in peptide nanochannels is reviewed.

Table 2.2. State of the Art: Computational Approaches for Transport Properties of Peptide Channels

Nanostructure	Contribution	Methods	Reference
α,γ-Peptide Nanotubes in Solution (different solvents)	Permeability and carrier properties based on polar character of the solvent.	Molecular dynamics and steered molecular dynamics.	[77] (2009)
Cyclic peptide nanotubes	H-bonds distribution, water transport, water structure	MD and CG-MD simulations with explicit solvent	(1998)[16] (2003)[78] (2009)[79] (2010) [80]
Cyclic peptide nanotubes	Ion transport	Atomistic and CG simulations	[81-83] (2006)
Lysozyme protein crystals	Electrophoresis of Na+ and Ca+	Non-equilibrium MD	[84](2008)
Natural membrane channels	Review of studies for water and ionic transport	MD simulations	[85](2009)
Alpha-helical peptides	Energy transport mechanism	Non-equilibrium MD	[86] (2010)
KcsA channel	Coordination number of Na+ and K+ ions	Quantum mechanics/MD Car-parinello simulations	[87] (2010)

2.2.3. Molecular Organization & Self-assembly

Understanding of the molecular organization, B-sheet characteristics and hydrogen bond distribution in peptide nanostructure is still a challenge for computational and experimental characterization techniques.

Studies on these patterns will contribute to the design of peptide materials and to unveil details of natural occurring processes and structures related with diseases. Below in Table 2.3., are listed recent studies related to this problem.

Table 2.3. State of the Art: Molecular Organization of Peptide Nanomaterials

Nanostructure	Contribution	Methods	Ref (Year)
Protein Nanotubes structures	Prediction of high resolution atomic-scale structures	Computational method is based on the symmetrical assembly of a repeating protein subunit into a nanotube	[88] (2009)
A6K Peptide Nanotubes	Structure and morphology of surfactant-like nanotubes	X-ray diffraction and MD	[89] (2010)
Crystalline peptides structures	Study of influences of symmetry of the head-to-tail chains, H-bonding type and amino acid sequence in peptide patterns.	Review of crystallographic studies in peptide patterns.	[90] (2010)

Via X-ray diffraction, the structure of single wall peptide nanotubes formed from the surfactant-like peptide A6K were studied [89]. Oriented X-ray diffraction patterns were obtained after capillary flow alignment of the sample. Preliminary molecular dynamic simulations reported a stable beta sheet antiparallel arrangement of di-peptides in a helical structure. A bilayer model, see Fig. 2.10. was studied via MD simulations, it was also found to be stable. Further molecular modeling for these systems is suggested [89].

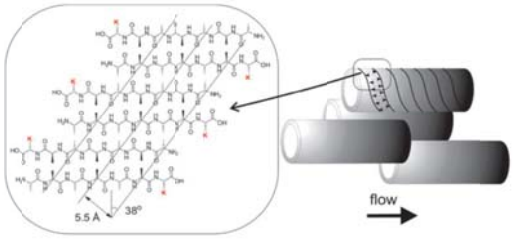

Figure 2.10. A6K Surfactant-like Peptide Nanotubes. Image taken from [89]

Peptide Self-assembly

Understanding the pathway and interactions leading the self-assembly processes of peptides have important implications not only for the prevention of amyloids aggregates that are related to several diseases but also in nanotechnology applications and in the design of peptide based nanostructures [2]. Molecular simulation provides an excellent option to study these processes; however, the large time scale and sizes present

a limitation and a challenge. In the following, we preview some experimental and computational techniques that have been used to study these self-association problems.

In order to reduce the degrees of freedom in the calculations, different approaches have been suggested. Coarse-grained (CG) methods have been recently reported as a powerful approach for simulating events on "biological" time scales and size scales[91]. Self-assembly studies are relevant because they contribute to understanding the formation ofnanostructures[36] and also the basis of the amyloid fibrils formation processes . Particularly, the MARTINI CG force field has been successfully used to study aggregation problems[92].

Molecular dynamics simulations were used to study self-assembly of polyglutamine into nanotubes. This structure reorganizes into an antiparallel double-stranded conformation with 22 residues per turn. These results suggest the polymorphism of polyglutamine structures and the possibility of different toxic oligomers and fibrils aggregates. The aggregation kinetics for the polyglutamine monomer was study from 250 to 700K, transitions between α-helical structure to random coil were observed and the nanotubes were formed from 40 peptide chains[93], see Fig.2.11.

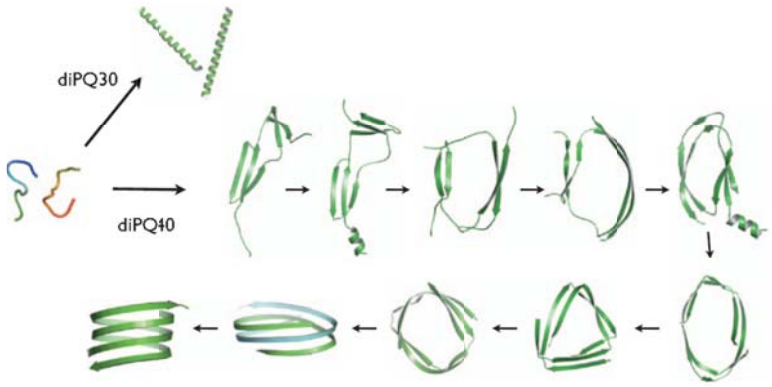

Figure 2.11. Polyglutamine Nanotubes Assembly Pathway. Image taken from Ref. [93]

Table 2.4. State of the Art: Self-assembly of Peptide Nanomaterials

Nanostructure	Contribution	Methods	Ref(Year)
Polyglutamine nanotubes	Implications in neurodegenerative diseases including Huntington's disease, spinocerebellar ataxias and muscular atrophy.	Replica exchange molecular dynamics	[93] (2010)
Diphenylalanine nanostructures	Implications in Nanotechnology (biosensing, nanowires) & Alzheimer's disease	Coarse-grained CG molecular dynamics (MD)	[94] (2009)
Peptide Amphiphile (PA)	Characterization of the size distribution of the aggregates as a function of the molecular interactions	Coarse grained model for PA molecules using the united atom model	[95] (2008)
Peptide Nanotubes into Lipid bilayers	The cyclo[(l-Trp-d- (Leu)3-l-Gln-d-Leu] ring is aligned parallel to the dimyristoyl phosphatidylcholine (DMPC) chains. Implications in transmembrane transport	Polarized attenuated total reflectance (ATR), grazing angle reflection−absorption and transmission Fourier transform infrared (FT-IR) spectroscopy methods	[19] (1998)
Peptide Nanotubes into Lipid bilayers	Tubes formed by 8 × cyclo[(−d-Ala-l-Glu-d-Ala-l-Gln−)2] and 8 × cyclo[(−Trp-d-Leu−)4] spontaneously insert into lipid bilayer membranes.	Coarse-grained (CG) molecular dynamics (MD) simulation	[83] (2008)
Lanreotide Octapeptide Nanotubes	Results show three assembly stages and three intermediates steps	Analytical centrifugation, NMR and X-ray scattering	[30] (2010)
Peptide self-assembled structures	Review of self-organization properties of peptides.	Theory and experimental methods	[2] (2007)
Amyloid Peptide	Aggregation structures of (GGVVIA) peptides	CG Montecarlo Simulations	[96] (2010)
Polyglutamine peptides	PRIME model of monomers for DMD simulations.	Discontinuous Molecular dynamics	[97] (2007)
Beta-amphiphilic peptides	Analysis of influence in sequence and residue type.	Coarse Grained model and monte carlo simulations.	[98] (2010)

2.2.4. Applications of Peptide-based Nanostructures

Peptide nanostructures have been used as biosensors, for fabrication of nanowires and as tissue scaffolds and recently as peptide nanowires, among others applications, see Fig.2.13.

Lim et al. reported nanoparticles with very good control over the morphology, size, and aggregation of the resulting peptide-coated nanostructures formed by Tat cell-penetrating peptide (Tat CPP) and hydrophobic lipid segments. By manipulation of the

lipid block, different geometries were constructed, and properties were manipulated[99], see Fig. 2.12.,. Table 2.5. shows a list of recent applications.

Figure 2.12. Bioactive Tubular Micelles. Image taken from Ref. [99]

Another example is the fabrication of peptide nanowires from amorphous diphenylalanine films, which are treated with aniline vapor at high temperatures to form tubular structures; cobalt oxide is used to fabricate composite nanowires. Potential applications for electrodes in batteries were evaluated with promising results for future uses in energy storage. See Fig. 2.13. for the steps of fabrication for peptide naonwires from diphenylalanine.

#

#

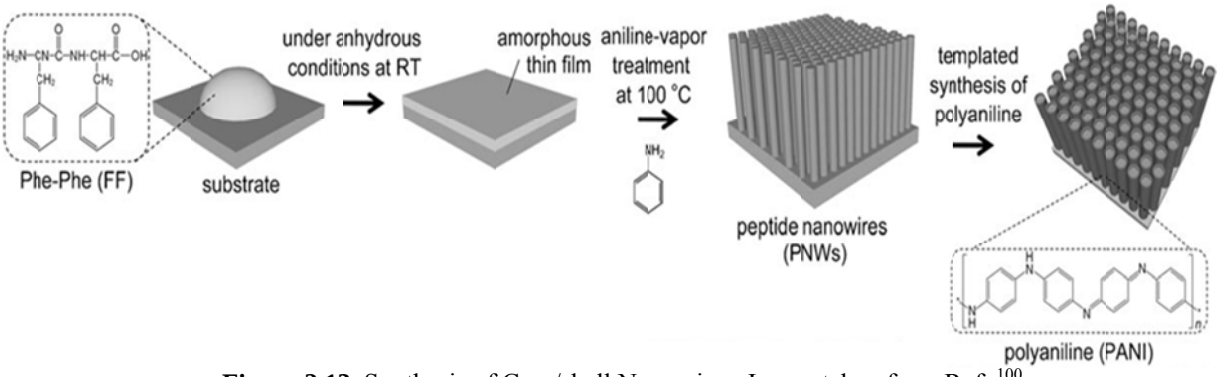

Figure 2.13. Synthesis of Core/shell Nanowires. Image taken from Ref. [100]

Table 2.5. Recent Applications for Peptide Nanostructures.

Application	Contribution	Ref(Year)

Coaxial Nanowires	A scaffold of self-assembled peptide nanotubes was used to produce coaxial nanocables	[38] (2006)
Diphenylalanine/Polyaniline Core/Shell Conducting Nanowires	Experimental work where self-assembled peptide nanowires were used as a template for the synthesis of hollow polyaniline (PANI) nanotubes	[100] (2009)
Bioactive Nanostructures	Review of functional peptides with dendritic lipid groups forming nanoparticles with controlled morphologies and assembled in aqueous solution	[99] (2007) [101] (2008)
Quantum Dots (QDs) in tertbutoxycarbonyl-Phe-Phe-OH (Boc-FF) peptide networks	Experiments/Theory showed optical absorption of QDs with luminescence of excitons	[102] (2009)
Peptide nanostructured electrodes	Implications in Ultra- Sensitive Enviromental Monitoring.	[103] (2010)
Piezoelectric Peptide Nanotubes	High effective piezoelectric coefficient of about 60 pm/V (shear response) was reported for Self-assembled diphenylalanine peptide nanotubes (PNTs).	[35] (2010)
Electronic Conductor Based on β-3-thienylalanine	Using quantum mechanical calculations, MD and QM/MM simulations reported the optimal conditions for design of a nanowire.	[104] (2009)
Peptide scaffolds	Peptide scaffolds are used for for neurite outgrowth and synapse formation, they are formed by self-assembly of ionic self-complementary oligopeptides.	[3] (2000)

2.3. Fundamentals of Computational Methods

2.3.1. Molecular Dynamics

Molecular Dynamic (MD) is a technique that allows the calculation of dynamic properties for classical many-body systems. In MD, the contributions to the total energy of the system from covalent and non-bonded interactions are included in a mathematical function or "potential function" known as Force Field. In general, all physical properties are the result of these intermolecular interactions and are expressed as time averages, derivatives or fluctuations of the functions of interaction potentials[105]. Hence, molecular dynamics in principle provides important information about the system under study from molecular level interactions, see Fig. 2.14.

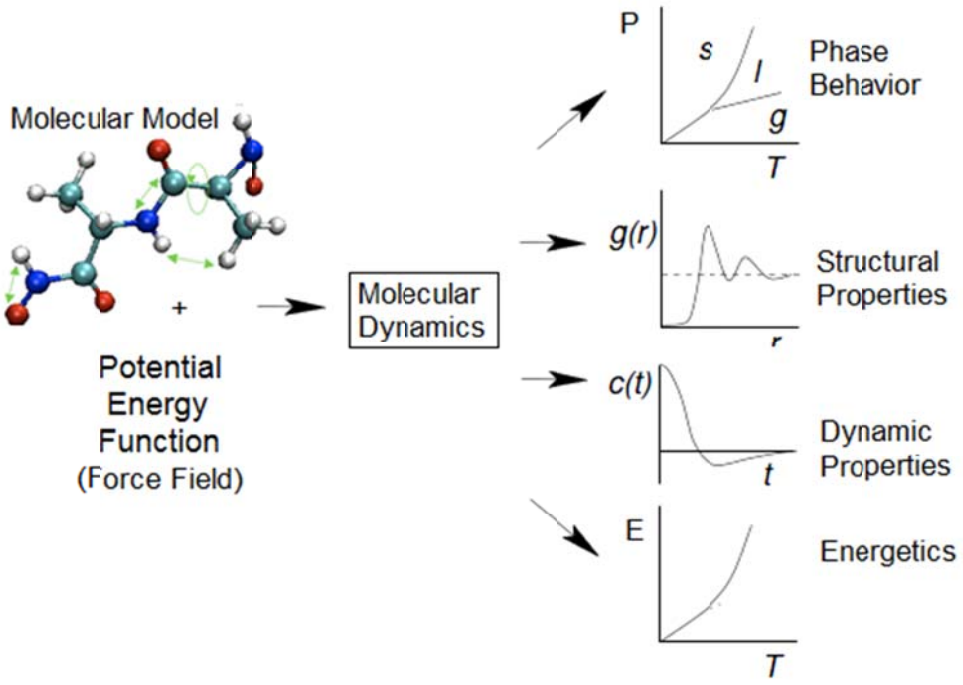

Figure 2.14 Properties from Molecular Dynamics

In molecular dynamics simulations we refer to "ensembles" to describe the thermodynamic state, an ensemble is the assembly of all possible microscopic states that will satisfy the conditions of the macroscopic state[105]. The thermodynamic state defined by fixed number of atoms, N, fixed volume, V, and fixed energy, E, correspond to an isolated system as in known as Microcanonical Ensemble (NVE). The case of fixed number of atoms, N, fixed volume, V, and fixed temperature, T, is known as the Canonical or isothermal-isochoric Ensemble (NVT); the isothermal-isobaric (NPT) Ensemble is defined by a fixed number of atoms, N, a fixed pressure, P, and a fixed temperature, T; the isoenthalpic-isobaric (NhP) with constant N, pressure and enthalpy (h) and finally the Grand canonical Ensemble (μVT) is characterized by a fixed chemical potential, μ, a fixed volume, V, and a fixed temperature, T. Below the basic steps performed in a molecular dynamics code are shown in Fig.2.15.

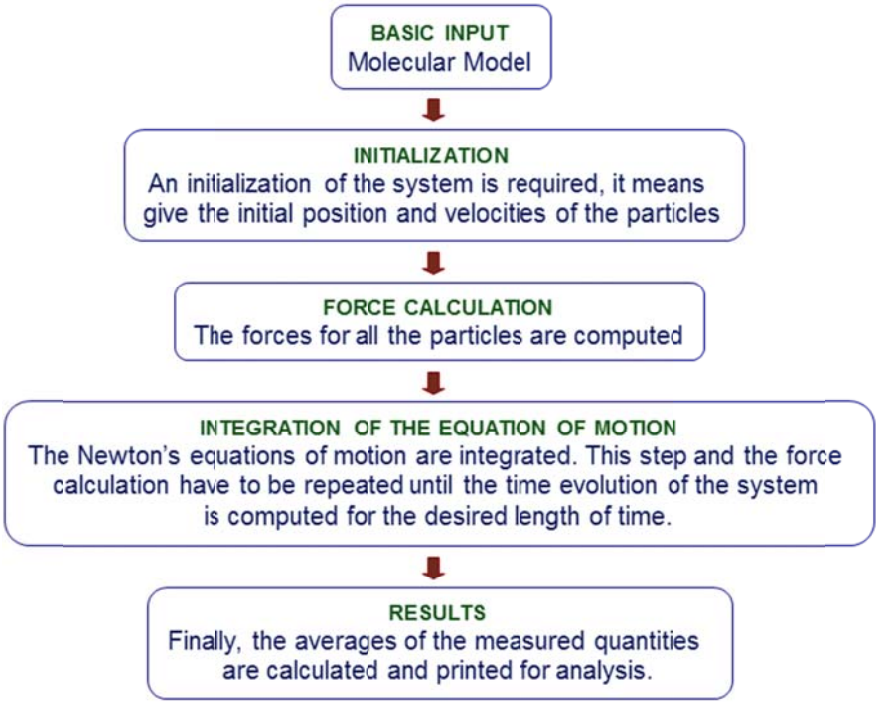

Figure 2.15. Basic Steps in Molecular Dynamics

The equations of motion for each atom are given by the classic formulation and may be written as: $m\ddot{r}_i = f_i$, these forces can be derived from the potential energy function as $f_i = -\nabla_i U$, where U is the total potential energy, r_i is the position vector of the atom, m is the mass and f_i represent the force.

In this work, the CHARMM[106] (Chemistry at HARvard Macromolecular Mechanics) Force Field was used to describe the interactions between atoms of the systems studied; the NAMD software was used to perform molecular dynamic simulations. NAMD is a high performance molecular dynamics code developed by the Theoretical and Computational Biophysics group at the University of Illinois at Urbana-Champaign[107]. NAMD has reported excellent parallel performance and it is an open-source code. Additionally, NAMD can be efficiently combined with the Visual Molecular Dynamics (VMD)[108] software to perform trajectory and molecular visualization analysis.

The CHARMM force field was developed by Dr. Martin Karplus group at Harvard University[106] in 1983. It is an all-atom force field designed for molecular modeling and molecular dynamics which has successfully been used in computational studies for proteins and peptide systems. The potential energy function implemented in NAMD is given by:

$$U_{TOTAL}=U_{bond}+U_{angle}+U_{dihedral}+U_{vdW}+U_{Coulomb} \tag{2-1}$$

where, U_{TOTAL} represents the total energy, which accounts for contributions from stretching (U_{bond}) , bending (U_{angle}), torsion ($U_{dihedral}$), van der Waals (U_{vdw}) and Coulomb ($U_{Coulomb}$) interactions. The mathematical expression for each term is given by:

$$U_{bond}=\sum_{i(bonds)}k_i^{bond}(r_i-r_{0i})^2 \tag{2-2}$$

$$U_{angle}=\sum_{i(angles)}k_i^{angle}(\theta_i-\theta_{0i})^2 \tag{2-3}$$

$$U_{dihedral}=\sum_{i(dihedrals)}\begin{cases}k_i^{dihe}\left[1+\cos(n_i\phi_i-\gamma_i)\right], n_i\neq 0\\ k_i^{dihe}(0_i-\gamma_i)^2, n=0\end{cases} \tag{2-4}$$

$$U_{vdW}=\sum_i\sum_{j>i}4\varepsilon_{ij}\left[\left(\frac{\sigma_{ij}}{r_{ij}}\right)^{12}-\left(\frac{\sigma_{ij}}{r_{ij}}\right)^{6}\right] \tag{2-5}$$

$$U_{Coulomb}=\sum_i\sum_{j>i}\frac{q_iq_j}{4\pi\varepsilon_0 r_{ij}} \tag{2-6}$$

The parameters required in the previous potential functions (k_i^{bond}, r_{0i}, etc.) are taken from the latest version of the CHARMM force field[109]. These values were determined by combination of empirical and quantum mechanical calculations.

Finally, it is important to mention that in order to simulate a complete representation of the system and to be able to approach the bulk behavior, a set of periodic boundary conditions (PBC) are defined. This will create infinite copies of the simulated unit cell in three dimensions, the atoms in the central simulation box boxes behave in the same manner as their replica images, and can freely cross box boundaries. Under periodic boundary conditions the linear momentum of the system will be conserved.

2.3.2. Nosé-Hoover Langevin Piston Barostat

The Nosé-Hoover Langevin Piston method is a modification of the Nosé-Hoover method[110] in which the fluctuations in the barostat are controlled through a Langevin Dynamics method[111]. In order to simulate the NPT ensemble, it requires to be combined with a temperature control method. The equations of motion are expressed as:

$$\dot{r}_i = \frac{p_i}{m_i} + \frac{1}{3}\frac{\dot{V}}{V} r_i \tag{2-7}$$

$$\dot{p}_i = F_i - \frac{1}{3}\frac{\dot{V}}{V} p \tag{2-8}$$

$$\ddot{V} = \frac{1}{W}\left[P(t) - P_0\right] - \gamma \dot{V} + R(t) \tag{2-9}$$

where, r is the position, p the momentum, m the mass, V the volume and F_i is the force of each atom. P(t) is the instantaneous pressure, P_0 is the external imposed pressure, W is the mass of the piston, γ is the collision frequency and R(t) is a random force taken from a Gaussian distribution with zero variance and mean. Below is the expression for R(t), where, k_B is the Boltzmann's constant.

$$\langle R(0)R(t)\rangle = \frac{2\cdot\gamma\cdot k_B\cdot T\cdot\delta(t)}{W} \tag{2-10}$$

2.3.3. Langevine Thermostat

In order to correctly control the temperature, the system is coupled with a reservoir or heat bath; The Langevine thermostat[107] models the influence of a heat bath by adding a small random noise and a frictional force directly proportional to the velocity of each particle. These two terms are balanced to maintain a constant temperature. The heat trapped in localized modes is removed using this model when each particle is coupled to a heat bath. The mathematical model for Langevine Dynamics is shown below.

$$M\cdot\dot{v} = F(r) - \gamma\cdot v + \sqrt{\frac{2\cdot\gamma\cdot k_B\cdot T}{W}}R(t) \tag{2-11}$$

where M is the mass, v is the velocity, F is the force, r is the position, γ is the friction coefficient, k_B is the Boltzmann constant, T is the temperature, and $R(t)$ is a random term. The coupling is applied by adding the fluctuation and frictional forces (last two terms) to the Newton's equations of motion[107].

2.3.4. Constrains: SHAKE/RATTLE Algorithm

In molecular dynamics, constrains are applied to the systems. Generally the simulations are carried out so that the internal coordinates satisfy bond-length and bond angle constrains. Also explicit or implicit constrains forces can be applied to bond and angle lengths. The constraint algorithms should be implemented effectively in order to prevent expensive and long computation times.

The SHAKE method[112] is based on the Verlet algorithm in which only the atomic positions are constrained; RATTLE is the velocity Verlet version of SHAKE where both positions and velocities are constrained[113]. SHAKE requires previous information for

the positions while RATTLE can calculates the new positions and velocities without earlier history. RATTLE also uses cartesian coordinates to describe the configuration of internal constrains in a molecule and like SHAKE is based on the Verlet algorithm. RATTLE is of higher precision than SHAKE on computers of fixed precision and it is convenient in molecular dynamics simulations at constant temperature and pressure where the velocities need to be rescaled[113].

2.3.5. Electrostatics: Particle Mesh Ewald (PME)

The Ewald summation[114] is the conventional method used to evaluate long-range electrostatic interactions in systems where periodic boundary conditions are applied. The infinite sum of charge-charge Coulomb interactions for a charge-neutral system is conditionally convergent.

Ewald summation sums over each box first, then sum over spheres of boxes of larger radius. This method is considered more reliable than a cutoff scheme, although it is noted that the artificial periodicity can lead to bias in free energy. The particle–mesh Ewald (PME) method[115] is a fast numerical method to compute the Ewald sum for large periodic systems.

CHAPTER III
THERMO-MECHANICAL CHARACTERIZATION OF PEPTIDE NANOTUBES*

3.1. Overview

Peptide nanostructures present wide range of opportunities for potential device and applications in biomedicine and bio-nanotechnology; hence thermo-mechanical stability studies on these materials are important and crucial for the design of their applications.

Recently, the interest in deformation and fracture of protein materials has intensified[116]; the mechanical stability of collagen tissues, beta-sheet structures and alpha helical structures has been studied using atomistic simulations and multi-scale modeling methods[117]. These findings, have illustrated the potential of peptide materials for nano-scale and biomedical applications[3]. However understanding the effect of molecular scale organization in the macroscopic mechanical behavior of these peptide based materials still remains in the earlier stages. Therefore, further experimental and theoretical studies have an important role contributing to the rational design of new functional peptide nanostructures.

Different theoretical approaches have been proposed to calculate the elastic constants of materials. These methods include empirical force-constant models [118,119], second derivative methods[120], molecular-dynamics simulations using fluctuation formulas [121,122] and finite elasticity theory based deformation methods[123-126]. One of the pioneers in the investigation of mechanical properties using atomistic simulations was Andersen [127], in his method the pressure was held constant and the volume of the system represented a dynamical variable.

---

*Part of this chapter is reprinted with permission from "Thermo-mechanical stability and strength of peptide nanostructures from molecular dynamics: self-assembled cyclic peptide nanotubes" by Carvajal-Diaz, J. A. & Çağin, T. *Nanotechnology* **21**, 115703 (2010). doi: 10.1088/0957-4484/21/11/115703

Parrinello and Rahman [128,129] method allow changes in both the size and shape of the molecular dynamics cell. A matrix h was defined from the molecular dynamics simulation cell parameters as h = (**a**, **b**, **c**); where **a**, **b**, and **c** are the cell vectors and constitute the columns of the h-matrix. In the Parrinello-Rahman approach h is a dynamical variable that describes the shape and size variations of the molecular dynamics cell. Ray and Rahman[130] showed how the MD theory can be used together with the theory of finite (or nonlinear) elasticity[131]. They defined the *EhN* ensemble; in which not only the volume (V= det (*h)*) is kept constant but also the shape of the molecular dynamics simulation cell. The introduction of the h matrix into the theory, allows a full description of the elastic properties of a system of arbitrary symmetry. In this study, we apply strains of arbitrary magnitude to the system and the finite theory of elasticity is used for the calculation of the second order elastic constants.

The calculations of elastic constants using atomistic simulations have become useful to provide a complete description of the elastic response of materials such as metals [7], ceramics[8], polymers[9], carbon nanotubes[132] and minerals, among others. Gupta and coworkers have demonstrated the use of the finite strain theory of homogeneous elastic deformation with first principles methods to calculate second order elastic constants (SOEC) and third order elastic constants (TOEC) for crystals of low symmetry, illustrating the general applicability of the method. They found out that fitting the energy-strain relation is more robust numerically than fitting the stress-strain relation and the coefficients derived from fitting the calculated total energy are less sensitive to the details of computations compared to stress-based approaches[133].

In the present work, we have used Lagrangian strain tensors characterized by a single strain parameter, and each strain tensor is applied to the crystal lattice, using the definition of the h matrix given by Ray and Rahman[130]. The elastic strain energy is calculated from the molecular dynamics simulations, hence including the temperature effect. The second-order (isothermal) elastic constants are obtained from a polynomial fit to the calculated energy-strain relation obtain from constant temperature simulations. This work focuses on a specific system: peptide based nanostructures self-assembled in

nanotubes forming a two-dimensional ordered structure following the model of cyclic peptide nanotubes synthetized by Ghadiri[13]. The use of periodicity in the third dimension makes up a 3-dimensional infinite crystal. In these peptide nanotubes, the peptides subunits present covalent interactions between the amino acids forming each ring; the hydrophobic side chains interact through VDW forces providing stability between the tubes. The hydrogen bonding between the peptide subunits represents the strongest intermolecular forces of the system and directs the self-assembly of these tube-like peptide nanostructures. Anisotropic behavior is expected for the mechanical properties of this system due to the different nature of interactions present along different directions.

Up to date, there is not report of mechanical characterization of these nanotubes. Therefore, the study and understanding of the mechanical stability and strength of these materials is important in order to be able to predict and design the previously mentioned applications.

In this chapter, a homogeneous deformation method is combined with the finite elasticity theory and molecular dynamics simulations (MD) is presented for the calculation of second order anisotropic elastic constants; additionally thermodynamic properties are also reported for the model formed by self-assembled cyclic peptide nanotubes.

3.2. Description of the Model

The results presented here are related to the first experimentally synthesized peptide nanotubes, obtained by Ghadiri[13]. These nanotubes form a crystalline network, which has been characterized experimentally and cell parameters known[13]. One tube is made out of cyclic peptide subunits formed by eight amino acid residues, each represented as Cycle[-(D-Ala-Gln-D-Ala-Glu)$_2$-]. The D,L amino acids are: Glutamine (Gln), D-Alanine (Ala) and Glutamic Acid (Glu). The octa-peptide subunit and nanotube structure is shown in Fig. 3.1.

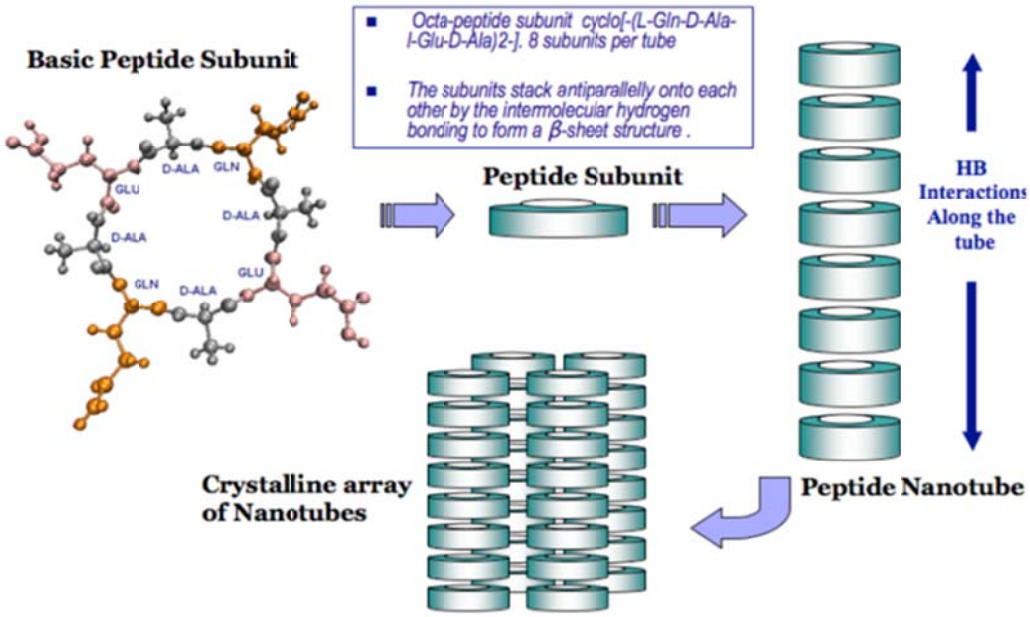

Figure 3.1. Self-assembly Scheme for Cyclic Peptide Nanotubes

The cyclic peptide nanotubes membrane is classified as an anisotropic. This character is explained based on the differences in the interactions between the tubes in the x-y plane and along the tubes (z direction). The mechanical properties are expected to be different depending on direction (see Fig. 3.2.).

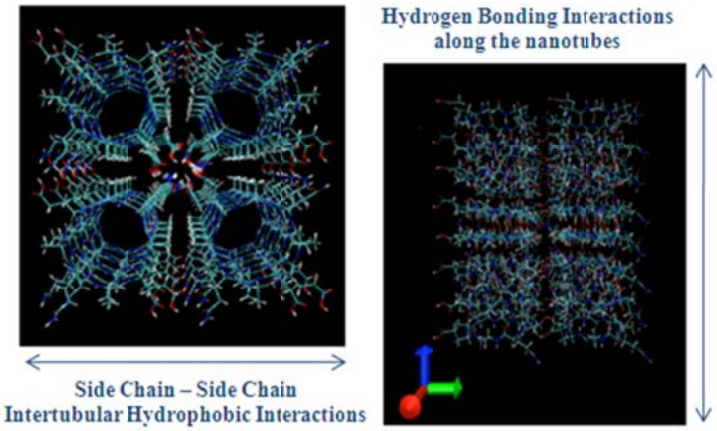

Figure 3.2. Anisotropy of Interactions in Self-assembled Cyclic Peptide Nanotubes. Axial view (right) and Longitudinal view **(**left).

3.2.1. Optimization of Initial Model

In order to obtain properties from MD simulations, it is necessary to build a model consistent with the crystallography results. The development of this model is an important goal before the prediction of any property. This strategy may be used for other nanostructured models. Minimization of the initial structure is followed by several NPT simulations at temperatures ranging from 0K to 700K, the procedure was repeated until the system fully relaxed to zero stress-pressure state. (see Fig. 3.3.) This state serves as the stress free state-reference state for the definition of h_o.

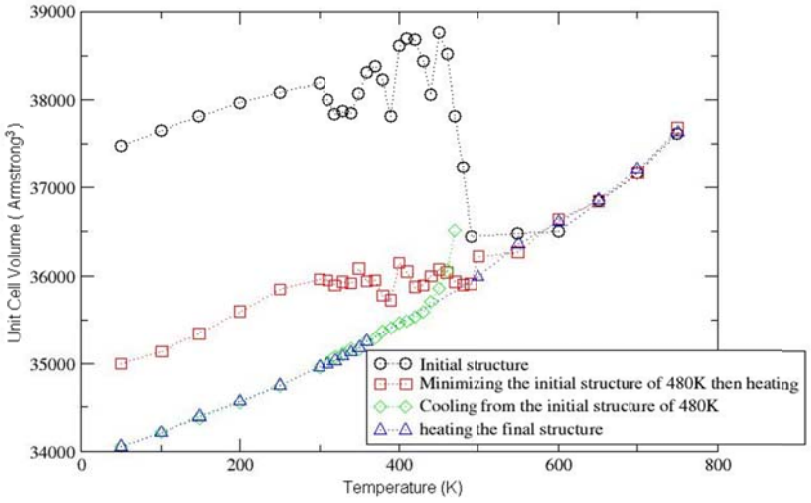

Figure 3.3. Variation of unit Cell Volume during Thermal Treatment of Self-assembled Cyclic Peptide Nanotube Structures. Optimized Structure and Volume are Obtained through a Successive Thermal Treatment and Minimization Strategy.

After the optimization, the calculated cell parameters and density of the systems are in good agreement with the reported experimental values (see Table 3.1).

Table 3.1. Comparison between Experimental and Calculated Cell Parameters

Unit Cell parameter	*Experimental*	*Simulation*
a (A)	9.5	9.6
b (A)	15.1	15.3
c (A)	15.1	15.1

3.3. Thermodynamic Properties

3.3.1. Computational Details

Molecular Dynamics simulations give the first-order properties such as internal pressure, internal energy and density in time and averages over time yield the thermodynamic observables. The second-order properties are the thermodynamic and mechanical response functions such as the specific heat capacity, the isothermal compressibility, the thermal expansion coefficient, the elastic constants, etc., these may be obtained from the first order properties using numerical differential methods, or statistical fluctuation formulas derived from definition of entropy or free energy [134,135].

$$C_P = \left(\frac{\partial E}{\partial T}\right)_P \; ; \; V\kappa_T = -\left(\frac{\partial V}{\partial P}\right)_T \; ; \; V\alpha_P = \left(\frac{\partial V}{\partial T}\right)_P \tag{3-1}$$

We have used exclusively the NAMD2.5[107] program with the CHARMM force field representing the interatomic interactions in the model system. Isothermal-isochoric and isothermal-isobaric ensembles were used in the calculations of thermodynamic properties such as specific heat capacity, bulk modulus and thermal expansion coefficient of the peptide nanostructures. NPT dynamics are used to determine bulk properties at atmospheric pressure. Temperature was increased from 100K to 700K using the Langevine thermostat as temperature control method.

3.3.2. Results and Discussion

Thermodynamic properties were calculated using the NPT (isothermal-isobaric) ensemble. The thermal expansion coefficient and the specific heat capacity were calculated from NPT simulations from 0 GPa to 16 GPa and the isothermal compressibility factor value is reported at 300K (see Fig. 3.4 and Table 3.2.).

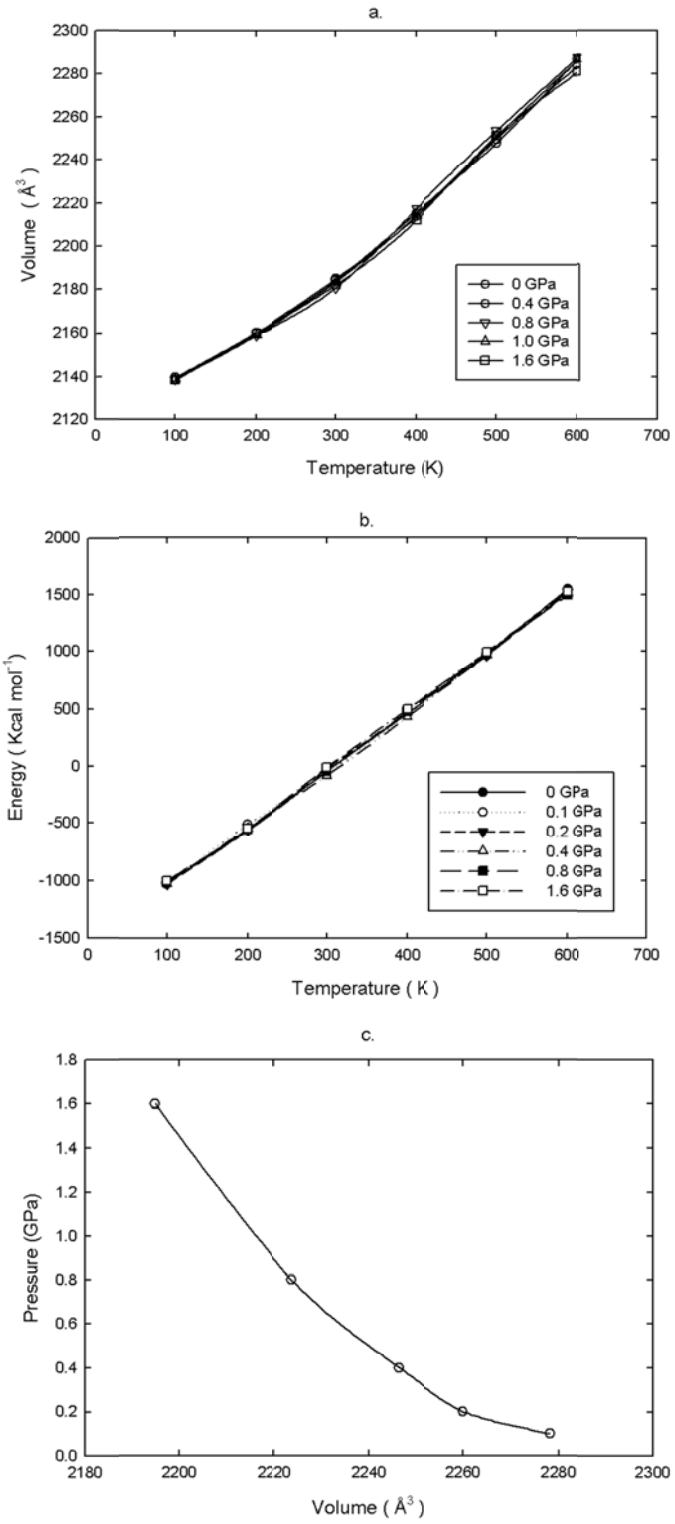

Figure 3.4. Thermodynamic Properties: Variation of Volume, Internal Energy as a Function of Temperature and Variation of Pressure vs. Volume.

Table 3.2. Thermodynamics Properties of Crystalline Cyclic Peptide Nanotubes at 300 K

Cp (Kcal/mol)	1.32
κ(GPa^{-1})	2.9x10^{-2}
α (1/K)	1.3x10^{-4}

3.4. Anisotropic Elastic Constants

3.4.1. Homogeneous Deformation Method

Taking a reference state is needed in order to describe a strained state of a system, one needs to define a reference. We can define the h-matrix, which represent the shape and the size of the system, and in an arbitrary coordinate frame in terms of its unit cell vectors as its columns:

$$h = \begin{pmatrix} a_x & b_x & c_x \\ a_y & b_y & c_y \\ a_z & b_z & c_z \end{pmatrix} \tag{3-2}$$

The h-matrix transforms the fractional/crystallographic coordinates (ξ, η, ζ) to Cartesian coordinates (x, y, z) as follows:

$$\begin{pmatrix} x \\ y \\ z \end{pmatrix} = h \begin{pmatrix} \xi \\ \eta \\ \zeta \end{pmatrix} \tag{3-3}$$

If the ZYX-crystallographic convention assumed, it becomes a lower triangular matrix, with $b_x = c_x = c_z = 0$.

One can write the h matrix in terms of components of cell vectors as well as the more commonly used cell parameters, (a,b,c, α, β, γ,) as follows:

$$h = \begin{pmatrix} a_x & 0 & 0 \\ a_y & b_y & 0 \\ a_z & b_z & c \end{pmatrix} = \begin{pmatrix} a\sin\beta\sin\gamma^* & 0 & 0 \\ a\sin\beta\cos\gamma^* & b\sin\alpha & 0 \\ a\sin\beta & b\cos\alpha & c \end{pmatrix} \tag{3-4}$$

where, $\gamma^* = \dfrac{\cos\gamma - \cos\alpha\cos\beta}{\sin\alpha\sin\beta}$ (3-5)

This zero stress state value of this matrix h_o represents the cell size and shape before application of any deformation and it is therefore used as the reference state to define the strain tensor of finite theory of elasticity[122] as:

$$\varepsilon = \frac{1}{2}\left(\tilde{h}_0^{-1} G h_0^{-1} - I\right) \tag{3-6}$$

where G matrix is defined as; $G = \tilde{h}h$, the tilde indicates matrix transposition[122]. The finite strain expression can trivially be inverted to express the metric tensor, G,

$$G = \tilde{h}_0(2\varepsilon + I)h_0 \tag{3-7}$$

in turn, the cell parameters are defined as a function of applied strain; first the cell lengths:

$$a = \sqrt{G_{11}};\ b = \sqrt{G_{22}};\ c = \sqrt{G_{33}} \tag{3-8}$$

and the nonzero components of **a** and **b** from

$$a_z = G_{13}/c;\ b_z = G_{23}/c;\ b_y = \sqrt{b^2 - b_z^2};\ a_y = \left(G_{12} - a_z b_z\right)/b_y;\ a_x = \sqrt{a^2 - a_z^2 - a_y^2} \tag{3-9}$$

In this work, after establishing how to apply the strain properly to the molecular level models, we combine the method of homogeneous but finite deformations with the total-energy calculations from molecular dynamics simulations to provide the general method for determining second order elastic constants of self-assembled cyclic peptide nanotubes at elevated temperatures, in particular at 300K.

To establish the basis of our calculations, we start by defining the strain energy with respect to reference, unstressed state. If a body is deformed, then its strain energy can be expressed as a Taylor series expansion in strain as:

$$\Delta E = \frac{V_0}{2!}\sum_{i,j,k,l} C_{ijkl}\varepsilon_{ij}\varepsilon_{kl} + \frac{V_0}{3!}\sum_{ijklmn} C_{ijklmn}\varepsilon_{ij}\varepsilon_{kl}\varepsilon_{mn} + O(\varepsilon^4) \tag{3-10}$$

For generality we have given the expression up to third order elastic constants. We can express the strain energy in commonly encountered Voigt notation; where the Voigt notation uses a 6-vector notation utilizing the inherent symmetries of the strain tensor and elastic constants:

$$\Delta E = \frac{V_0}{2!}\sum_{I,J} C_{IJ}\eta_I\eta_J + \frac{V_0}{3!}\sum_{I,J,K} C_{IJK}\eta_I\eta_J\eta_K + O(\eta^4) \tag{3-11}$$

$$\begin{pmatrix} \varepsilon_{11} & \varepsilon_{12} & \varepsilon_{13} \\ \varepsilon_{12} & \varepsilon_{22} & \varepsilon_{23} \\ \varepsilon_{13} & \varepsilon_{23} & \varepsilon_{33} \end{pmatrix} \Rightarrow \begin{matrix} \eta_1 = \varepsilon_{11} & \eta_6 = 2\varepsilon_{12} \\ \eta_2 = \varepsilon_{22} & \eta_5 = 2\varepsilon_{13} \\ \eta_3 = \varepsilon_{33} & \eta_4 = 2\varepsilon_{23} \end{matrix} = \begin{pmatrix} \eta_1 & (1/2)\eta_6 & (1/2)\eta_5 \\ (1/2)\eta_6 & \eta_2 & (1/2)\eta_4 \\ (1/2)\eta_5 & (1/2)\eta_4 & \eta_3 \end{pmatrix} \tag{3-12}$$

Elastic constants are obtained from a polynomial fit to the calculated energy-strain relation. Fitting the energy-strain relation, rather than the stress-strain relation, provides a more robust procedure and enables the use of certain first-principles codes where the stress tensor cannot be determined directly as well.

3.4.2. Energy-Strain Relationships and Elastic Constants

After expanding the elastic energy per unit volume of specific strained systems and fitting the energy values with respect to the value applied of ξ, the second order elastic constants (SOEC) are obtained from the coefficients of the second order terms of the expression. Results are plotted in Fig. 3.5 (a-h).

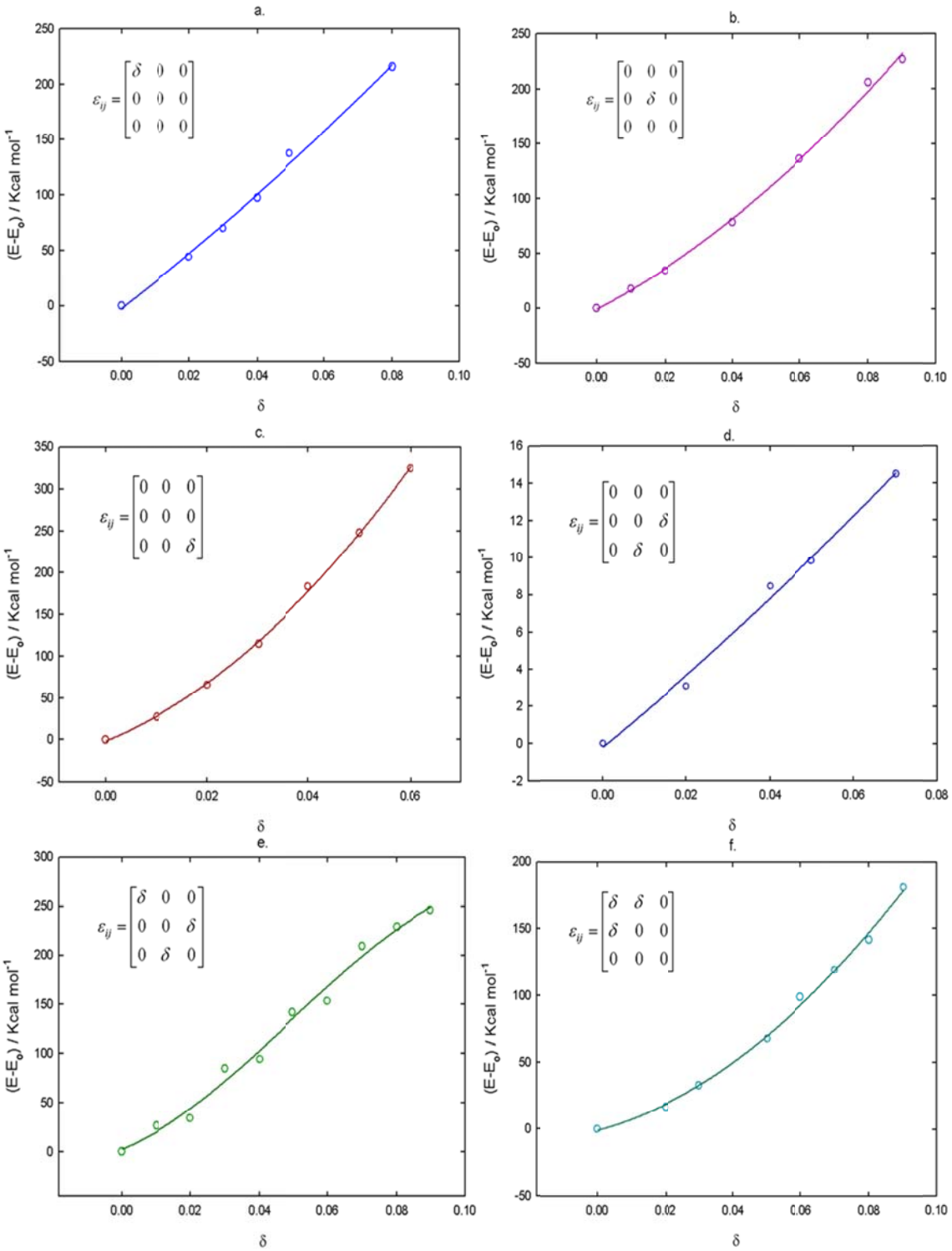

Figure 3.5. Variation of Strain Energy (E-Eo) as a Function of Different Applied Strain Tensors used in Calculating the Anisotropic Elastic Properties of the Cyclic Peptide Nanotubes. The Applied Strain Tensors are displayed as Insets for each Elastic Constant. The Y-Axis (E-Eo) has units of Kcal/mol.

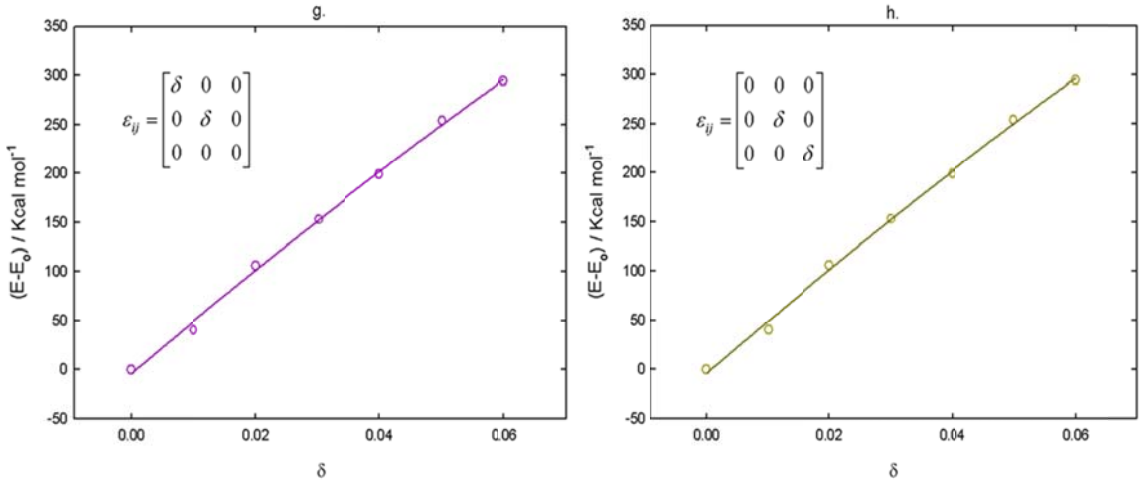

Figure 3.5. Continued.

As the applied strain values is increased, an expected yield behavior was observed, see Fig. 3.6, at a value of strain, ξ above 6% in z direction (along the tube axis).

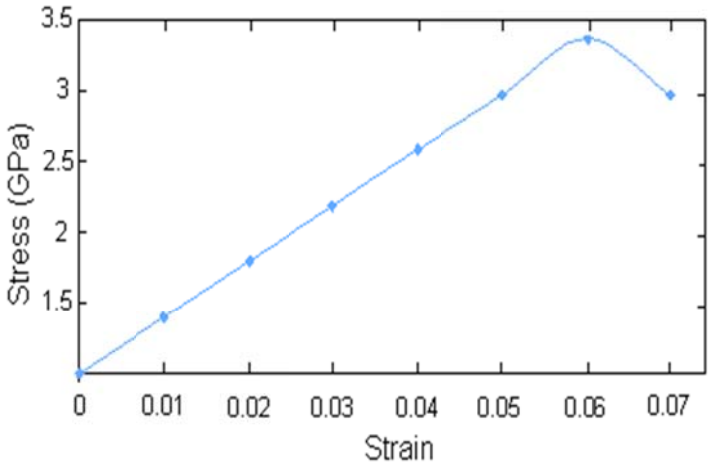

Figure 3.6. Stress-strain Behavior along Tube axis in Assembled Cyclic Peptide Nanotubes, and Yield Behavior at around 6% Tensile Strain.

This behavior has to be further investigated in order to obtain a better understanding of the yield phenomena, our hypothesis is that the yield is observed as consequence of hydrogen bond breaking in z direction for high strain values (>6%). The values for the Second Order Elastic Constants (SOEC) are reported in Table 3.3, results

are consistent with the various mechanical stability relations given in terms of anisotropic elastic constants for trigonal crystals.

Table 3.3. Anisotropic Elastic Constants of Cyclic Peptide Nanotubes

C_{ij}	(GPa)	C_{ij}	(GPa)
C_{11}	8.09	C_{66}	0.77
C_{22}	10.16	C_{12}	6.56
C_{33}	19.65	C_{13}	9.56
C_{44}	1.23	C_{14}	0.57
C_{55}	1.23	C_{23}	9.59

The value found for C_{33} is highest as expected due to the strong intermolecular forces (Hydrogen-bonds) along z (tube axis) direction. The difference between C_{11} and C_{12} is larger than zero, indicating tetragonal shear stability, but corresponding tetragonal shear constant is 0.7 GPa is an indication of delicate nature of this tetragonal shear stability. The values of C_{44}, C_{55} and C_{66} are small compared to the other constants, this is an indication of the weakness of the shear stability of the membrane, but still these numbers are high enough to keep the system self-assembled and intact. The smallest value is C_{66} and this is in plane xy pure shear value. This resulted is as expected and quite close in value to corresponding tetragonal shear, C_t= (C11-C_{12})/2. The values for C_{11} and C_{22} are smaller compared with the C_{33} coefficient, since these two constants are mainly representation of van der waals and electrostatic forces. However, these values are still noticeably larger than most of the amorphous polymers.

The Young's modulus can be approximated to the value of the C_{33} elastic constant. The Young's Modulus calculated from molecular dynamics is 19.65 GPa, this value is higher than the C_{11} and C_{22} components; this confirms the anisotropy of the system and its more rigid character in z direction can be attributed to the hydrogen bonds that assemble the peptide subunits of the nanotubes. There is no experimental value of the Young's modulus for this particular system, however the peptide nanotubes made up of diphenyl alanine peptides is reported to have a Young's modulus of 19 GPa[33] which is in close agreement with our finding.

3.5. Summary

Peptide Nanostructures are mechanically stable materials with huge possibilities to be studied and a promising number of applications in biomedicine and bio-nanotechnology. Here, the anisotropic elastic constants for cyclic peptide nanotubes at 300K were reported. This methodology can be used to obtain a better understanding in the mechanical stability of different peptide materials with known cell parameters.

It is important to design a methodology to optimize the initial structure of the molecular model in order to represent the experimental model. CHARMM force field was validated to predict peptide materials properties accurately. The behavior of the elastic properties at different temperatures can be further investigated as well as the thermal stability of the system. The ordered conformations in which the peptide subunits and nanotubes are self-assembled influence favorably the stability of the membrane. The result for the Young's modulus is in good agreement with previous reported results for similar peptide nanotubes and protein crystalline systems. The yield behavior could be explained as a consequence of breaking the Hydrogen-bonds when applying the tensile strain deformation, this have to be further investigated.

CHAPTER IV
TRANSPORT PROPERTIES UNDER NANOSCALE IN PEPTIDE NANOTUBES*

4.1. Overview

The exploration of transport behavior and structure of fluids in nanoscale confinement is common to many systems and problems: water channels[136,137], separation of multicomponent molecular mixtures[138], biological channels[139] and confinement effect on glass transition[140]. Nanoscale diffusion mechanism changes depending on the relative size of molecule and pores. The decrease in pore size leads to different modes of diffusion at molecular level: from a normal-mode to a transition-mode and then subsequently a single-file mode[141]. Understanding the change in structure and transport of fluids under nanoscale confinement conditions can contribute to design better nano-fluidic devices and as well as help to understand biological function of cell membranes.

Experimentally, it is necessary to have a defect-free nano-porous materials of known size and narrow size distribution in order to study nanoscale transport and confinement mechanisms[142,143]; however it is still very difficult and expensive to produce small inner diameter and uniform nano-pores on a macroscopic membranes.

Due to the channel structure and the interaction between channel and molecules, transport mechanism studies are essential to get fundamental insight of nanoscale transport phenomena. Fortunately, a similar but less complicated structure or model is always a good substitute to study its primary characteristic. Molecular dynamics (MD) is an efficient method to study molecular transport and confinement phenomena inside nano-pores such as zeolites, carbon nanotubes and biological channels.

---

*Part of this chapter is reprinted with permission from "Structure and Dynamics of Water Within Single Wall Carbon Nanotubes and Self-Assembled Cyclic Peptide Nanotubes" by Carvajal-Diaz, J. A., Liu, L. & Cagin, T. *Journal of Computational and Theoretical Nanoscience* **6**, 894-902 (2009). Copyright 2009 by American Scientific Publishers.

MD can help to predict the new materials properties, contributing to optimize their rational design, while saving time and investment[144].

4.2. Transport of water in single wall Carbon Nanotubes

Carbon nanotubes (CNT) have uniform pore size and composition, with a quasi-one-dimensional feature and continuously smooth walls. It has several promising applications for its interesting properties, such as selective molecular filter[145], support material for catalyst[146] and nanofluidic devices[147] . It is also a good prototype for those more complicated channel structures, especially biological channels, and is amenable to study by MD method for its simplicity, stability and small size[148].

In 2001, Hummer et al. showed the potential application of single wall carbon nanotube as a water channel[149]. Although there were several other computational studies on carbon nanotubes published earlier, Hummer was the first to propose that hydrophobic carbon nanotube can serve as water channel. Mao and Sinnott later studied the dynamic flow and molecular diffusion of small organic molecule such as methane, ethane and ethylene[150,143] and their mixture in carbon nanotube; and theoretically have shown the possibility of use of carbon nanotubes as membrane filters. Their study of diffusive flow through nanotubes shows that nanotube diameter has significant effect on molecular diffusion mechanism. If the molecules have strong interaction with nanotubes, the dynamics of flow will be further slowed down.

Walther et al. studied water and carbon nanotube energetics for solvated systems, i.e. water interaction with the external surfaces of nanotube[151]. Martí and Gordillo studied the temperature effect on static and dynamic behavior of water inside carbon nanotube[152]. They analyzed the distribution of hydrogen-bonding network, hydrogen and oxygen density in nanotube as a function of temperature. They have reported that there are no complex hydrogen-bond structures in narrow tubes.

Several water transport models in carbon nanotube have been proposed prevously. In 2002, Berezhkovski and Hummer proposed the continuous-time random walk model [153] [154]. They used this model to describe the concerted motion of confined

molecules and calculate single-file transport properties. Zhou et al. proposed the one dimensional lattice gas model[155], which has the same shortcoming as above model. Zhu et al. proposed a collective diffusion model based on a statistical mechanics treatment[156], this model is limited to single-file channels and it can be used to study equilibrium and non-equilibrium transport phenomena establishing the quantitative relationship between spontaneous water movement and pressure induced water flux; it provides an analysis tool for nanoscale transport phenomena. However, even though these studies have contributed, confined water behavior in nanopores is still far from being fully understood. Here, we present molecular dynamics simulations to study confined water transport, the results from confined water in CNTs is compared with CPNTs channels under the same simulation conditions.

4.2.1. Computational Details

For the case of carbon nanotubes, armchair and zigzag nanotube membrane was constructed by hexagonally packing of identical carbon nanotubes. In the membrane, due to close packing, the gaps between tubes were so narrow that water molecules could not enter. The nanotubes were fixed in space, the channels were initially empty and water molecules flowed into the nanotubes (from the reservoir domains) during the simulations. There were enough water molecules in the reservoir section of the simulation box, see Fig.4.1.; bulk water was always present away from the entrances of the nanotubes, this model can avoid the "image" effect between conducted water.

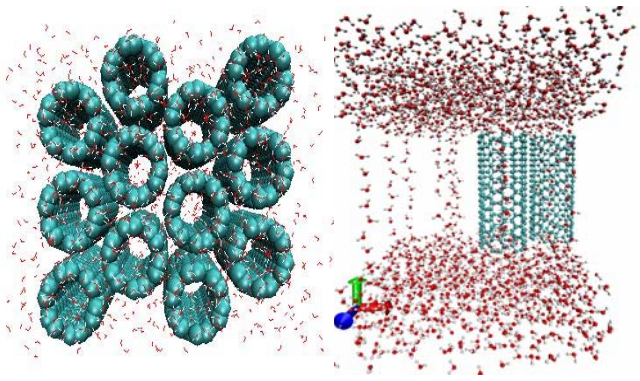

Figure 4.1. Carbon Nanotubes in Water Simulation Box

For the cases of CNT armchair (n,n) and zigzag (n,0) chirality, two different length and several diameters were constructed for the analysis. The types of CNT studied in this work are listed in Table 4.1. where van der Waals diameter means the distance between van der Waals surfaces of carbon atoms along nanotube diameter.

Table 4.1. Simulated Geometries of Carbon Nanotubes

CNT geometry	Length (Å)		VDW diameter (Å)
(6,6)	23.37	97.17	4.5
(7,7)	23.37	97.17	5.9
(8,8)	23.37	97.17	7.2
(9,9)	23.37	97.17	8.6
(10,10)	23.37	97.17	9.9
(15,15)	23.37	97.17	16.8
(10,0)	24.15	100.84	4.3
(14,0)	24.15	100.84	7.4
(16,0)	24.15	100.84	8.9
(18,0)	24.15	100.84	10.5
(26,0)	24.15	100.84	16.8

All simulations were performed using NAMD2.5 and the CHARMM force fields, under constant temperature (300K) and constant pressure (1 atm = 1.013 bars) conditions. Model systems were run for 3 ns and the last 2 ns were used for analysis with coordinates recorded every 1 picosecond (ps). The nanotubes were constrained and just the water molecules were allowed to move. Time step of integration was 1fs. Periodic Boundary conditions were used. The SHAKE/RATTLE algorithm was imposed for fixing the O-H bonds during evaluating the equations of motions. For the interaction of waters transferable intermolecular potential (TIP3P) water model was employed and in evaluating electrostatic interactions Particle Mesh Ewald (PME) algorithm was used. After the equilibration of the system self-diffusion coefficient and dipole correlation functions were calculated. Self-diffusion coefficient calculation and hydrogen bond

analysis were based on 300 ps long simulation trajectory with the coordinates recorded every 50 fs in the NPT ensemble (300 K, 1.013 bars). Dipole moment study was based on 30 ps long simulation trajectory with coordinates recorded every 10fs.

4.2.2 Results and Discussion

The cross sectional views of equilibrium water configuration inside nanotube are shown in Fig 4.2. Water molecules form layer structure inside nanotubes Fig 4.2. shows that a single-file water chain is occupying the pore of (6, 6) nanotube and water molecules, linked by hydrogen bonds, are cyclically stacking inside (8, 8) nanotube. Here the single-file water chain in (6, 6) nanotube is recognized as one layer whose radius is almost zero.

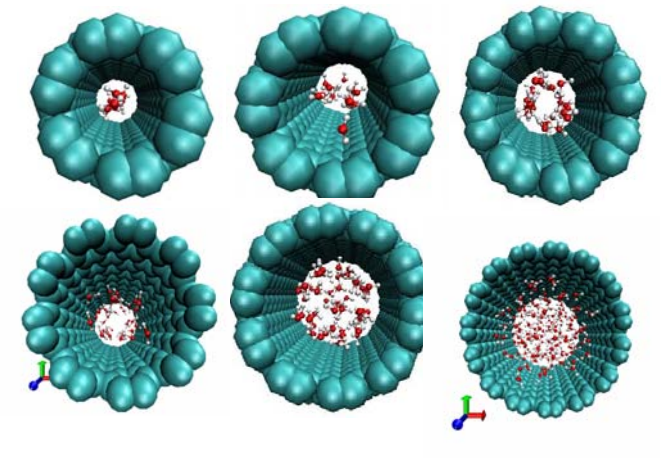

Figure 4.2. Cross-sectional view of Water Equilibrium Profile inside Armchair CNTs

To characterize water configuration quantitatively, water radial distribution probability curve along nanotube radius is shown in Fig 4.3, while reduced water density distribution along nanotube axis is shown in fig 4.5. From Fig.4.3, water radial distribution probability curve inside (6, 6), (7, 7), (8, 8) nanotube are unimodal, which means water molecules form single layer structure inside these three types of nanotube.

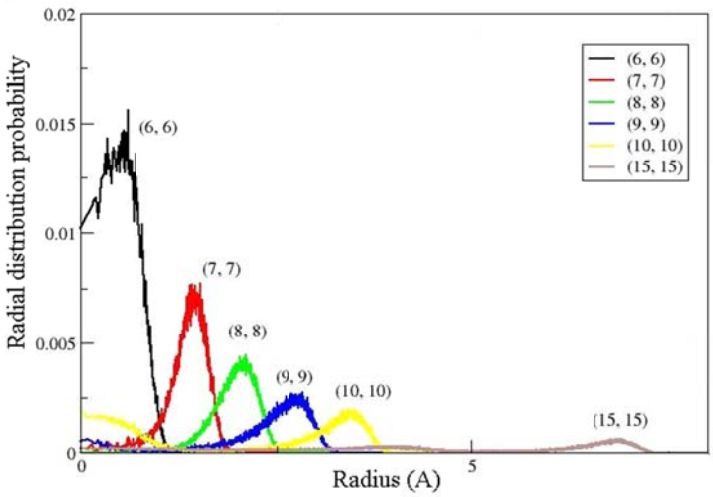

Figure 4.3. Water radial Distribution within Carbon Nanotubes of Different Diameter

In nanotubes with larger VDW diameter, water radial distribution probability curve has two or more peaks. From Fig 4.4, water in (7, 7) and (8, 8) nanotube has similar reduced axial density, so as in (9, 9) and (10, 10) nanotube. The wave like water axial reduced density distribution in (6, 6) nanotube is in good agreement with the single file transport mechanism that water molecules are hopping along axial direction under the driving force of density difference. However the wave like density distribution is not obvious in larger diameter nanotube. This is due to the availability of larger space inside the nanotube and water behavior tends to approach bulk water behavior.

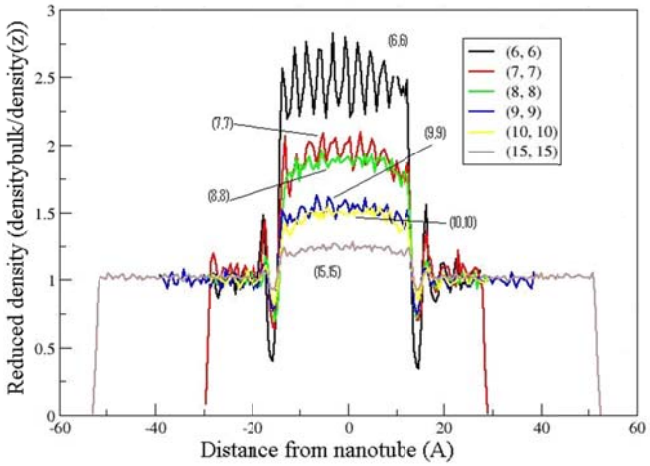

Figure 4.4. Water Reduced Density Distribution along Nanotube Axis. Nanotube Length : 2.337 nm.

In Fig 4.3., there is one water peak and one valley near each end of each type of nanotube. The water peak is caused by the attraction of carbon atoms on water molecules, while the valley is for the reason of repulsion of carbon atoms on water molecules. From Fig 4.4, the magnitude of density fluctuation at entrance is determined by the nanotube VDW diameter and nanotube length. The larger the nanotube VDW diameter, the smaller the fluctuation will be. The water density fluctuation at (6, 6) nanotube entrance becomes smaller for longer tube while that of nanotubes with larger diameter will not change much as shown in Fig 4.5.

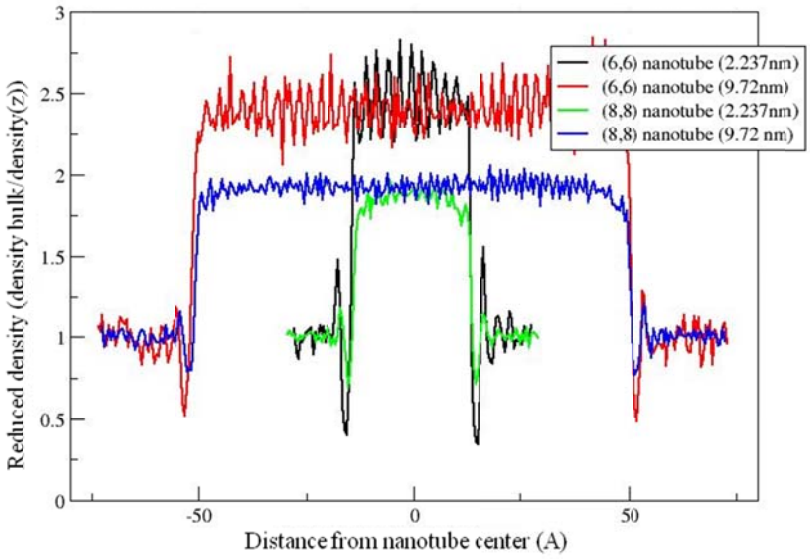

Figure 4.5. Water Reduced Density Distribution along Nanotube Axis. Effect of Length.

To study dynamic properties of confined water, the mean square displacement along axial direction are obtained and shown in Fig 4.6, where the studied armchair CNTs were 2.337nm long. The water self-diffusion coefficients along axial direction are calculated according to Einstein's relationship:

$$msd(t) = \left\langle \left| r_i(t) - r_i(t_0) \right|^2 \right\rangle = d * D * t \tag{4-1}$$

where d depends on the space dimensionality (6 for three dimensions, 4 for two dimensions, 2 for one dimension).

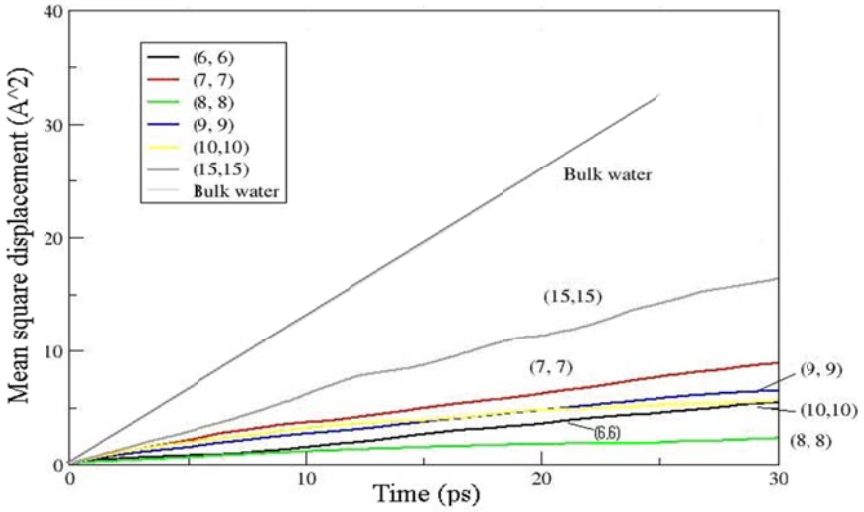

Figure 4.6. Mean Square Deviation

Dipole moment autocorrelation function of single water molecule, $\langle p_i(0) \bullet p_i(t) \rangle / \langle p^2 \rangle$, is calculated to study the water reorientability inside nanotube and shown in Fig.4.7.

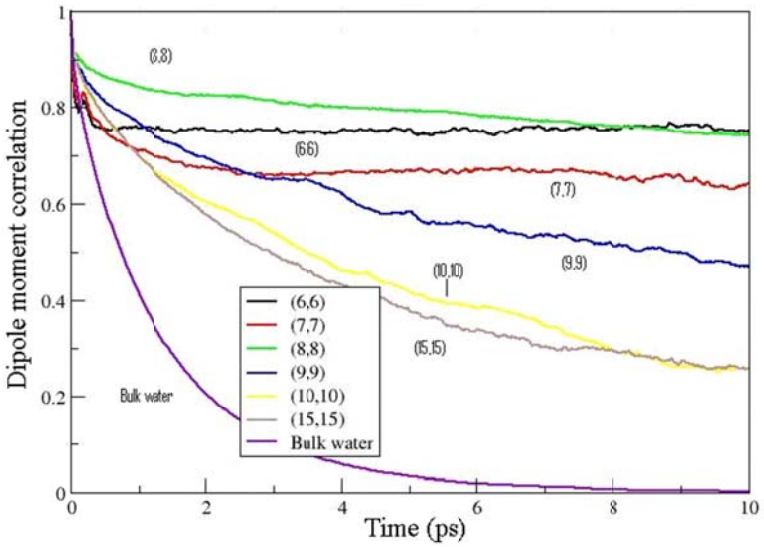

Figure 4.7. Single Water Molecule Dipole Autocorrelation

Dipole-dipole correlation function is calculated to further study water dynamics behavior inside nanotube as shown in Fig.4.8. Water dipole-dipole correlation functions in (6, 6), (7, 7) and (8, 8) nanotube decay slowly. While in (10, 10) nanotube and nanotube with larger diameter, water dipole-dipole correlation is limited within the next two neighbors. So with the increasing VDW diameter, the dipole-dipole correlation changes from long-range to short-range.

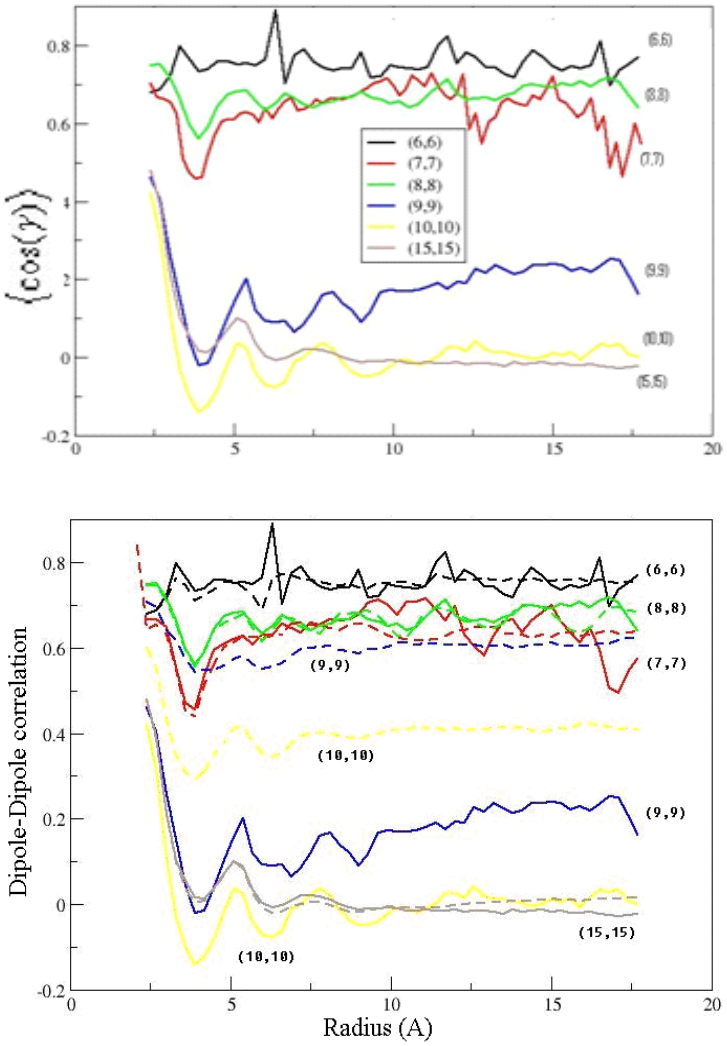

Figure 4.8. Dipole-dipole Autocorrelation Function (γ is the angle between dipole moments of water molecules that are separated by the distance r). Solid line Represents the dipole-dipole Correlation Function in 2.337 nm Nanotube and dash line is the result in 9.717nm Nanotube.

The probability distribution of the angle between hydrogen bond and nanotube axis is showed in Fig.4.9. The probability distribution for the angles in (6, 6) nanotube is a unimodal curve whose peak is around 160 degrees. And the probability distribution of angle in (8, 8) nanotube is a bimodal curve that has two peak values, one at 10 degrees and the other at 75 degrees. In nanotube with larger VDW diameter, the probability distribution of the angle becomes more even and approach that of bulk water.

To understand the length effect on water reorientability, we also examined the dipole correlation function in longer nanotube. The observation of Fig.4.8. indicates that length effect is mainly related to the nanotube diameter. For narrow nanotube, short tube will demonstrate most of the confinement effect. And for very wide nanotubes, such as (15, 15) nanotube, the length effect are not significant for their transport mechanism have to studied by combining other mechanism such as capillary mechanism. Length effect is very import for those intermediate nanotubes, such as (9, 9) and (10, 10) nanotubes, which only show significant confinement effect with long enough tube length.

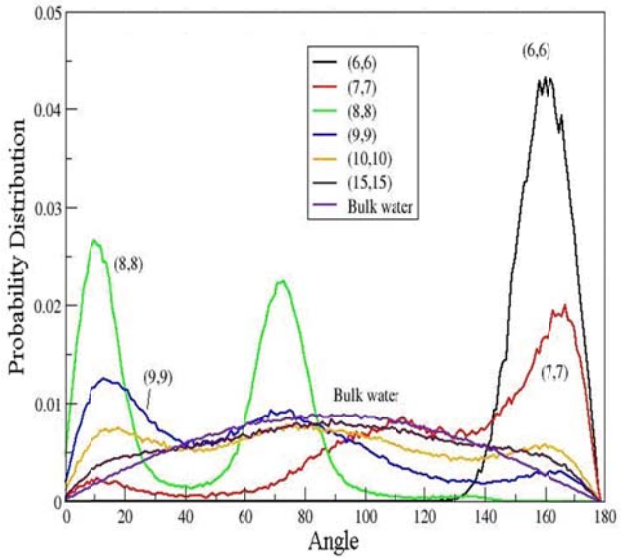

Figure 4.9. Probability Distribution of Angle between Hydrogen Bond and Tube Axis

Our study demonstrates that nanotube chirality doesn't have significant effect on water static behavior, which is consistent with previous research. Water distribution

patterns are similar to those in armchair nanotube, which are not shown here. By examining the dipole correlation function, we found nanotube chirality does not affect the water reorientability, which is mainly determined by the available space in nanotube and the nanotube length. The comparison between self-diffusion coefficient of water in armchair and zigzag nanotube infers that chirality doesn't affect water diffusion.

4.3. Transport of Water in Cyclic Peptide Nanotubes

Nature forms complex three-dimensional structures through spontaneous association of molecules termed "molecular self-assembly". In this study, we will focus on peptide-based self-assembled nanotubes to study its transport properties. Here, we present the cyclic peptide nanotube designed by Ghadiri[4] as alternate water channel, in order to compare its transport properties with equivalent sizes of carbon nanotubes (CNTs). The internal diameter of the nanotubes ranges between 7-8 Å and 13-15 Å and it can be controlled by changing the number of the amino acids in the cyclic peptide sequence[14,4].

Various applications were offered for these tubular structures. One of the first applications was based on their membrane interactions. As the cyclic peptide nanotubes are toxic to bacteria, they were demonstrated to serve as novel antibiotic agents[15]. Other potential applications include drug delivery, and application in material sciences, since new composite material can be formed by nucleation of inorganic materials into the peptide structures[15]. Structures consisting of eight[13], ten[17], and twelve[157] cyclic peptide subunits form tubular structures with the diameter of the internal van der Waals pore estimated to be 7, 10, and 13 A°, respectively. These structures have been shown to be large enough to serve as a conduct for water[16], function as size-selective ion and mediate the transport of biologically relevant molecules[158,159].

In 1995, Engels, Bashford and Ghadiri by the first time studied the dynamic behavior of water in self-Assembled peptide nanotubes[16]. They suggested that water diffusion could be understood as a series of "hops" between zones, which can cause

transient local deviations from the ideal number of water molecules in a zone. They also suggest longer simulations for a better estimation of the diffusion process in these nanotubes. Peptide nanotubes can be self-assemble into complex multimeric entities that constitute nanopores, or ‘‘barrel staves’’. Just like multi helix trans-membrane proteins, these nanopores result from the association of individual nanotubes through favorable interactions of their polar residues—constituting the hydrophilic interior of the pore—whereas the no polar ones are exposed to the aliphatic chains that form the hydrophobic core of the lipid bilayer. The ability to tailor surface characteristics of the nanotubes by changing the amino acid side chain functionality enable the design of trans-membranes and nanochannels with competitive transport efficiencies compared with other common used materials.

Both of the systems described previously, carbon nanotubes and cyclic peptide nanotubes present a uniform environment apart from the distinct character of their specific interactions with water. Carbon nanotubes have hydrophobic cylindrical core in contrast with the hydrophilic core structure presented by cyclic peptide nanotubes. In this study, we intended not only investigate the structural stability and dynamics of water in both types of nanotubes, but also analyze the most interesting factor: the influence of the interactions channel-water in the nanotubes on the diffusion properties of the water molecules.

4.3.1. Computational Details

The same parameters and software as used in the CNTs case was used. For cyclic peptide nanotubes, structure is a β-sheet-like hydrogen bonded stacks of cyclic subunits. The starting tube was constructed according to the model proposed by Ghadiri[13]. Nanotubes with eight, ten and twelve amino acid residues were formed by cyclic [-(D-Ala-Gln-D-Ala-Glu)$_2$-] subunits using the VMD visualization package and Matlab. The peptide membranes with different number of peptides lead different configurations of packing of tubes (with different diameters as well). Packing of CPNTs for two different diameters is shown in Fig. 4.10. Different diameters of CPNT are shown in Fig 4.11

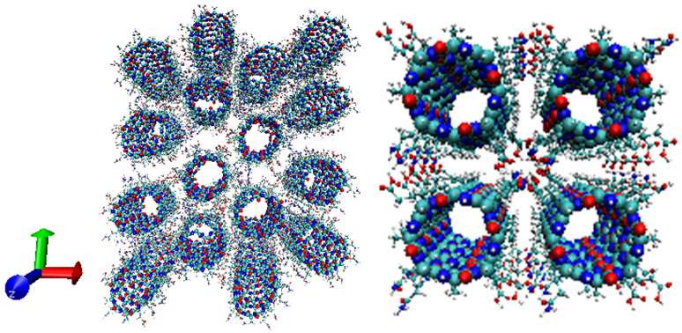

Figure 4.10. Two-dimensional Packing Arrays for 12-peptide and 8-peptide-based CPNTs.

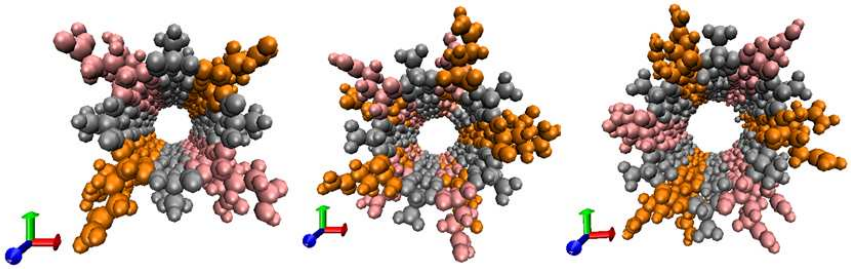

Figure 4.11. Cross Sectional View of the Peptide Nanotubes

4.3.2. Results and Discussion

For the case of Peptide nanotubes, the average water molecules of the octapeptide nanotube is 31.5, this result agrees with the results found by Engels and Co-workers[16]. They found an average of 32.8 molecules in an octa-peptide nanotube of 10 subunits, equilibrium water number for this system is shown in Fig.4.12.

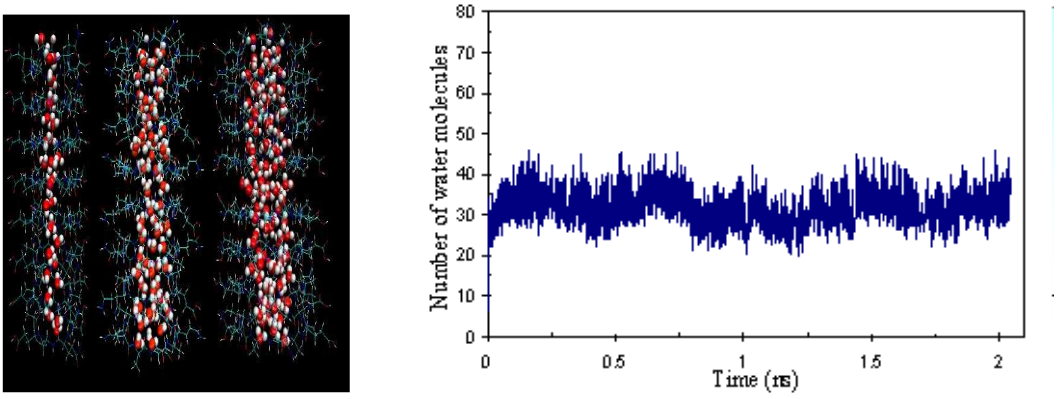

Figure 4.12. Equibrium Number of Water in octa-CPNT

The peptide nanotube shows unimodal radial distribution probability of the water molecules, as seen in Fig.4.13., the water molecules form single layer structure inside the nanotubes for the case of small diameter, for larger diameter the radial distribution becomes more even and more molecules are founded in the tubular cavity.

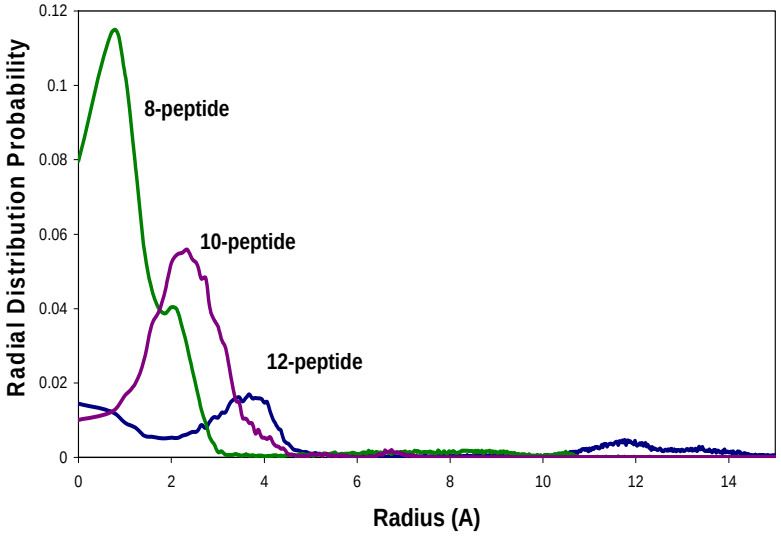

Figure 4.13. Radial Distribution Probability and Reduced Density

The reduce density along the nanotube shows the reduction of density of water molecules once they enter into the nanotube. Single file mechanism is suggested as transport mechanism for the octapeptide nanotubes; the water molecules are hopping along the axial direction under density difference as driving force. Inside the nanotube the interactions between the water molecules and the amino acids of the nanotube increases, the interactions slow down the motion of water molecules.

The axial distribution of water in the nanotubes shows that there are more zones populated than others, see Fig.4.14., it occurs between the rings because the water molecules find more space available to move, and those zones are more hydrophilic than the alpha carbon plane due to the H-bonds presence.

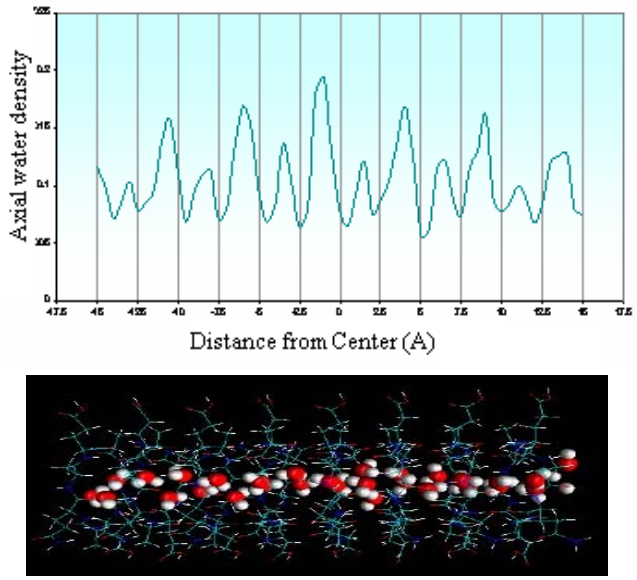

Figure 4.14. Occupancy of Water in CPNTs

The molecular diffusion is analyzed through the time evolution of the mean square displacement (MSD), as described previously for the case of CNTs. See Fig. 4.15.

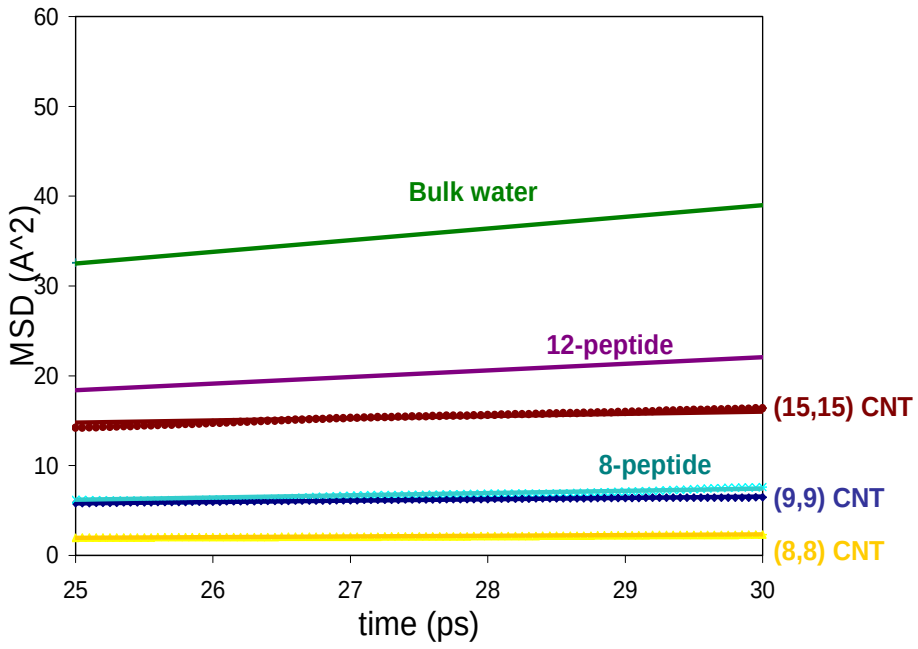

Figure 4.15. MSD Curve for CPNTs

In Table 4.2 the calculated diffusion coefficients for equivalent diameters of CNT and Peptide Nanotubes are listed. All the values were higher for the case of the peptide nanotubes.

Table 4.2. Comparison of Diffusion Coefficients for Water in CPNTs vs CNTs

System	**Diameter (A)**	**Diff. Coeff. (calc) (10^{-9} m^2/s)**
Bulk water	-----	2.17
12-peptide	14	1.23
(15,15) CNT	15	0.41
8-peptide	8.8	0.41
(9,9) CNT	8.6	0.25
(8,8) CNT	7.2	0.13

These results verify the favorable character of peptide nanotubes due to their hydrophilic tubular core compared with the hydrophobic character of the tubular core of CNT. Peptide nanotubes can constitute promising materials in areas such biotechnology and biomedicine due to their nature and properties.

The Probability of Hydrogen Bonds inside of peptide nanotube shows to be unimodal for octapeptide and the peaks tend to disappear for larger diameters, see Fig 4.16. It is very similar to the probability of equivalent diameter of CNTs. Dipole-dipole autocorrelation function was also calculated to represent the re-orientability of the water molecules inside of the nanotube (γ is the angle between dipole moments of water molecules that are separated by the distance r).

As in the case of CNTs when increasing the diameter, the hydrogen bond probability becomes more even and approach the bulk water behavior, as seen for the 12-peptide/ring nanotubes in Fig. 4.16. This behaviour is expected because the water molecules have larger available space to complete the typical hydrogen bond distribution found in bulk water. For smaller diameters the water reorientation is restricted and water movement is limited due to confinement.

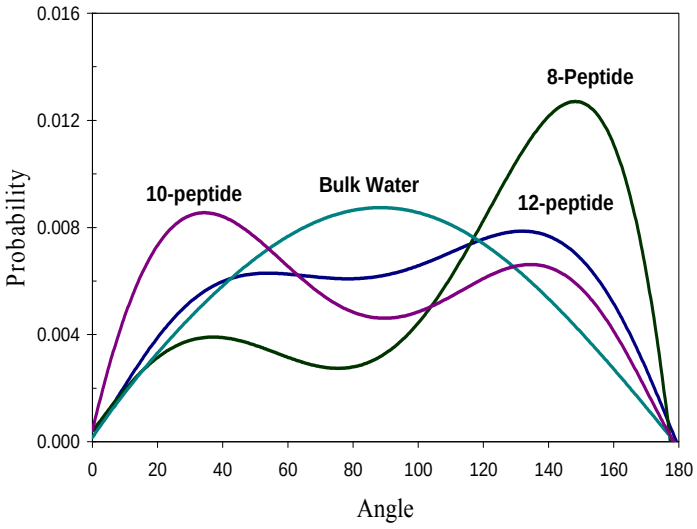

Figure 4.16. Hydrogen Bond Probability in CPNTs

Dipole-Dipole Correlations are shown in Fig. 4.17.; the curve decay faster for smaller diameters in CPNTs . Then, we can conclude that the correlations change from long range to short range when decreasing the diameter.

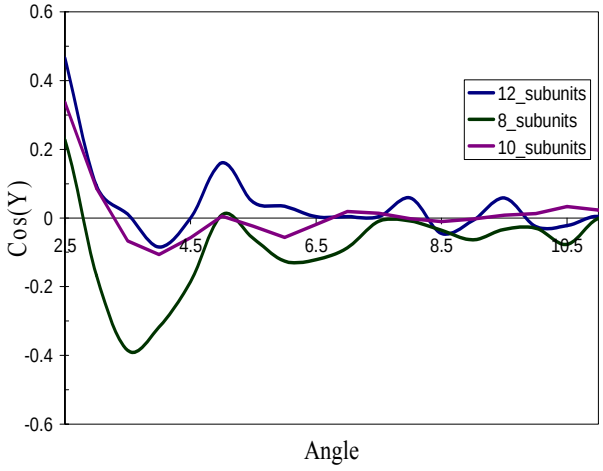

Figure 4.17. Dipole-Dipole Autocorrelation Function in CPNTs

4.5 Summary

For the case of CNTs, it was found that the water static behavior is dominated by the available space inside nanotube, which is directly related to the nanotube's diameter. Chirality and nanotube length do not have a significant effect on water dynamics within the nanotubes. Results demonstrated that the effect of nanotube length is significant for transport properties of water in intermediate carbon nanotubes. Water self-diffusion coefficient and reorientability present significant changes in these intermediate nanotubes. However, nanotube chirality does not have any influence on water dynamic behavior.

The transport of water was favored in peptide nanostructures compared with equivalent sizes of CNTs. The hydrophobic side chain interactions allow the aggregate to form a crystalline stable structure.

The more hydrophilic zones of the nanotube are located between the rings and are the more populated zones of water molecules. The diffusion mechanisms of water in the octa-peptide nanotube correspond to single file diffusion. The greater diffusion coefficients within cyclic peptide nanotubes is attributed to the hydrophilic character of the hollow tubular structure due to the high hydrogen bond density[79].

CHAPTER V
ELECTROPHORETIC TRANSPORT OF Na+ AND K+ IONS WITHIN CYCLIC PEPTIDE NANOTUBES

5.1. Overview

Cyclic peptide nanotubes play an important role as potential candidates for artificial ion channels. Experimentally, it was shown that these hollow tubular structures will conduct ions at higher rates than natural ion channels and present an alternative to antibacterial agents for therapeutic applications[17]. Fernandez-Lopez et al. demonstrated, with experiments, that cyclic peptide nanotubes can induce the death of bacteria by forming nano-scale channels in its membrane[15]. Additionally, by using coarse grained molecular dynamics simulations, the self-assembly of cyclic peptide nanotubes into lipid bilayer membranes was reported by Hwang et.al.[160]. Interesting possibilities to improve the selectivity and ion rectification exist for these artificial ion channels[161]. Due to the low molecular weight, d,l-peptides offer an attractive complement to the current natural antibiotics and represent new options against infectious diseases, bio-sensing and drug delivery applications. For this reason, it is important to understand the insights of ion transport mechanisms while engineering these artificial ion channels to be able to mimic and control the features found in biological channels. Furthermore, understanding ion transport in nano-channels is important to explore engineering applications in nanofluidics, as well as clarifying the role of intermolecular forces (between ions, water and the inner surface of channels) on transport properties under confinement effects.

Channels in cell membranes have been studied experimentally and theoretically in the past[162]. In particular, natural channels have been widely studied due to their importance in biological processes and their relation to many diseases; previous studies have focused mainly on natural ion channels, natural water channels (aquaporins) and other membrane transporter channels[85]. Two of the most important natural ion channels

are the gramicidin channel and the KcsA potassium channels. Gramicidin is known as a natural antibiotic because it can alter the electrochemical potential across cell membranes; this channel was studied by Neher and Sakmann[163], who won the Nobel prize in Physiology and Medicine in 1991 for their studies. The KcsA potassium channel was study by Mackinnon[164], Nobel prize in Chemistry 2003; in this channel the combined effects of the ion's energy and the electrostatic field of the helix give rise to selectivity for monovalent cations. Computational studies of ion transport in gramicidin have been reported by Mackay et al.[165], Jordan et al.[166,167], Roux et al[168], Chiu et al.[169] among many others. For the case of KcsA channel, Fowler et al. investigated K+ selectivity via molecular dynamics (MD)[170], Noskov et al. studied the effect of carbonyl groups[171] and hydration[172] in K+ selectivity via molecular dynamics, Cordero-Morales et al. studied the molecular driving forces important in the KcsA inactivation mechanisms via MD simulations[173]; other computational studies have also contributed to understanding the mechanisms of transport in the KcsA channel[87,174-176]. On the other hand, continuum dynamics methods have been used to study ion transport in membranes with the Poisson-Nernst-Plank (PNP) theory[82,177,178]; however to study nanofluidic transport in scales smaller than 5 nm, molecular dynamics methods are generally preferred due to different confinement effects[179].

Molecular dynamics simulation is one of the best methods available to elucidate ion channel mechanisms; however, in order to achieve a complete description, it is necessary to design simulations that are long enough to observe ion translocation. Also, it is important to choose a realistic and appropriate potential function to represent the ion-channel, ion-solvent and solvent-channel interactions properly and ideally the influence of typical potentials across cell membranes have to be included for a complete representation. Molecular dynamic simulations have revealed key information and principles about selectivity and transport in membrane channels, this technique provides details that are currently not easy to obtain experimentally due to the spatial and temporal resolution required for the analysis.

Previously, Lynden-Bell et al.[180] studied transport properties of ions and

uncharged molecules in nano-channels; they investigated the influence of water in ion transport at room temperature and calculated free energy profiles for different diameters of the channel. His work suggested that ion dynamics inside nanopores is affected by the non-uniform water density distribution and ionic hydration. Quiao et al.[181] carried out molecular dynamics simulations of electro-osmotic transport of NaCl solutions in carbon nanotubes (CNTs) with different surface charges. They observed that the dependence of electro-osmotic transport on the surface charge was significantly different from the results obtained using conventional continuum theories. Tang et al. reported molecular dynamics simulations for the transport properties of KCl electrolyte solutions in a nanopore, showing the influence of confinement through the decrease of ion hydration as well as in hydrogen bonding and a strong influence of electric field magnitude in the orientation of water molecules[182]. Dzubiela et al. conducted MD simulations of water and ion permeation controlled with applied electric fields through a nanopore[183]; they found that the transport, density and structure of water are highly dependent on the field intensity. Hu et al.[84] studied the electrophoresis of water and ions in protein crystals via non-equilibrium molecular dynamics; the effect of electric field in coordination numbers of ions and stability of the protein crystals was reported.

Studies including the effect of electric field in membrane channels are important because the permeability and diffusion rate of molecules can be enhanced and manipulated. This enhancement has been proposed for potential applications like drug delivery, cancer treatment and gene therapy[84]. Then, the study of ion transport under the influence of electric field can lead us to possible manipulation of ion rates as well as induced open-closed states for the artificial ion channels.

The first work in which cyclic peptide nanotubes were considered as artificial ion channels was reported in 1994 by Ghadiri et al.[17]. They measured ion channel conductance for Na+ and K+ to be up to three times faster compared with the Gramicidin channel. The first computational studies on ion transport in peptide nanotubes were reported in 2006 by Hwang et al.; this group performed steered molecular dynamics simulations where the potential of mean force for a single ion

passing through CPNTs was calculated. The results showed energy barriers of around 2.4 kcal/mol at the channel entrances and energy wells in the middle of the tube[81]. In addition, they also studied ionic transport in CPNTs with sequences of eight and ten cyclo[(-l-Trp-d-Leu-)4] using the PNP continuum theory. The results indicated agreement of ion currents curves, compared with experiments for low ion concentration, and overestimation for high concentrations[82]; in addition, limitations of PNP theory for these systems were discussed. Dehez et al. studied free energy profiles for one sodium ion transported in a peptide nanotube. It was found that the ion permeation depends on the nanotube structure and the location of the open-end of the channel with respect to the membrane surface where it is inserted[184].

In this chapter, the theoretical investigation of cyclic peptide nanotubes as candidates for artificial ion channels is investigated via molecular dynamics simulations; dynamic properties for transport of Na+ and K+ are studied through statistical thermodynamics analysis (mean square deviation curves), and structural analysis was performed via radial distribution functions and the estimation of coordination numbers; additionally, the influence of electric field and temperature in the motion and hydration of ions within these CPNTs was investigated for the first time to the best of our knowledge.

5.2. Computational Details

The cyclic peptide nanotubes model was constructed in agreement with the 12-peptide/ring model synthesized by Ghadiri et al.[4]. These peptide tubes present a radius of 13 Å and a channel length of 37 Å. The tubes were solvated in a 0.5 M solution of NaCl and KCl respectively. Periodic boundary conditions were used in all directions. The long-range electrostatic interactions were evaluated using the Particle Mesh-Ewald (PME) method. Simulations were performed using the NAMD2.6 software with the CHARMM force field. The system was initially minimized, and then it was equilibrated using NPT dynamics at 300K and 1Bar for 0.5 ns. Finally the electric field was applied

and ion transport was simulated for 10 ns in the Canonical ensemble (NVT) at 300 K. Analysis for the calculation of mean square deviation curves was carried out for the last nanosecond of the simulation. The integration time step was 1fs. The electric field was applied along the z direction and the applied field varied from 0.1, 0.2, 0.3, 0.4, to 0.5 V/nm. These values were chosen in accordance with previous studies for electrophoretic motion of ions in protein crystal channels[84].

5.3. Stability of CPNTs under electric field

The stability of the peptide nanotubes under electric field was maintained up to 0.4 V/nm; for the case of 0.5 V/nm the Root Mean Square Deviation (RMSD) increased drastically as shown in Fig.5.1.a. After this analysis, it was decided to keep the cyclic peptide nanotubes constrained and only water and ions were allowed to move for all of the ion transport simulations presented here.

a. 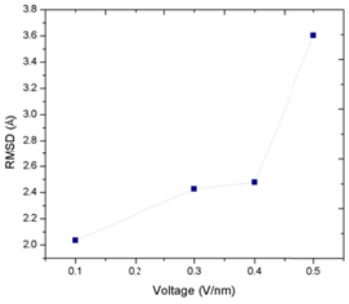

b. 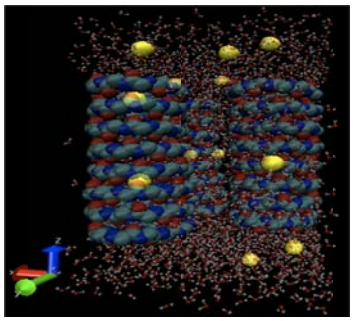

Figure 5.1. a) RMSDs Curves for CPNTs under Electric Field, b) Ionized CPNTs

5.4. Diffusion of Na+ and K+ within CPNTs

For all simulations it was observed selectivity for cations over the anions (Cl-) for the transport inside the cyclic peptide nanotubes. The positive ions start diffusing into the nanotubes after equilibration and application of the electric field in z direction. Translocation occurs in different stages as suggested by Hwang et al.[81], depending on the

position of the ion in z direction: First the ion is in one of the bulk water cavities and surrounded by water molecules. Here, the first energy barrier (known as dielectric barrier) is encountered as the ion experiences a desolvation of some waters present in the hydration shell. However, for this particular case, the nanotube has relatively large diameter (13 Å), and the energy penalty is expected to be smaller compared with channels of lower diameter. Second, when the ion is inside the nanotube it can be located in two zones: between the two rings or in the plane of the ring. In the plane of the ring the positive ion will experience attraction forces from the negatively charged carbonyl groups of the peptide backbone, between the two rings this force should be weaker and interaction with water may be stronger due to the larger population of water in these zones (Chapter IV). Finally at the exit, the ion overcomes the final energy barrier and reaches into bulk water and complete solvation again. See Fig. 5.2. for a schematics of the process described above.

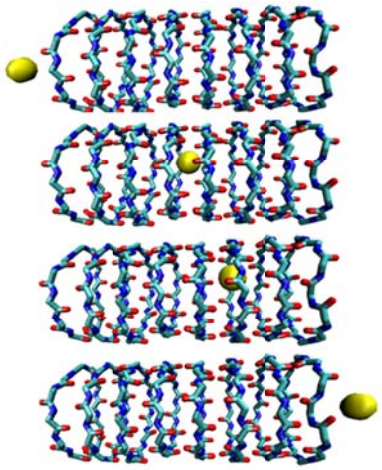

Figure 5.2. Stages of ion Transport within Cyclic Peptide Nanotubes in Backbone Representation

For the calculation of the diffusion coefficients, the Einstein's relationship and the mean square deviation curves (MSD) were used for both (Na+, K+) ions; the mean-square displacement of the ions along z was calculated as follows:

$$MSD_z(t) = \left\langle \frac{1}{N} \sum_{i=1}^{N} (z_i(t) - z_i(0))^2 \right\rangle \qquad (5\text{-}1)$$

where N is the number of ions permeating the channel, t is time of a translocation event and z_i is the position of ion i along z. Initial inspection of the results shows that the mobility of Na+ is higher than K+. The calculated diffusion coefficients are in good agreement with diffusivities previously calculated in equivalent sized protein crystals channels[84]. In Fig 5.3. and Fig 5.4. the comparison between transport of Na+ versus K+ is shown for E=0.5V/nm; all other applied fields revealed the same trend, and the calculated diffusion coefficients are shown in Table 5.1. For the Cl- ions, no translocation events were recorded, this behavior is explained due to repulsive electrostatic interactions between the anion and the inner surface of the peptide nanotubes.

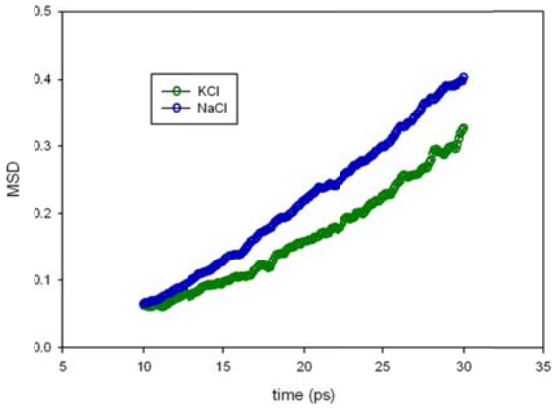

Figure 5.3. Comparison of MSD Curves for Different Ionic Species at $E_{0.5v/nm}$

Table 5.1. Comparison of Diffusion coefficients of Na+ and K+

Ion	Dion (10^{-9} m^2/s)
K+	0.0699
Na+	0.0895

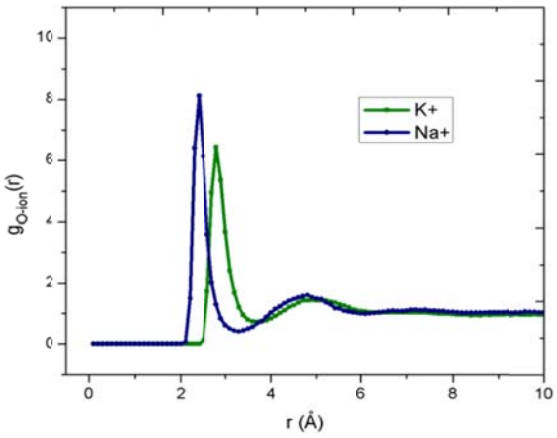

Figure 5.4. Comparison of Radial Distribution Functions for Na+ and K + at $E_{0.5v/nm}$

Understanding hydration interactions of ions under confinement is important because it can be an important factor for the translocation rate of ions. Hydration can be associated with the increase of enthalpy required to break the ion-water interactions in solution and facilitate the ion transport within the nano-channel.

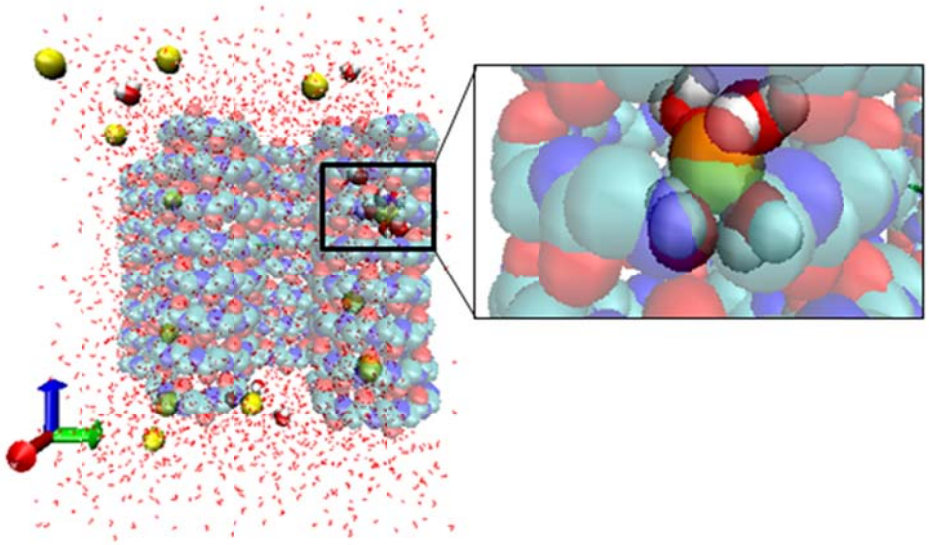

Figure 5.5 Water-Ion Interactions inside the Cyclic Peptide Nanotubes. First Hydration Shell is shown for Na+

The first hydration shell of the ions within the peptide nanotubes can be analyzed through the radial distribution function between the ion and the oxygen of the water molecules. The radial distribution function ($g_{O\text{-}ion}(r)$) represents the relative number of water molecules around a distance r from the ion in the channel. In the cyclic peptide nanotube, the first peak in the radial O-Na+ distribution function is located at 2.27 Å and the second is at 4.75 Å. In the case of K + the first peak in the radial O-K+ distribution function is at 2.82 Å, and the second peak is located at 4.60 Å. Water forms the first hydration layer of thickness of ~ 0.32 nm for Na+ and of ~0.35 for K+; this value correspond to the r of the first minimum in the $g_{O\text{-}ion}(r)$ function. It can be observed in Fig. 5.5 that the oxygen of the waters is pointing toward the ion. This is because around cations, the waters are oriented in such a way that their dipole moments lie in the same line with the cation charge. In the obtained result, a change in the maximum value

of the ion-water radial distribution function was observed, see Fig.5.6. This behavior indicates a small effect in the ion-water interaction due to variations in intensity of the electric field.

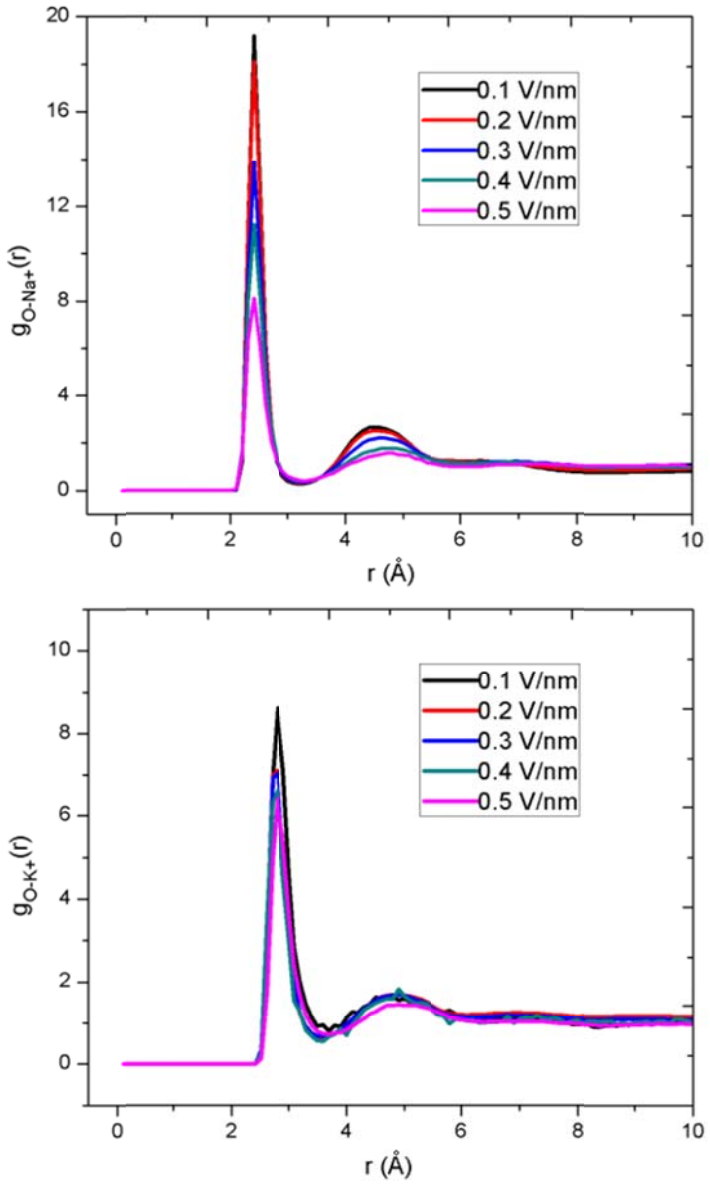

Figure 5.6. Radial Distribution Function Comparison, water-Na+ Interaction (top) & OH2-K+ Interaction (down)

Additionally, the coordination numbers (hydration numbers) were calculated by integrating the radial distribution function up to the fist minimum, which is the area under the first peak. The coordination number for this case can be calculated from:

$$N_{water}^{ion}(r) = 4\pi\rho \int_{0}^{r\min} g_{O-ion}(r) r^2 dr \qquad (5\text{-}2)$$

where ρ is the number density of water and $g_{ion\text{-}O}$ is the radial distribution function.

The coordination number did not change significantly for different applied electric fields. In the case of zero field, the coordination number was 5.8 for Na+; and 7.1 for K+. The coordination number or hydration number is plotted in Fig.5.8. for all values of electric field, and in both cases little effect was observed for different fields. Also, the calculated values are very close to the coordination number in bulk water. These values are in good agreement with previous electrolyte studies in nanopores[87]. Table 5-2. shows a comparison of coordination number for Na+ and K+ in different channels and bulk water and Fig. 5.7 shows an axial view of the hydrated ion.

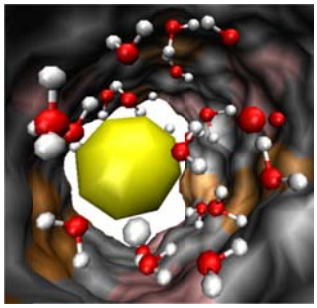

Figure 5.7. Axial snapshot of Na+ within CPNT and Waters up to the Second Hydration Shell Radius (~ 6 Å from the ion)

Table 5.2. Coordination Numbers of Na+ and K+ in Different Nanopores

System	*Na+*	*K+*	*Ref.*
Bulk water	5.9	6.9	(2003)[185]
CPNTs	5.8	7.1	This work
CNTs	4.9	8.0	(2008)[186]
KcsA	6.0	6.7	(2003)[87]

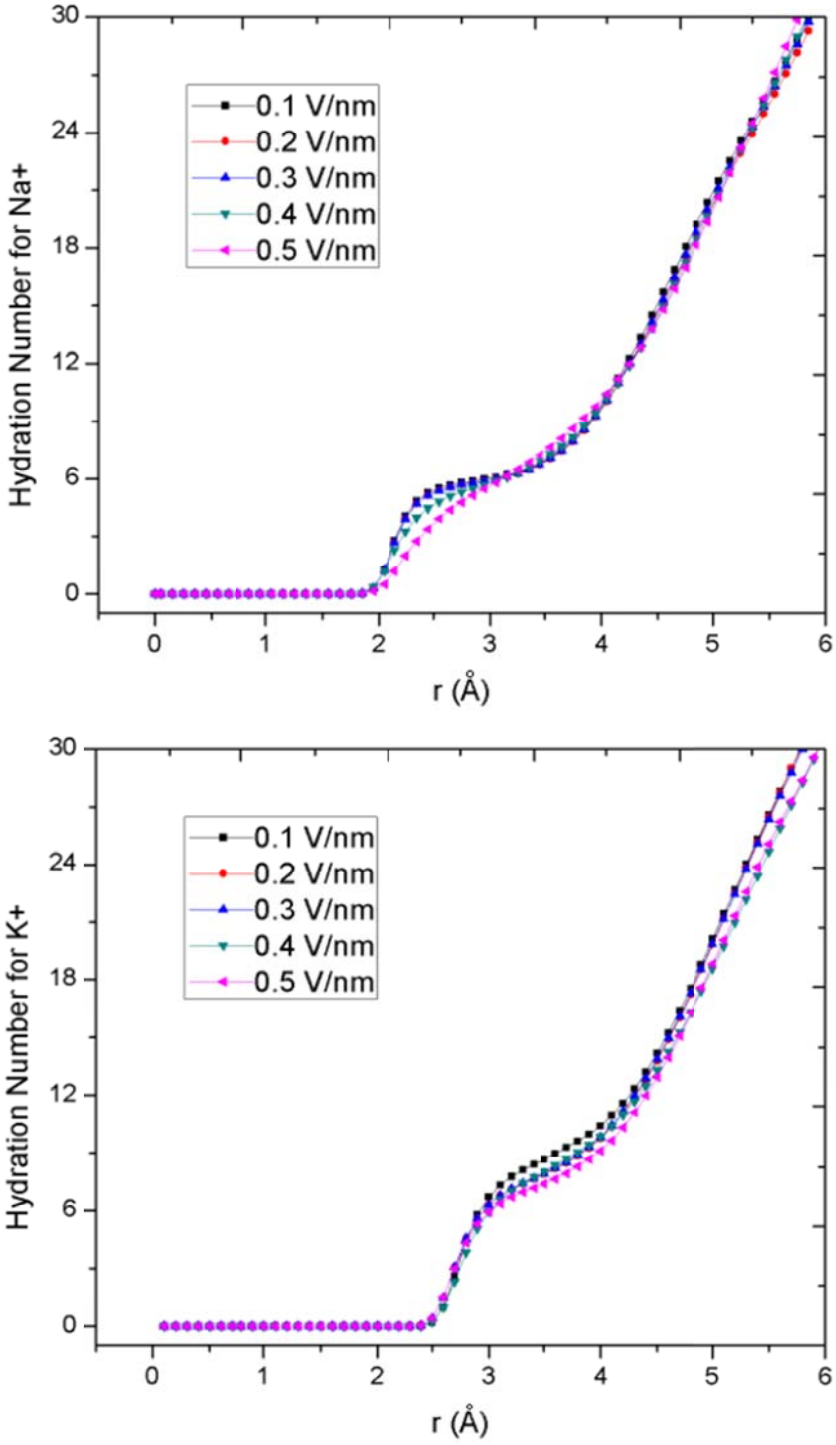

Figure 5.8. Hydration Number for Na+ and K+ in CPNT under the Influence of Different Electric Fields

For the calculation of the diffusion coefficients, first the z coordinates are recorded for all ions during the simulation. The analysis is carried out with the z coordinates values inside the nanotubes through translocation times. The MSDs are averaged over the total number of permeation events. Results are shown in Fig. 5.3. The calculated diffusion coefficients are given in Table 5-3 below.

Table 5.3. Diffusion Coefficients at Different Electric Fields for Na+ and K+ Transport at 300K

Efield (V/nm)	D_{Na+} (10^{-9} m^2/s)	D_{K+} (10^{-9} m^2/s)
0.1	0.0001	ND
0.2	0.0007	0.0009
0.3	0.0183	0.0016
0.4	0.0526	0.0205
0.5	0.0895	0.0699

5.5. Current – Voltage (I-V) Relation

Current-voltage curves can be obtained from the MD simulations. The ionic current is calculated as described in the equation below, the charge (q_i) and position (z_i) coordinates are recorded from the MD trajectory:

$$I(t) = \frac{1}{\Delta t L_z} \sum_{i=1}^{N} q_i [z_i(t + \Delta t) - z_i(t)] \qquad (5\text{-}3)$$

To compute an average current, we first integrate the instantaneous current I(t) to produce a cumulative current curve as in the method proposed by Schulten et. al.[187].

The current voltage relation for Na+ ion, Fig.5.9, shows that for higher electric fields the current value increases exponentially and more ions go through the peptide nanotubes with time. Values are reported in Table 5.4.

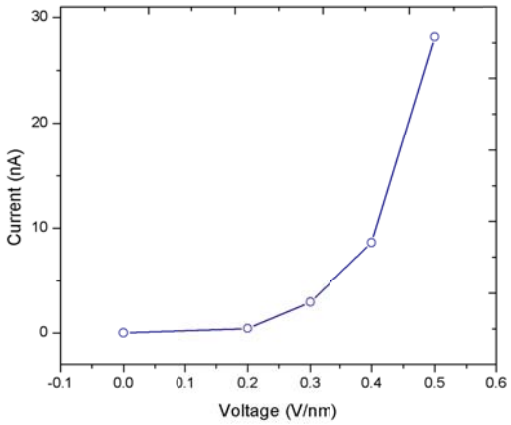

Figure 5.9. Current-Voltage Curve for Na+

Table 5.4. Current-Voltage Values Calculated from MD Simulations for Na+

Voltage (V/nm)	Current (nA)
0	0.00
0.2	0.42
0.3	2.95
0.4	8.64
0.5	28.19

5.6. Temperature Effects

It has been proven that the orientation of water molecules and the coordination number of an ion can be influenced by temperature in nano-channels[186]. Here, the effect of temperature was investigated for the Na+ transport within CPNTs; all simulations were performed at two temperatures (300K, 500K). The diffusion rates are higher for 500K, and the diffusion rate for the cation is increased for 500K as shown in Fig.5.10a, However, the size of the first ionic hydration shell does not seem to be affected with the increase of temperature; as it is observed in the Fig.5.10.b, the peak (r) positions of the radial distribution function are unchanged for the two different temperatures. For all the other electric field values the same trend was observed for the radial distribution function and the MSDs curves. The height of first peak in the radial distribution function decreased when the temperature increases, it is in accordance with the tendency in bulk solutions[186].

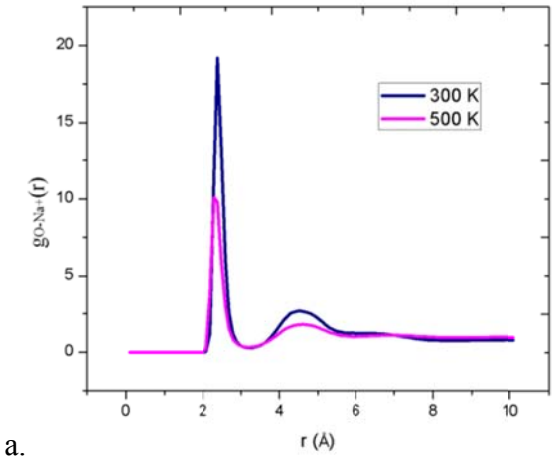

a.

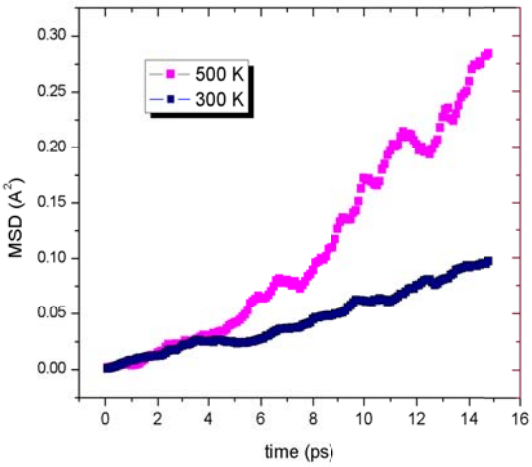

b.

Figure 5.10. Temperature Effect on Na+ transport (top) $g_{(o\text{-}Na^+)}(r)$ (bottom) MSDs Curves, 0.5V/nm

Results of diffusion coefficients calculated at 500K are listed in Table. 5.5. As observed in the case of 300K, there is an increase of diffusion rate as the applied electric field increases. The mean square displacement curves and radial distribution functions for 500K are shown in Fig. 5.11.

Table 5.5. Diffusion Coefficients of Na+ for Different Electric Fields at 500K

Efield (V/nm)	**D** (10^{-9} m^2/s)
0.1	0.0035
0.2	0.0095
0.3	0.0150
0.4	0.0461
0.5	0.0983

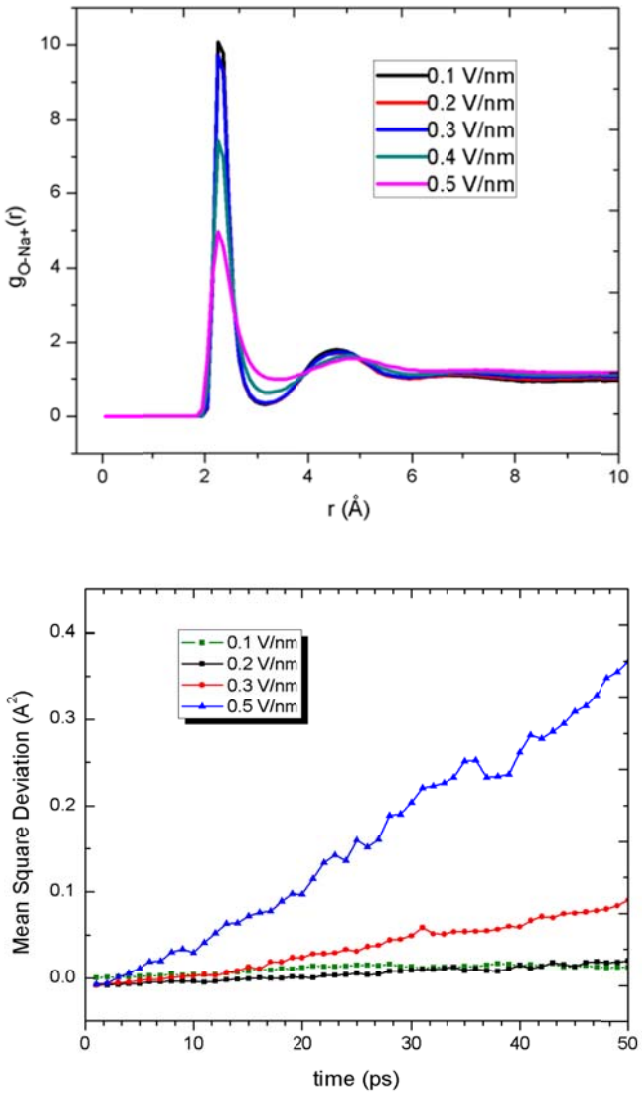

Figure 5.11. Radial distribution function (top) and MSDs (bottom) Curves for Na+ at 500K and Different Electric Fields.

5.7. Summary

The results presented here show the motion of ions within CPNTs under the influence of electric fields. This scenario is important to be able to mimic conditions of cell membranes, which are naturally polarized due to differences in concentration of ions across them. Also, we can predict diffusion rates as a function of externally applied

fields for design and manipulation. Selectivity for cations was observed for all simulations. The chlorine ions did not go through the peptide nanotubes. Then, counter-ion interactions are eliminated in these systems and the channel can transport higher number of positive ions. This may be explained as a consequence of a strong repulsion force experienced by the anion due to the oxygen present in the backbone of the rings forming the nanotube.

One of the limitations of using molecular dynamics for ion channels studies is that long simulations are required (at least 10 ns) to observe ion transport through the nanochannel. No experimental data has been reported for these peptide nanotubes; however the calculated diffusion constants are in the same order of magnitude compared with previous reported values for similar diameter of protein crystals[84].

With the aim of studying the ion-channel interaction under the effect of different electric fields, **t**he radial distribution functions between the oxygens of water and ion within the CPNTs and coordination numbers were analyzed. The first and second peaks in the radial of the ions-water distribution functions were reduced when external electric fields applied. However, the position of the peaks was unaltered, and no effect was observed on the coordination number. This can be explained as a result of the larger diameter of the 12-peptide nanotube studied here. As indicated in Chapter III, this diameter of the peptide nanotube approaches bulk behavior, and there is enough free space available to achieve larger densities of water inside the nanotube compared with the octa and deca-peptide nanotubes. In smaller channels the effect in coordination number can be expected to be more noticeable due to confinement effects.

The 12-peptide/ring nanotube studied here has proved to work as an artificial ion channel and will have larger available space for the transport of molecules and biosensing applications while still keeping important inner-surface electrostatic forces, important for selectivity. These results provide insights about ionic transport in CPNTs and are expected to contribute to future manipulation of transport rates for biotechnology applications of these artificial ion channels.

CHAPTER VI
MOLECULAR ORGANIZATION OF PHENYLALANINE (F) DIPEPTIDES NANOSTRUCTURES

6.1. Importance of Phenylalanine Peptide Nanostructures

The phenylalanine dipeptide is the core recognition motif of the Alzheimer's β-amyloid, it can also self-assemble into stable peptide nanostructures with different morphologies[36]. Because of this , it has become one of the most important and recently studied peptide building blocks.

In 2003, while investigating the tendency of short aromatic peptides to form amyloid fibrils, Gazit et.al discovered that stable and stiff peptide nanotubes were formed from phenylalanine dipeptides[21] (NH_2-Phe-Phe-COOH). This research group also suggested that aromatic interactions play an important role in the self-assembly process and can favor stable molecular organization of peptides into amyloid fibrils[188].

The phenylalanine dipeptide (FF) nanotube was first synthetized by dissolving the diphenylalanine peptide monomer in 1,1,1,3,3,3-hexafluoro-2-propanol (HFIP) at high concentrations (≥100mg/mL) and then diluting this into an aqueous solution at a final μM concentration range; fast assembly was observed[21].

An alternative method avoiding the use of the fluorinated alcohol was proposed by Song and co-workers in 2004; first a lyophilized dipeptide (HN_2-D-Phe-D-Phe-COOH) was dissolved in 5 mL water at 65 °C; the solution was equilibrated for 30 min and then gradually cooled down to room temperature. They also demonstrated that the concentration of the building peptides plays a key role in the final nanostructure morphology, when for diluted solutions, vesicles were observed in addition to the nanotubes[189], see Fig. 6.1.

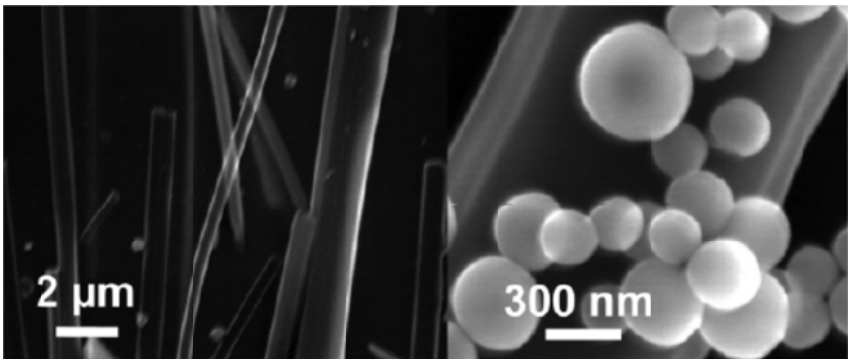

Figure 6.1. SEM Images (left) Peptide Nanotubes and (right) Mixture of Nanotubes and Nanovesicles

Investigations for the molecular structure, chemical, physical and thermal stability are important in the development of future applications of these peptide nanotubes. In 2006, Adler-Abramovich and co-workers studied their chemical and thermal stability in aqueous solution and under dry conditions; by SEM analysis they showed how the FF nanotubes were chemically stable in organic solvents such as ethanol, methanol, 2-propanol, acetone and acetonitrile[34]. Thermally the nanotubes were stable up to 100°C; for temperatures above 150°C the tubular and secondary structure was altered and the nanotubes were degraded to the original dipeptide building blocks[190]. Recently, stability up to 200°C was reported for diphenylalanine/polyalanine core/shell peptide nanowires[191]. Also, the fabrication and application of diphenylalanine/Co_3O_4 composite nanowires as novel materials for energy storage was demonstrated[39].

In order to enable the technological applications of FF peptide nanotubes, it is necessary to be able to control their molecular organization. Reches and Gazit reported the first attempt in 2006. They achieved vertical alignment of FF nanotubes by applying the FF peptide monomers dissolved in the organic solvent onto siliconized glass; they also were able to align horizontally the FF nanotubes by assembling the phenylalanine dipeptide monomers in the presence of a ferrofluid and then exposing formed nanotubes to an external magnetic field[192]. Later, it was reported that thanks to the magnetic torque on the structure generated by the diamagnetic anisotropy of the aromatic rings, it is possible to align the FF nanotubes by applying a magnetic field without additional treatments[193]. Recently a vapor deposition method[42] was developed to generate self-

assembled arrays of aligned peptide nanotubes, which showed how peptide nanotubes can easily be produced at larger scales as well as their potential to be used to develop highly hydrophobic self-cleaning coatings, new electrodes for energy storage applications, and microfluidic chips[42].

6.1.1. Molecular Organization of FF Nanotubes

The molecular organization of FF nanotubes is not completely understood yet. This problem is particularly important because the molecular forces stabilizing these nanotubes and directing the self-assembly may be related to the forces present in amyloids. Transmission Electron Microscopy (TEM) studies indicated that the structures of FF nanotubes were well-ordered elongated nanotubes with no branching and low content of amorphous aggregates (<1%), which is in contrast to other peptide aggregates in which a mixture of ordered and aggregated structures are frequently observed. Görbitz determined X-ray powder diffraction patterns for FF nanotubes and proposed a tentative model for their molecular structure. In his model, the aromatic groups generate a three-dimensional aromatic stacking arrangement serving as a glue between the hydrogen-bonded cylinders of peptide main chains[47]. It was also suggested that exceptional strength could result from the laminated construction of the peptide nanotube. However, the exact configuration of the inner dipeptide arrangement into nanotube crystals suggested in the model proposed by Gorbitz has not been well elucidated yet[47]. In this model, six diphenylalanines form each tube in the crystal with the aromatic groups pointing outward and the peptide termini pointing toward the center of the tube . The crystalline information suggests that it could be possible to use only two diphenylalanines as the tube's thickness to create the peptide nanotube[194].

In this research work, different configurations and orientations of the phenylalanine dipeptide, leading to stable tubular structures, were investigated. A geometrical search combined with fist principle molecular simulations were used to optimize parameters that have resulted in a stable structure. The thermal stability was also explored by NVT and NPT molecular dynamics simulations.

6.2. Computational Details

All simulations were performed using NAMD2.6 and the CHARMM force field. Time step of integration was 1fs. The SHAKE/RATTLE algorithm was imposed for fixing the O-H bonds during evaluating the equations of motions. For the evaluation of electrostatic interactions Particle Mesh Ewald (PME) algorithm was used.

6.3. Two-dimensional Structures from Phenylalanine

6.3.1. Sheet Configurations of Phenylalanine Dipeptide

The basic peptide subunit was built from two dipeptide monomeric blocks and the dipeptides were arranged in accordance with an optimized model reported previously[194]. Two dimensional planar sheets where built by defining the position of the center of mass of each subunit along a sheet characterized by the parameters (*n, m, a, b*, and β) ; where a is the unit cell lattice value in x direction, b is the unit cell lattice value in y direction, n and m are the number of repetitive units in x and y direction respectively and β is the angle between the unit vectors along the unit cell lattice directions. After assigning different a,b values and performing an initial molecular minimization, the optimized unit cell lattice values were calculated, the values found are a=6.8 Å and b=10.1 Å, which are in close agreement with a previous study[194]. The angle β was kept equal to 90 degrees. In Fig. 6.2. below is shown the planar structure for the optimized lattice; the different parameters assigned and final energies are shown in Table.6.1.

Table 6.1. Sheet Configuration Parameters for di-Phenylalanine

Parameter	System A	System B	System C (optimized)
a (Å)	7.0	7.0	6.8
b (Å)	10.1	9.8	10.1
Energy/unit cell (Kcal/mol)	-99.94	-138.65	-148.77

After minimization, only the optimized system rearranged in a uniform lattice, in the A and B systems, described in Table 6.1. the unit cells did not show a compact

packing as in the optimized system. Also, this system had the lowest normalized energy/unit cell.

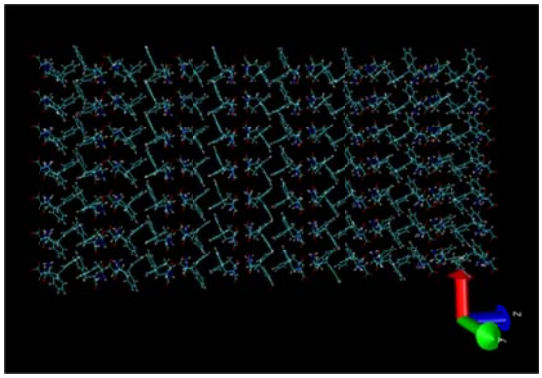

Figure 6.2. Molecular Structure for 2-D Sheet from Phe

6.3.2. Ring Configurations of Phenylalanine Dipeptide

Planar ring conformations from the described unit cell were also studied; for this geometry, two different orientations of the peptide backbone were used, the first one in which the unit cell contains the dipeptides parallel to the z axis of the ring and the second, with the peptide backbones perpendicular to the z axis of the ring, as shown in the Fig 6.3. below.

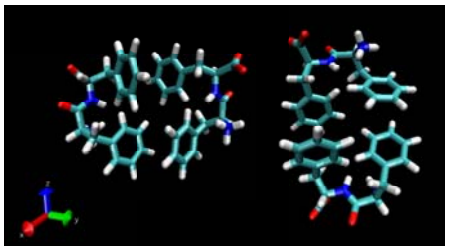

Figure 6.3. Two Different Orientations of the Phe-Phe Unit Cell

The rings were built by assigning the positions for the center of mass of the unit cell to a point along the ring with parameters (l, and r), where l is the spacing between adjacent units cells in the ring and r is the radius, translation and rotation operations were applied to the coordinates of all atoms contained in the cell. As in the 2-D planar

sheet case, these parameters were optimized in order to obtain a low energy configuration and an ordered peptide arrangement within the ring. The positions are assigned first, calculating the angle corresponding to the circular segment $\theta_0 = l/r$ and the number of segments (unit cells) that will be forming the ring is calculated as $n = 2*\pi/\theta_0$, then coordinates translated and rotated for all atoms in the unit cell to the new coordinates (x,y), where: $x = r*\cos(\theta_0 * k)$, $y = r*\sin(\theta_0 * k)$ and k is the unit number (this step is repeated for all n unit cells). Table 6.2 list the configurations studied for radius of 25 Å and the optimized structure (system 3).

Table 6.2. Ring Configuration Parameters for di-Phenylalanine

System	l (Å)	n	Energy/cell (Kcal*mol^{-1})
1	7.85	20	-111.5
2	8.73	18	-88.06
3	11.22	14	-141.9

The final structure of the system number 1 (see Table 6.2.) was completely destroyed after minimization; a stable structure configuration after the simulation was found for r=25 **Å** when 14 units were equally distributed in the ring. The molecular structures for the three systems before and after the minimization are shown in Fig. 6.4.

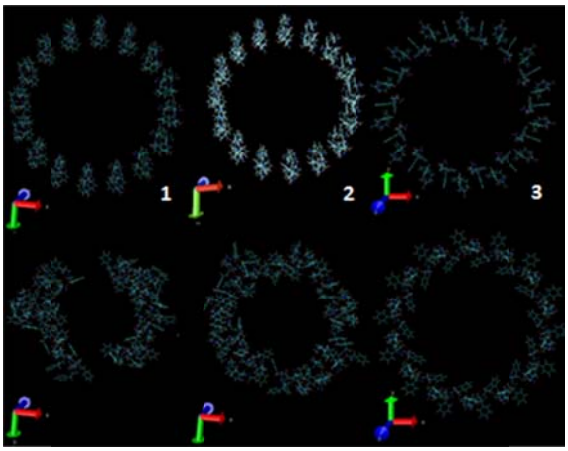

Figure 6.4. Molecular structure before (up) and after (down) energy minimization.

Additionally, double layer rings were created to explore the feasibility of double wall peptide rings or nanotubes. The double layer structure was unstable after minimization, see Fig.6.5. This instability needs to be further explored.

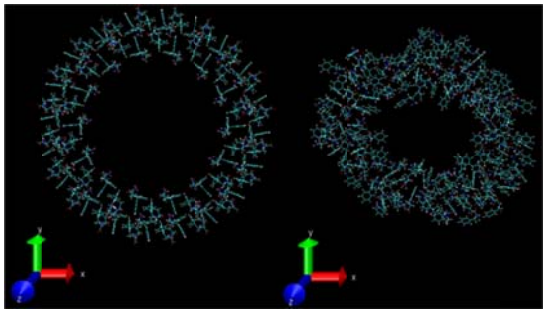

Figure 6.5. Molecular Structure before (left) and after (right) Energy Minimization

6.4. Peptide Nanotube Structures from Phenylalanine

The tubular structures were constructed as stacking of the planar rings; two and four rings were stacked along z direction to check the stability of the tubular structure. After taking the optimized ring structure and optimizing the tubular structure formed by four rings, the minimization leaded to a stable configuration. After obtaining stable tubes, periodic boundary conditions were applied in z direction to represent infinite nanotubes. The peptide backbone orientated in a helical distribution, after minimization of three different diameters (25 Å, 50 Å and 100 Å); structures for the optimized phenylalanine nanotubes are shown in Fig.6.6:

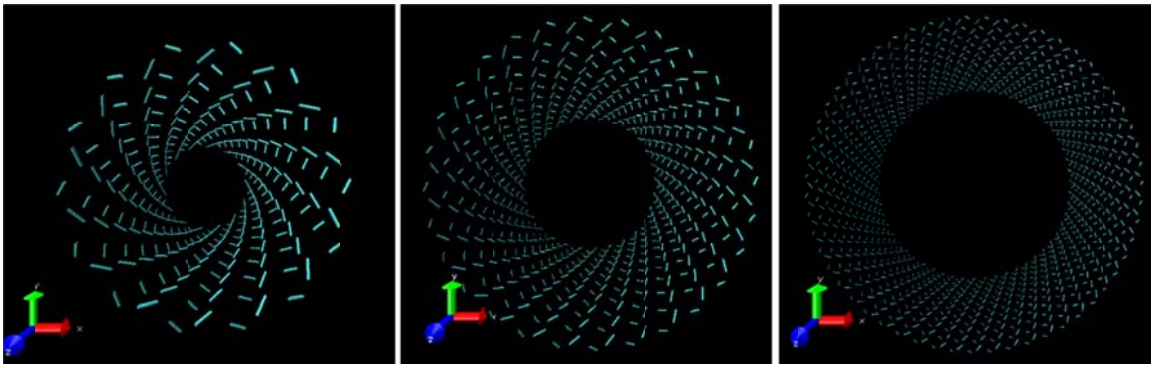

Figure 6.6. Optimized Tubular Structures for Radius of 25 Å, 50 Å and 100 Å

After minimization, the three tubes showed a helical distribution of the peptide backbone. All three tubes remained stable after minimization for 50 ps (50000 steps) in the NPT ensemble during molecular dynamics simulations performed with NAMD2.6 and the CHARMM force field. Periodic boundary conditions were used; the tube was replicated infinitely in z direction. Minimization curves are shown in Fig.6.7.

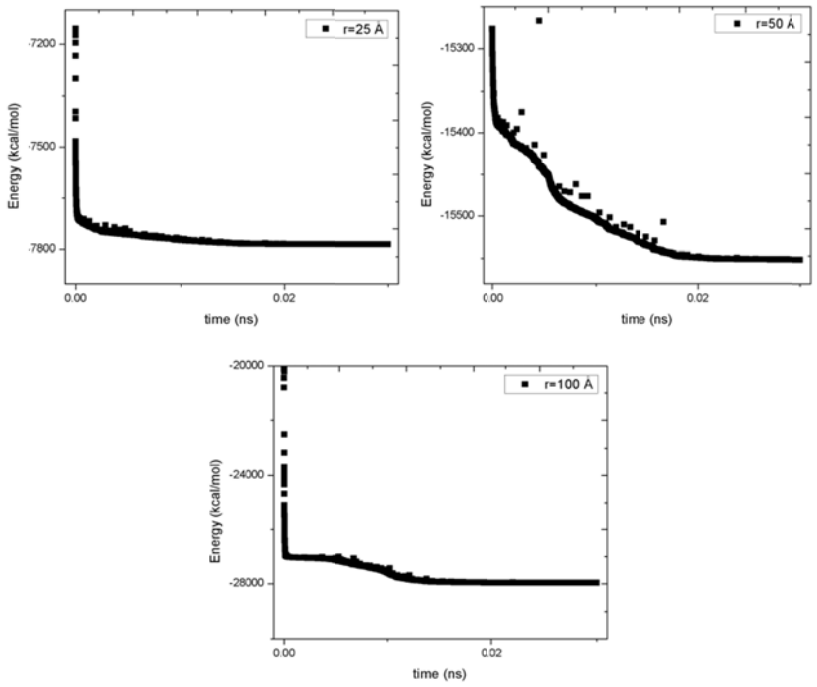

Figure 6.7. Energy Minimization Curves for 25 Å, 50 Å and 100 Å tubes

Fig. 6.8 shows the optimized structures for the three diameters 25 Å, 50 Å and 100 Å.

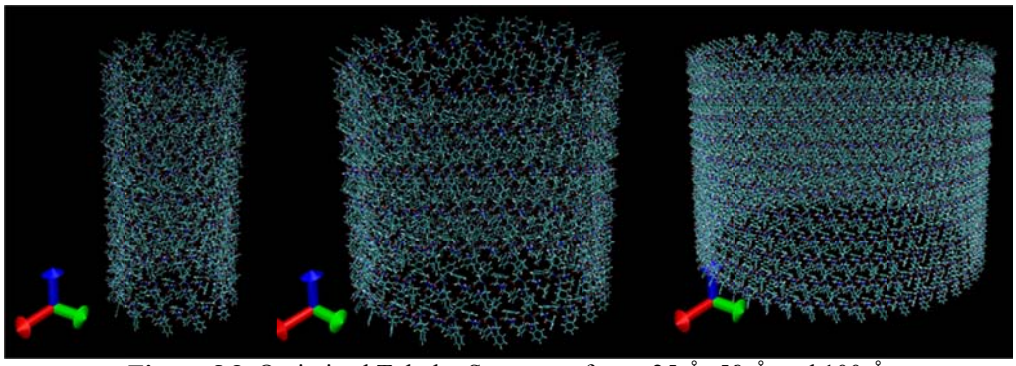

Figure 6.8. Optimized Tubular Structures for r= 25 Å, 50 Å and 100 Å

The normalized energy was calculated for the three different diameters and three lengths of the nanotubes. Results are plot in Fig.6.9.

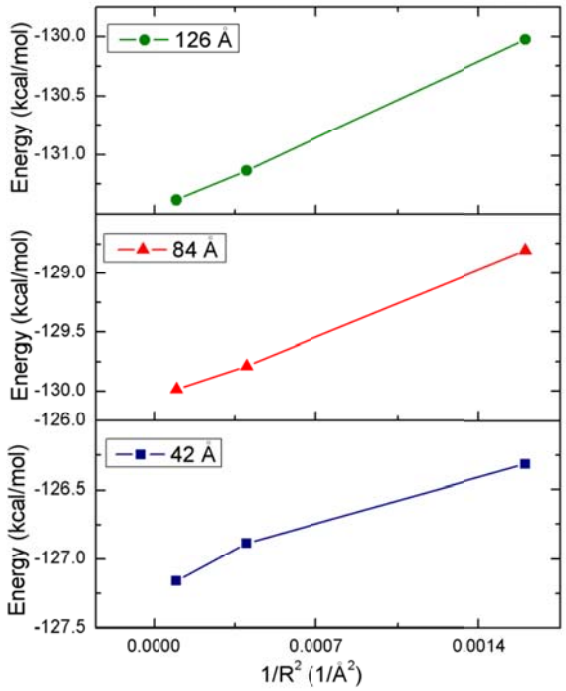

Figure 6.9. Strain Energy as Function of $1/R^2$ for Bending Modulus

In order to perform molecular dynamics with correct periodic boundary conditions applied, it is necessary to analyze the chirality of the tube and determine what would be the correct number of rings in z direction that will match the helicity of the structure without introducing strain to the system. A preliminary calculation of the bending modulus, using the method described by Gao[120], gives $\kappa = 7.1$ GPa.

Chirality analysis for the phenylalanine dipeptide nanotube

The position of an individual phenylalanine peptide was tracked and the angle with respect to the original angle for the Ring configuration of system number 1, specified in Table 6.2., was plotted. There was a linear relation between the angle and the ring number (which is proportional to the Z coordinate). In Fig. 6.10 are shown the

structures and Fig.6.11 show the absolute values of the angular increase versus the z coordinate for the FF-nanotubes; where $r_{min}=(x^2+y^2)^{0.5}$ and $\theta_Z=\text{asin}(y/r)$.

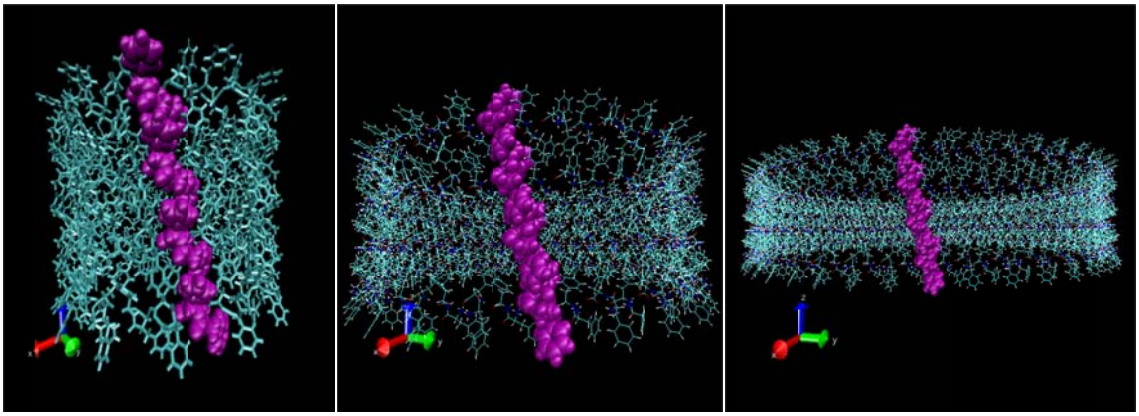

Figure 6.10. Orientation for Repetitive Unit of 25 Å, 50 Å and 100 Å Nanotubes

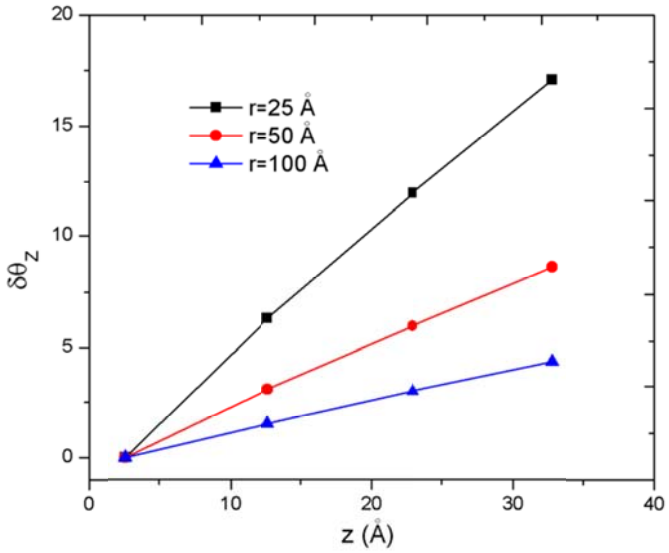

Figure 6.11. Change in Angular Position of Unit Cell along z Direction for r= 25 Å, 50 Å and 100 Å

When tracking the dipeptide unit cell along the tube, energy minimization calculations lead to structures where the orientation of peptides is maintained in the arrangement (see purple, white, red pairs in the middle of the FF tube in Fig.6.12. When tracking the center of mass for the dipeptide system, an increase of 6.5 degrees/ring for each unit cell was calculated, for the case of r=25 Å.

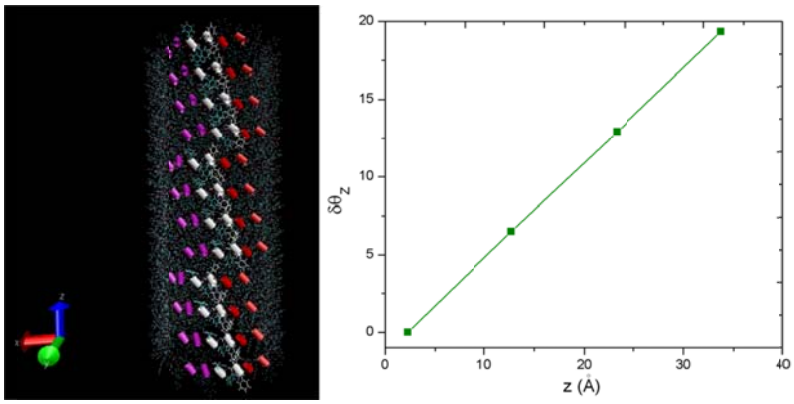

Figure 6.12. Chirality along Peptide Nanotube for r= 25 Å

6.5. Thermal Stability of Phenylalanine Nanotubes

Simulations were carried out in the NPT ensemble at three different temperatures to investigate thermal stability. The software used was NAMD2.6 with the CHARMM parameter force field. From the variation of the energy vs temperature for the r=25 Å and r=50 Å cases, a linear behavior is observed and after normalizing the energy vs No. of units, the correlation found is almost identical for both cases. In the experiments[34], thermal stability of phenylalanine di-peptide (FF) nanotubes up to 90*C in aqueous solution, and up to 150*C in dry conditions, was reported. In general, after including the effect of temperature in the simulations, the tubes keep the hollow conformation; however the perfect pattern organization is disrupted for high temperatures. The results from NPT dynamics show a linear increase of the total energy with the temperature as seen in the Fig. 6.13 below. The calculated heat capacity was C_p=0.4644 Kcal/mol-K.

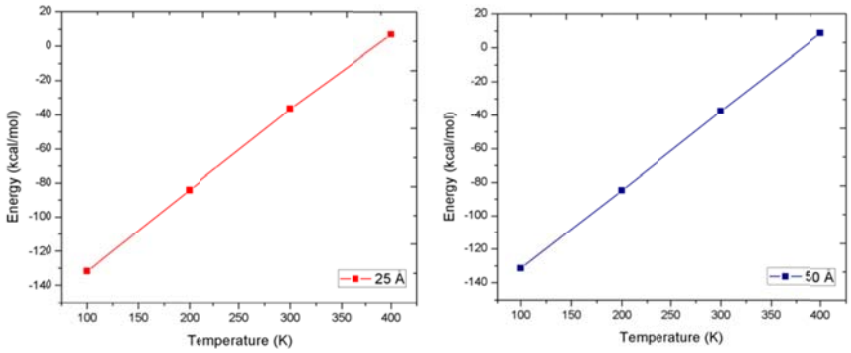

Figure 6.13. Increase in Energy with Temperature for Radius of 25 Å and 50 Å Nanotubes

Fig. 6.14 shows the total energy after equilibration and the change of cell parameters vs the number of steps. It shows how the volume of the unit cell is preserve after 0.5 ns

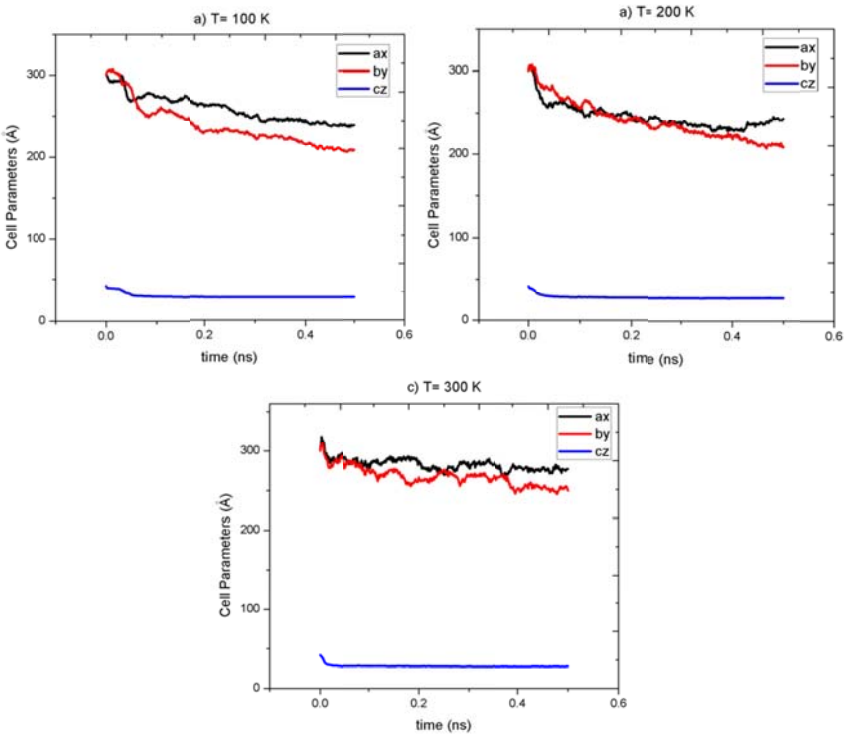

Figure 6.14. Change in Lattice Constant Values in the NPT Ensemble for 100K, 200K, 300K

The thermal stability was also studied using the NVT ensemble to confirm the values obtained from NPT dynamics and to observe if the change of cell parameters was influencing the results. Comparison of results in shown in Fig. 6.15.

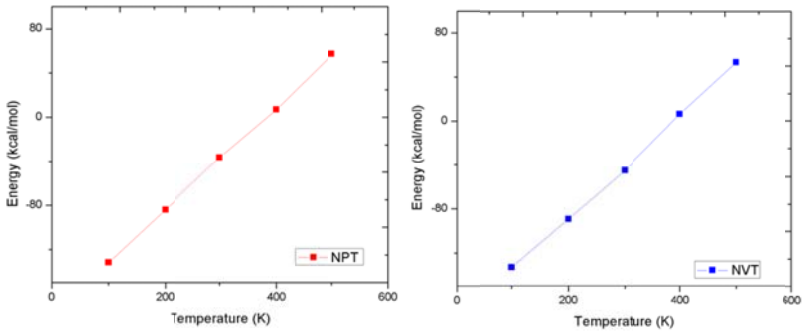

Figure 6.15. Comparison between NPT (left) and NVT (right) Simulations, r=25 A

To further investigate the thermal stability, a slow heating procedure was employed through gradually increasing the temperature first and then performing the NVT equilibrium simulations. The obtained results are more stable and ordered structures were kept stable up to 400K, in agreement with experiments[34]. The slope from Fig.6.16, obtained after correlation of the total energy with temperature is 8% smaller compared with the previous value calculated in NPT simulations.

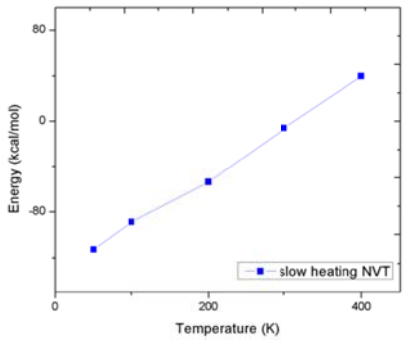

Figure 6.16. Total Energy after Slow Heating of Peptide Nanotubes, r=25 Å

In Fig.6.17, the axial views of the phenylalanine after equilibration at different temperatures are shown, the structure was ordered up to about 400 K.

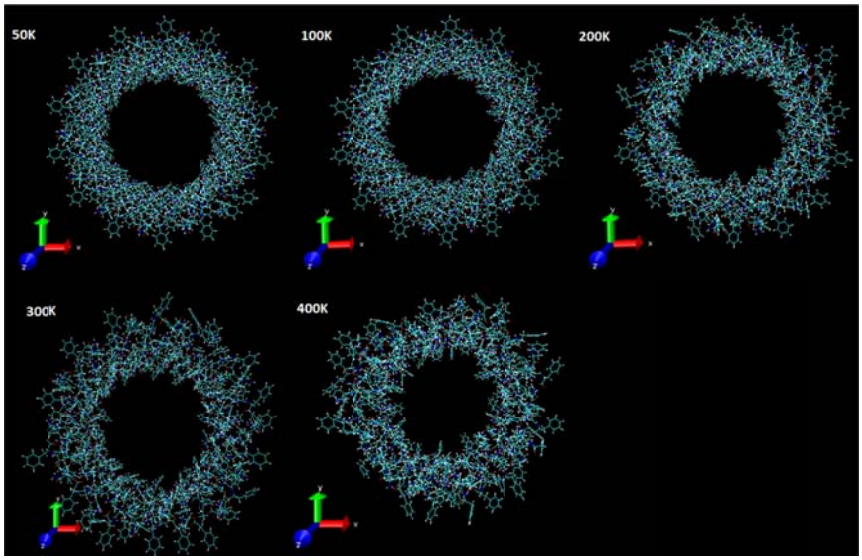

Figure 6.17. Final Equilibrated Structures at Different Temperatures, r=25 A

The effect of temperature on the number of hydrogen bonds was also analyzed. Fig.6.18. shows how the number of hydrogen bonds (H-bonds) decreases as the temperature increases; this can be related to the loss of stability in the tubular structure as the temperature increases, H-bonds play an important role in keeping the dipeptides units together in the nanotubes. The donor acceptor distance used was 3 Å and the angle cutoff was 2 Å.

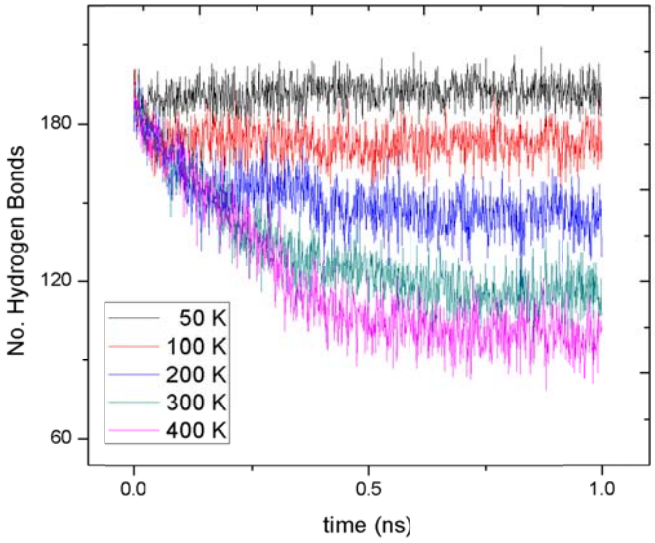

Figure 6.18. Effect of Temperature on Hydrogen-bonding in Peptide Nanotube for r=25Å

6.6. Summary

A two dimensional ring configuration of the phenylalanine dipeptide was found to be stable and nanotubes models of different diameters were successfully built with stable structural stability. The tubes are kept stable through aromatic and H-bonding interactions. The dipeptide subunits formed a helical pattern along the tubes for all diameters. Additionally, thermal stability was explored using MD simulations in two different thermodynamic ensembles (NPT &NVT). After slow heating the tubes were found to be stable up to 400K in agreement with experimental reports. H-bonds in the nanotube decreased as the temperature was raised, explaining the loss in its stability.

CHAPTER VII
CONCLUSIONS

7.1. Summary

Peptide Nanostructures are mechanically stable materials with various possibilities to be studied and a promising number of applications in biomedicine and bio-nanotechnology. Hence, the study of their properties by theoretical and experimental methods will contribute to the rational design of these novel materials. This work has been focused on peptide nanotubes as models for peptide nanostructures.

First, an efficient optimization strategy has been established, we successfully obtained an initial model of D,L cyclic peptide nanotubes, which is consistent with the experimental result. The CHARMM force field was validated and demonstrated to predict peptide materials and structure accurately.

The mechanical properties for cyclic peptide nanotubes were calculated by combining non-linear elasticity theories, a homogeneous deformation method and molecular dynamics for a complete consideration of the system's anisotropic nature. The result for the Young's modulus is in agreement with previous reported results for similar peptide nanotubes and protein crystalline systems. Yield behavior was observed for high strain values and could be explained as a consequence of breaking the hydrogen bonds when applying values of tensile strains above 6%. The anisotropy of the cyclic peptide nanotubes was confirmed through the obtained values for elastic constants. The C33 value is remarkable higher compared with the C11 and C22 values; this is in agreement with the fact that the tube is stabilized through hydrogen bond interactions longitudinally and that hydrophobic interactions between the tubes are weaker.

Additionally, the results from transport of water under confined conditions for carbon nanotubes (CNTs) and cyclic peptide nanotubes (CPNTs) as channel models indicated that water transport is indeed influenced by confinement. The transport of water was favored in CPNTs compared with equivalent sizes of CNTs due the

hydrophilic character of the hollow tubular zones of the peptide nanotube. Different diameters were studied for both systems and the density distribution function and dipole time correlations functions showed how the water molecules reduce the possibilities for hydrogen bond structure in confined spaces. For the smaller diameter, single file diffusion of water was observed while for larger diameters, bulk transport behavior was approached. This tendency was observed for both channels.

In order to explore the potential application of cyclic peptide nanotubes as artificial ion channels for transmembrane transport and other nano-transporter applications, the transport of Na+ and K+ ions under the influence of electric field was studied. The transport of ions across nanochannels is a complex problem with a high number of degrees of freedom. The channel-ion, Ion-water, channel-water interactions play important roles in the transport mechanisms. Also, the transmembrane potential, which can be represented in terms of an external electric field along the channel, can influence these interactions and polarize water and channel to induce gating and alter the transport properties. However, these effects were not accounted for in this work, because it is necessary to have a potential functions that precisely includes many-body polarization effects. These force field limitations should be addressed in future research. Here, we have studied the influence of electric field in the ion-water interactions and in the diffusion rates for two different systems. We observed selective transport for cations through the peptide nanotubes, the Cl- ions stayed in the bulk water cavities and did not diffuse into the nanotubes, and this selectivity was explained as a consequence of electrostatic repulsions due to the negative carbonyl oxygen present in the inner surface of the peptide nanotube. This kind of selectivity has been previously observed in channels like Gramicidin.

The diffusion rates calculated through mean square deviations indicated that the electric field accelerates the transport of ions but do not have any significant effect in the hydration number for Na+ and K+. However, a small effect was observed in the maximum value of the radial distribution functions. Also, when exploring the

temperature effect on the diffusion rates, it was observed that an increase in temperature also increases the rate at which ions move along the tube, as expected.

Finally, stable molecular models for nanotubes, with different diameter, from non-bonded phenylalanine dipeptide chains were successfully optimized; these nanotubes are stabilized through π-π aromatic interactions and hydrogen bonding that lead to helical organization of the dipeptide subunits. Thermal stability results agree with previous experimental reports; the nanotubes are stable up to around 400K and for higher temperatures the hydrogen bonding decreases drastically and the dipeptides lose their organization pattern.

7.2 Recommendations

Experimental and theoretical studies have significantly increased the knowledge in the area of peptide nano-materials in the last two decades. However, many properties and characteristics are still not fully understood. Opportunities for theoretical studies on peptide nanoscale properties such as stability in different solvents, transport dynamics, deformation properties, energy landscapes and inter and intra-molecular forces important for stability, are still open. Based on the research presented in this dissertation, future research could focus on:

1. Molecular transport with Cyclic Peptide Nanotubes: An interesting problem is the molecular transport of relevant molecules, like glucose, across the cyclic peptide nanotubes. Previous experimental studies have proved that these nanotubes will transport glucose[195]; furthermore, recently experimental and theoretical studies investigated the transport for the anti-tumor drug 5-Fluorouracil[196] within cyclic peptide nanotubes. An initial model was prepared and preliminary equilibration simulations were performed. See Fig.7.1 below

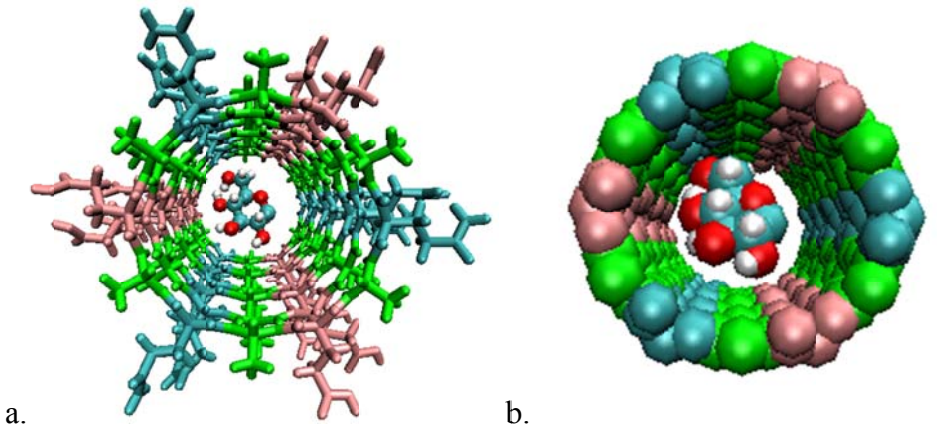

Figure 7.1. Molecular Model for a Cyclic Peptide Nanotube with a Glucose Molecule Inside. a) The Cyclic Peptide Nanotube colored by Amino-acid type in Bond Representation and b) the Backbone Representation colored by Amino-acid type in Van der Waals Representation

2. Mechanical properties of relevant anisotropic peptide systems such as: Phenylalanine peptide nanotubes and collagen fibrils. This can be addressed by using homogeneous deformation methods, non-linear elasticity theory and MD simulations as described in this work. A relative comparison between the modulus of phenylalanine nanotubes and relevant biomaterials is shown in Fig. 7.2.

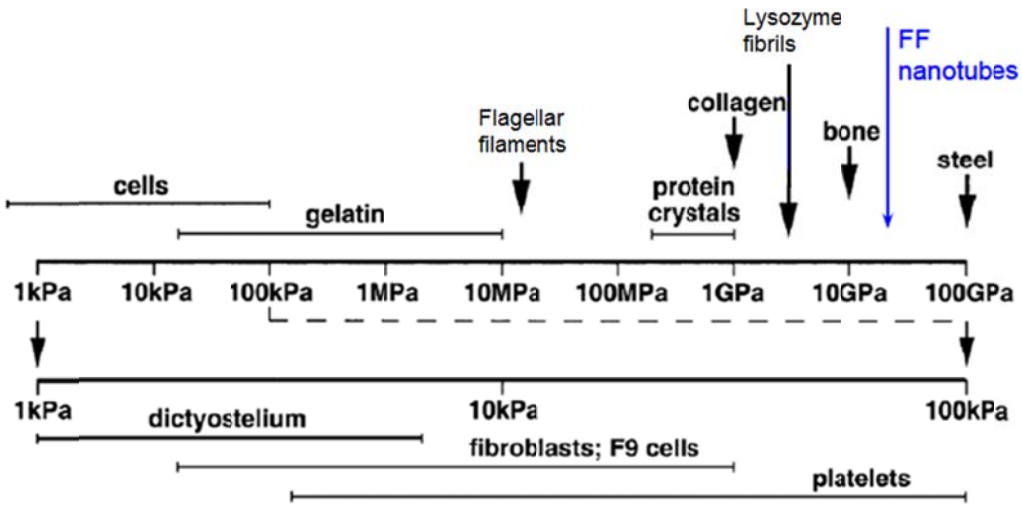

Figure 7.2. Comparison scheme for Mechanical Properties of Biomaterials with those of FF Peptide Nanotubes

The optimized molecular model (from this work) for phenylalanine nanotubes in longitudinal and axial views is shown in Fig. 7.3.

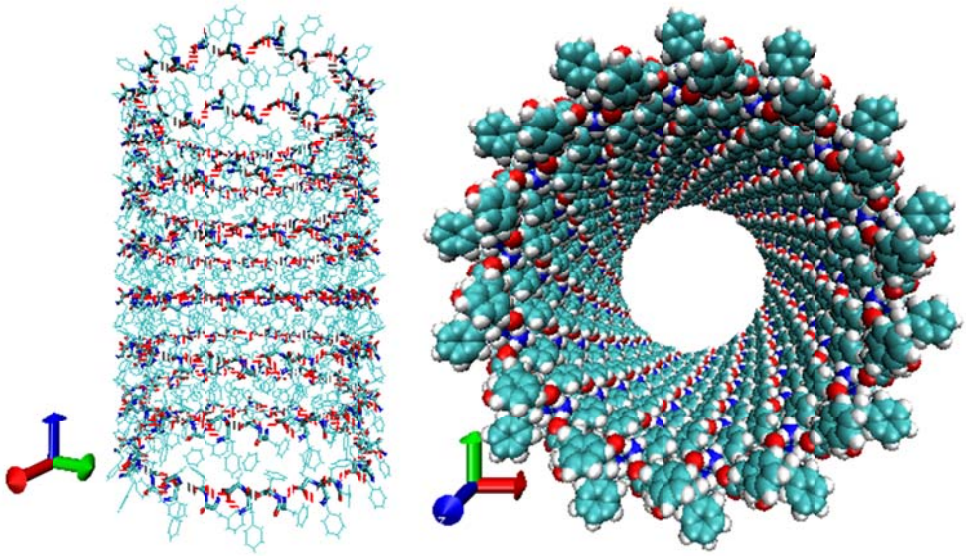

Figure 7.3. Longitudinal and axial views for FF nanotube, Radius of 25Å

3. Property Prediction and analysis of different peptide nanomaterials (Fibrils and Nanospheres) and Nanotubes (DNA nanotubes, surfactant nanotubes and other cyclic peptide nanotubes reviewed in Chapter II).

4. Studies of interactions between water and phenylalanine nanotubes for coating applications that were recently suggested experimentally.

5. Development of coarse grain models of peptide nanotubes that accurately reproduce the properties obtained from atomistic simulations.

6. Analysis of dipole time correlation functions and changes of dielectric properties in confined water for the artificial ion transport applications of cyclic peptide nanotubes.

REFERENCES

1 Gazit, E. Self-assembled peptide nanostructures: the design of molecular building blocks and their technological utilization. *Chemical Society Reviews* **36**, 1263-1269 (2007).

2 Colombo, G., Soto, P. & Gazit, E. Peptide self-assembly at the nanoscale: a challenging target for computational and experimental biotechnology. *Trends in Biotechnology* **25**, 211-218 (2007).

3 Holmes, T. C., de Lacalle, S., Su, X., Liu, G., Rich, A. Extensive neurite outgrowth and active synapse formation on self-assembling peptide scaffolds. *Proceedings of the National Academy of Sciences of the United States of America* **97**, 6728-6733 (2000).

4 Ghadiri, M. R., Granja, J. R., Milligan, R. A., McRee, D. E. & Khazanovich, N. Self-assembling organic nanotubes based on a cyclic peptide architecture. *Nature* **366**, 324-327 (1993).

5 Cellmer, T., Bratko, D., Prausnitz, J. M. & Blanch, H. Protein-folding landscapes in multichain systems. *Proceedings of the National Academy of Sciences of the United States of America* **102**, 11692-11697, doi:10.1073/pnas.0505342102 (2005).

6 Boudreault, P.-L., Arseneault, M., Otis, F. & Voyer, N. Nanoscale tools to selectively destroy cancer cells. *Chemical Communications* **18**, 2118-2120 (2008).

7 Cagin, T., Dereli, G., Uludogan, M. & Tomak, M. Thermal and mechanical properties of some fcc transition metals. *Physical Review B* **59**, 3468 (1999).

8 Uludogan, M., Guarin, D.P., Gomez, Z. E., Çağin, T., Goddard, W. A., DFT studies on ferroelectric ceramics and their alloys. *Computer Modeling in Engineering and Sciences* **24**, 215-38 (2008).

9 Fan, C. F., Cagin, T., Chen, Z. M. & Smith, K. A. Molecular modeling of polycarbonate. 1. Force Field, static structure, and mechanical properties. *Macromolecules* **27**, 2383-2391, doi:10.1021/ma00087a004 (1994).

10 Zangi, R. & Mark, A. E. Bilayer ice and alternate liquid phases of confined water. *The Journal of Chemical Physics* **119**, 1694-1700 (2003).

11 Alba-Simionesco, C., Dosseh, G., Dumont, E., Frick, B., Geil, B. *et al.* Confinement of molecular liquids: Consequences on thermodynamic, static and dynamical properties of benzene and toluene. *The European Physical Journal E: Soft Matter and Biological Physics* **12**, 19-28 (2003).

12 De Santis, P., Morosetti, S. & Rizzo, R. Conformational analysis of regular enantiomeric sequences. *Macromolecules* **7**, 52-58, doi:10.1021/ma60037a011 (1974).

13 Ghadiri, M. R., Granja, J. R., Milligan, R. A., McRee, D. E. & Khazanovich, N. Self-assembling organic nanotubes based on a cyclic peptide architecture. *Nature* **366**, 324-327 (1993).

14 Hartgerink, J. D., Granja, J. R., Milligan, R. A. & Ghadiri, M. R. Self-assembling peptide nanotubes. *Journal of the American Chemical Society* **118**, 43-50, doi:10.1021/ja953070s (1996).

15 Fernandez-Lopez, S., Kim, H., Choi, E., Delgado, M., Granja, J. R., *et al.* Antibacterial agents based on the cyclic d,l-[alpha]-peptide architecture. *Nature* **412**, 452-455 (2001).

16 Engels, M., Bashford, D. & Ghadiri, M. R. Structure and dynamics of self-assembling peptide nanotubes and the channel-mediated water organization and self-diffusion. a molecular dynamics study. *Journal of the American Chemical Society* **117**, 9151-9158, doi:10.1021/ja00141a005 (1995).

17 Ghadiri, M. R., Granja, J. R. & Buehler, L. K. Artificial transmembrane ion channels from self-assembling peptide nanotubes. *Nature* **369**, 301-304 (1994).

18 Görbitz, C. H. Nanotube formation by hydrophobic dipeptides. *Chemistry – A European Journal* **7**, 5153-5159, (2001).

19 Kim, H. S., Hartgerink, J. D. & Ghadiri, M. R. Oriented self-assembly of cyclic peptide nanotubes in lipid membranes. *Journal of the American Chemical Society* **120**, 4417-4424, doi:10.1021/ja9735315 (1998).

20 Vauthey, S., Santoso, S., Gong, H., Watson, N. & Zhang, S. Molecular self-assembly of surfactant-like peptides to form nanotubes and nanovesicles.

Proceedings of the National Academy of Sciences of the United States of America **99**, 5355-5360 (2002).

21 Reches, M. & Gazit, E. Casting metal nanowires within discrete self-assembled peptide nanotubes. *Science* **300**, 625-627, doi:10.1126/science.1082387 (2003).

22 Horne, W. S., Ashkenasy, N. & Ghadiri, M. R. Modulating charge transfer through cyclic d,l-α-peptide self-assembly. *Chemistry – A European Journal* **11**, 1137-1144, doi:10.1002/chem.200400923 (2005).

23 Clark, T. D., Buehler, L. K. & Ghadiri, M. R. Self-assembling cyclic β3-peptide nanotubes as artificial transmembrane ion channels. *Journal of the American Chemical Society* **120**, 651-656, doi:10.1021/ja972786f (1998).

24 Sun, X. & Lorenzi, G. P. On the stacking of β-rings: The solution self-association behavior of two partially N-methylated cyclo(hexaleucines). *Helvetica Chimica Acta* **77**, 1520-1526, doi:10.1002/hlca.19940770607 (1994).

25 Seebach, D., Matthews, J. L., Meden, A., Baerlocher, C., McCusker, L. B. Cyclo-β-peptides: structure and tubular stacking of cyclic tetramers of 3-aminobutanoic acid as determined from powder diffraction data. *Helvetica Chimica Acta* **80**, 173-182, doi:10.1002/hlca.19970800116 (1997).

26 Amorín, M., Brea, R. J., Castedo, L. & Granja, J. R. The smallest α,γ-peptide nanotubulet segments: Cyclic α,γ-tetrapeptide dimers. *Organic Letters* **7**, 4681-4684, doi:10.1021/ol0518885 (2005).

27 Reiriz, C., Castedo, L. & Granja, J. R. New α,γ-cyclic peptides-nanotube molecular caps using α,α-dialkylated α-amino acids. *Journal of Peptide Science* **14**, 241-249, doi:10.1002/psc.984 (2008).

28 Valéry, C., Paternostre, M., Robert, B., Gulik-Krzywicki, T., Narayanan, T., *et al.* Biomimetic organization: Octapeptide self-assembly into nanotubes of viral capsid-like dimension. *Proceedings of the National Academy of Sciences of the United States of America* **100**, 10258-10262 (2003).

29 Valéry, C., Pouget, E., Pandit, A., Verbavatz, J., Bordes, L., *et al.* Molecular origin of the self-assembly of lanreotide into nanotubes: A mutational approach. *Biophysical Journal* **94**, 1782-1795 (2008).

30 Pouget, E., Fay, N., Dujardin, E., Jamin, N., Berthault P., *et al.* Elucidation of the self-assembly pathway of lanreotide octapeptide into β-sheet nanotubes: Role of two stable intermediates. *Journal of the American Chemical Society* **132**, 4230-4241, doi:10.1021/ja9088023 (2010).

31 Scanlon, S. & Aggeli, A. Self-assembling peptide nanotubes. *Nano Today* **3**, 22-30.

32 Laghaei, R. & Mousseau, N. Spontaneous formation of polyglutamine nanotubes with molecular dynamics simulations. *Journal of Chemical Physics* **132,** 165102 (2010).

33 Kol, N., Alder-Abramovich, L., Barlam, D., Shneck, R. Z., Gazit, E., *et al.* Self-assembled peptide nanotubes are uniquely rigid bioinspired supramolecular structures. *Nano Letters* **5**, 1343-1346, doi:10.1021/nl0505896 (2005).

34 Adler-Abramovich, L., Reches, M., Sedman, V. L., Allen, S., Tendler, S. j., *et al.* Thermal and chemical stability of diphenylalanine peptide nanotubes: implications for nanotechnological applications. *Langmuir* **22**, 1313-1320, doi:10.1021/la052409d (2006).

35 Kholkin, A., Amdursky, N., Bdikin, I., Gazit, E. & Rosenman, G. Strong piezoelectricity in bioinspired peptide nanotubes. *ACS Nano* **4**, 610-614, doi:10.1021/nn901327v (2010).

36 Yan, X., Zhu, P. & Li, J. Self-assembly and application of diphenylalanine-based nanostructures. *Chemical Society Reviews* **39,** , 1877-1890 (2010).

37 Yemini, M., Reches, M., Rishpon, J. & Gazit, E. Novel electrochemical biosensing platform using self-assembled peptide nanotubes. *Nano Letters* **5**, 183-186, doi:10.1021/nl0484189 (2004).

38 Carny, O., Shalev, D. E. & Gazit, E. Fabrication of coaxial metal nanocables using a self-assembled peptide nanotube scaffold. *Nano Letters* **6**, 1594-1597, doi:10.1021/nl060468l (2006).

39 Ryu, J., Kim, S.-W., Kang, K. & Park, C. B. Synthesis of diphenylalanine/cobalt oxide hybrid nanowires and their application to energy storage. *ACS Nano* **4**, 159-164 (2009).

40 Cipriano, T. C., Takahashi, P. M., De Lima, D., Oliveira Jr., V. X., Souza, J. A., *et al.* Spatial organization of peptide nanotubes for electrochemical devices. *Journal of Materials Science* **45**, 5101-5108 (2010).

41 Shklovsky, J., Beker, P., Amdursky, N., Gazit, E. & Rosenman, G. Bioinspired peptide nanotubes: Deposition technology and physical properties. *Materials Science and Engineering B: Solid-State Materials for Advanced Technology* **169**, 62-66 (2010).

42 Adler-Abramovich, L., Aronov, D., Beker, P., Yevnin, M., Stempler, S., *et al.* Self-assembled arrays of peptide nanotubes by vapour deposition. *Nat Nano* **4**, 849-854 (2009).

43 Yan, X., He, Q., Wang, K., Duan, L., Cui, Y., *et al.* Transition of cationic dipeptide nanotubes into vesicles and oligonucleotide delivery. *Angewandte Chemie International Edition* **46**, 2431-2434, doi:10.1002/anie.200603387 (2007).

44 Yan, X., Cui, Y., He, Q., Wang, K., Li, J., *et al.* Reversible transitions between peptide nanotubes and vesicle-like structures including theoretical modeling studies. *Chemistry – A European Journal* **14**, 5974-5980, doi:10.1002/chem.200800012 (2008).

45 Gorbitz, C. H. Nanotube formation by hydrophobic dipeptides. *Chemistry - A European Journal* **7**, 5153-5159 (2001).

46 Gorbitz, C. An exceptionally stable peptide nanotube system with flexible pores. *Acta Crystallographica Section B* **58**, 849-854, doi:10.1107/S0108768102012314 (2002).

47 Gorbitz, C. H. The structure of nanotubes formed by diphenylalanine, the core recognition motif of Alzheimer's [small beta]-amyloid polypeptide. *Chemical Communications* **22**, 2332-2334 (2006).

48 Görbitz, C. Microporous organic materials from hydrophobic dipeptides. *Chemistry – A European Journal* **13**, 1022-1031, doi:10.1002/chem.200601427 (2007).

49 Feldkamp, U. & Niemeyer, C. M. Rational design of DNA nanoarchitectures. *Angewandte Chemie International Edition* **45**, 1856-1876, doi:10.1002/anie.200502358 (2006).

50 Sobey, T. L., Rennel, S., Simmer, F. C. Assembly and melting of DNA nanotubes from single-sequence tiles. *Journal of Physics: Condensed Matter* **21**, 034112 (2009).

51 Seeman, N. An Overview of Structural DNA Nanotechnology. *Molecular Biotechnology* **37**, 246-257, doi:10.1007/s12033-007-0059-4 (2007).

52 Yang, D., Campolongo, M. J., Nhi Tran, T. N., Ruiz, R., Kahn, J. S., *et al.* Novel DNA materials and their applications. *Wiley Interdisciplinary Reviews: Nanomedicine and Nanobiotechnology*, n/a-n/a, doi:10.1002/wnan.111 (2010).

53 Yin, P., Hariadi, R. F., Sahu, S., Choi, H., Park, S., *et al.* Programming DNA tube circumferences. *Science* **321**, 824-826, doi:10.1126/science.1157312 (2008).

54 Adams, D. J., Holtzmann, K., Schneider, C. & Butler, M. F. Self-assembly of surfactant-like peptides. *Langmuir* **23**, 12729-12736, doi:10.1021/la7011183 (2007).

55 Zhao, X., Pan, F., Xu, H., Yaseen, M., Shan, M., *et al.* Molecular self-assembly and applications of designer peptide amphiphiles. *Chemical Society Reviews* **39**, 3480-3498 (2010).

56 Hartgerink, J. D., Beniash, E. and Stupp, S. I. Self-Assembly and mineralization of peptide-amphiphile nanofibers. *Science* **294**, 1684-1688, doi:10.1126/science.1063187 (2001).

57 Yuwono, V. M. & Hartgerink, J. D. Peptide amphiphile nanofibers template and catalyze silica nanotube formation. *Langmuir* **23**, 5033-5038, doi:10.1021/la0629835 (2007).

58 Zhang, S., Marini, D. M., Hwang, W. & Santoso, S. Design of nanostructured biological materials through self-assembly of peptides and proteins. *Current Opinion in Chemical Biology* **6**, 865-871 (2002).

59 Zhou, M., Smith, A. M., Das, A. K., Hodson, N., Collins, R., *et al.* Self-assembled peptide-based hydrogels as scaffolds for anchorage-dependent cells. *Biomaterials* **30**, 2523-2530 (2009).

60 Orbach, R., Alder-Abramovich, L., Zigerson, S., Mironi-Harpaz, I., Seliktar, D., *et al.* Self-assembled fmoc-peptides as a platform for the formation of

nanostructures and hydrogels. *Biomacromolecules* **10**, 2646-2651, doi:10.1021/bm900584m (2009).

61 Reches, M. & Gazit, E. Formation of closed-cage nanostructures by self-assembly of aromatic dipeptides. *Nano Letters* **4**, 581-585, doi:10.1021/nl035159z (2004).

62 Matsuura, K., Murasato, K. & Kimizuka, N. Artificial peptide-nanospheres self-assembled from three-way junctions of β-sheet-forming peptides. *Journal of the American Chemical Society* **127**, 10148-10149, doi:10.1021/ja052644i (2005).

63 Yan, X., Cui, Y., Qi, W., Su, Y., Yang, Y., *et al.* Self-assembly of peptide-based colloids containing lipophilic nanocrystals. *Small* **4**, 1687-1693, doi:10.1002/smll.200800960 (2008).

64 Wright, P. A. Opening the door to peptide-based porous solids. *Science* **329**, 1025-1026, doi:10.1126/science.1195176 (2010).

65 Rabone, J., Yue, Y., Chong, S., Stylianou, K. C., Bacsa, J., *et al.* An adaptable peptide-based porous material. *Science* **329**, 1053-1057, doi:10.1126/science.1190672 (2010).

66 Xu, Z. & Buehler, M. J. Mechanical energy transfer and dissipation in fibrous beta-sheet-rich proteins. *Physical Review E* **81**, 061910 (2010).

67 Buehler, M. J. & Keten, S. Colloquium: Failure of molecules, bones, and the Earth itself. *Reviews of Modern Physics* **82**, 1459 (2010).

68 Thompson, E. J., DePaul, A. J., Patel, S. S. & Sorin, E. J. Evaluating molecular mechanical potentials for helical peptides and proteins. *PLoS ONE* **5**, e10056 (2010).

69 Qin, Z. & Buehler, M. J. Molecular dynamics simulation of the alpha -helix to beta-sheet transition in coiled protein filaments: evidence for a critical filament length scale. *Physical Review Letters* **104**, 198304 (2010).

70 Nova, A., Keten, S., Pugno, N. M., Redaelli, A. & Buehler, M. J. molecular and nanostructural mechanisms of deformation, strength and toughness of spider silk fibrils. *Nano Letters* **10**, 2626-2634, doi:10.1021/nl101341w (2010).

71 Bertaud, J., Hester, J., Jimenez, D., & Buehler, M. Energy landscape, structure and rate effects on strength properties of alpha-helical proteins. *Journal of Physics: Condensed Matter* **22**, 035102 (2010).

72 Gautieri, A., Vesentini, S., Montevecchi, F. M. & Redaelli, A. Mechanical properties of physiological and pathological models of collagen peptides investigated via steered molecular dynamics simulations. *Journal of Biomechanics* **41**, 3073-3077 (2008).

73 Buehler, M. J. Nature designs tough collagen: Explaining the nanostructure of collagen fibrils. *Proceedings of the National Academy of Sciences* **103**, 12285-12290 (2006).

74 Tuszyński, J., Luchko, T., Portet, S. & Dixon, J. Anisotropic elastic properties of microtubules. *The European Physical Journal E: Soft Matter and Biological Physics* **17**, 29-35, doi:10.1140/epje/i2004-10102-5 (2005).

75 Diaz, J. A. C. & Çağin, T. Thermo-mechanical stability and strength of peptide nanostructures from molecular dynamics: Self-assembled cyclic peptide nanotubes. *Nanotechnology* **21**, 115703 (2010).

76 Bao, G. & Suresh, S. Cell and molecular mechanics of biological materials. *Nature Materials* **2**, 715-725 (2003).

77 García-Fandiño, R., Granja, J. R., D'Abramo, M. & Orozco, M. Theoretical characterization of the dynamical behavior and transport properties of α,γ-peptide nanotubes in solution. *Journal of the American Chemical Society* **131**, 15678-15686, doi:10.1021/ja903400n (2009).

78 Tarek, M., Maigret, B. & Chipot, C. Molecular dynamics investigation of an oriented cyclic peptide nanotube in dmpc bilayers. *Biophysical Journal* **85**, 2287-2298 (2003).

79 Carvajal-Diaz, J. A., Liu, L. & Cagin, T. Structure and dynamics of water within single wall carbon nanotubes and self-assembled cyclic peptide nanotubes. *Journal of Computational and Theoretical Nanoscience* **6**, 894-902 (2009).

80 Liu, J., Fan, J., Tang, M. & Zhou, W. Molecular dynamics simulation for the structure of the water chain in a transmembrane peptide nanotube. *The Journal of Physical Chemistry A* **114**, 2376-2383, doi:10.1021/jp910624z (2010).

81 Hwang, H., Schatz, G. C. & Ratner, M. A. Steered molecular dynamics studies of the potential of mean force of a na+ or k+ ion in a cyclic peptide nanotube. *The Journal of Physical Chemistry B* **110**, 26448-26460, doi:10.1021/jp0657888 (2006).

82 Hwang, H., Schatz, G. C. & Ratner, M. A. Ion current calculations based on three dimensional Poisson-Nernst-Planck theory for a cyclic peptide nanotube. *The Journal of Physical Chemistry B* **110**, 6999-7008, doi:10.1021/jp055740e (2006).

83 Hwang, H., Schatz, G. C. & Ratner, M. A. Coarse-grained molecular dynamics study of cyclic peptide nanotube insertion into a lipid bilayer. *The Journal of Physical Chemistry A* **113**, 4780-4787, doi:10.1021/jp8080657 (2008).

84 Hu, Z. Q. & Jiang, J. W. Electrophoresis in protein crystal: Nonequilibrium molecular dynamics simulations. *Biophysical Journal* **95**, 4148-4156, doi:10.1529/biophysj.108.140160 (2008).

85 Khalili-Araghi, F., Gumbart, J., Wen, P., Sotomayor, M., Tajkhorshid, E., *et al.* Molecular dynamics simulations of membrane channels and transporters. *Current Opinion in Structural Biology* **19**, 128-137, doi:DOI: 10.1016/j.sbi.2009.02.011 (2009).

86 Nguyen, P. H., Park, S.-M. & Stock, G. Nonequilibrium molecular dynamics simulation of the energy transport through a peptide helix. *The Journal of Chemical Physics* **132**, 025102 (2010).

87 Bucher, D., Guidoni, L., Carloni, P. & Rothlisberger, U. Coordination numbers of K+ and Na+ ions inside the selectivity filter of the KcsA potassium channel: Insights from first principles molecular dynamics. *Biophysical Journal* **98**, L47-L49, doi:DOI: 10.1016/j.bpj.2010.01.064 (2010).

88 Buch, I., Brooks, B. R., Wolfson, H. J. & Nussinov, R. Computational validation of protein nanotubes. *Nano Letters* **9**, 1096-1102, doi:10.1021/nl803521j (2009).

89 Castelletto, V., Nutt, D. R., Bucak, S., Cenker, C. & Olsson, U. Structure of single-wall peptide nanotubes: In situ flow aligning X-ray diffraction. *Chemical Communications* **46**, 6270-6272 (2010).

90 Görbitz, C. H. Structures of dipeptides: The head-to-tail story. *Acta Crystallographica Section B* **66**, 84-93, doi:10.1107/s0108768109053257 (2010).

91 Tozzini, V. Coarse-grained models for proteins. *Current Opinion in Structural Biology* **15**, 144-150 (2005).

92 Monticelli, L., Kandasamy, S., Periole, X., Larson, R., Tieleman, P., *et al.* The MARTINI coarse-grained force field: Extension to proteins. *Journal of Chemical Theory and Computation* **4**, 819-834, doi:citeulike-article-id:2677939 (2008).

93 Laghaei, R. & Mousseau, N. Spontaneous formation of polyglutamine nanotubes with molecular dynamics simulations. *The Journal of Chemical Physics* **132**, 165102 (2010).

94 Villa, A., Peter, C. & van der Vegt, N. F. A. Self-assembling dipeptides: Conformational sampling in solvent-free coarse-grained simulation. *Physical Chemistry Chemical Physics* **11**, 2077-2086 (2009).

95 Velichko, Y. S., Stupp, S. I. & de la Cruz, M. O. Molecular simulation study of peptide amphiphile self-assembly. *The Journal of Physical Chemistry B* **112**, 2326-2334, doi:10.1021/jp074420n (2008).

96 Mu, Y. & Gao, Y. Q. Self-assembly of polypeptides into left-handedly twisted fibril-like structures. *Physical Review E* **80**, 041927 (2009).

97 Marchut, A. J. & Hall, C. K. Effects of chain length on the aggregation of model polyglutamine peptides: Molecular dynamics simulations. *Proteins: Structure, Function, and Bioinformatics* **66**, 96-109, doi:10.1002/prot.21132 (2007).

98 Mondal, J., Sung, B. J. & Yethiraj, A. Sequence dependent self-assembly of beta-peptides: Insights from a coarse-grained model. *The Journal of Chemical Physics* **132**, 065103-065107 (2010).

99 Lim, Y. b., Lee, E. & Lee, M. Controlled bioactive nanostructures from self-assembly of peptide building blocks. *Angewandte Chemie International Edition* **46**, 9011-9014, doi:10.1002/anie.200702732 (2007).

100 Ryu, J. & Park, C. Synthesis of diphenylalanine/polyaniline core/shell conducting nanowires by peptide self-assembly. *Angewandte Chemie International Edition* **48**, 4820-4823, doi:10.1002/anie.200900668 (2009).

101 Gazit, E. Molecular self-assembly: Bioactive nanostructures branch out. *Nat Nano* **3**, 8-9 (2008).

102 Amdursky, N., Molotskii, M., Gazit, E. & Rosenman, G. Self-assembled bioinspired quantum dots: Optical properties. *Applied Physics Letters* **94,** 261907 (2009).

103 Adler-Abramovich, L., Badihi-Mossberg, M., Gazit, E. & Rishpon, J. Characterization of peptide-nanostructure-modified electrodes and their application for ultrasensitive environmental monitoring. *Small* **6**, 825-831, doi:10.1002/smll.200902186 (2010).

104 Rodríguez-Ropero, F., Zanuy, D., Assfeld, X. & Alemán, C. Modeling an electronic conductor based on natural peptide sequences. *Biomacromolecules* **10**, 2338-2343, doi:10.1021/bm900524v (2009).

105 McQuarrie, D. *Statistical Mechanics* (Harper & Row, New York, 1976).

106 Brooks, B. R., Bruccoleri, R. E., Olafson, B., States, D., Swaminathan, S., *et al.* CHARMM: A program for macromolecular energy, minimization, and dynamics calculations. *Journal of Computational Chemistry* **4**, 187-217, doi:10.1002/jcc.540040211 (1983).

107 Phillips, J. C., Braun, R., Wang, W., Gumbart, J., Tajkhorshid, E., *et al.* Scalable molecular dynamics with NAMD. *Journal of Computational Chemistry* **26**, 1781-1802, doi:10.1002/jcc.20289 (2005).

108 Humphrey, W., Dalke, A. & Schulten, K. VMD: Visual molecular dynamics. *Journal of Molecular Graphics* **14**, 33-38, doi: 10.1016/0263-7855(96)00018-5 (1996).

109 MacKerell, A. D., Bashford, D., Bellot, R., Dunbrack, R., Evanseck, J., *et al.* All-atom empirical potential for molecular modeling and dynamics studies of proteins. *The Journal of Physical Chemistry B* **102**, 3586-3616, doi:10.1021/jp973084f (1998).

110 Martyna, G. J., Tobias, D. J. & Klein, M. L. Constant pressure molecular dynamics algorithms. *The Journal of Chemical Physics* **101**, 4177-4189 (1994).

111 Feller, S. E., Zhang, Y., Pastor, R. W. & Brooks, B. R. Constant pressure molecular dynamics simulation: The Langevin piston method. *The Journal of Chemical Physics* **103**, 4613-4621 (1995).

112 Ryckaert, J.-P., Ciccotti, G. & Berendsen, H. J. C. Numerical integration of the cartesian equations of motion of a system with constraints: Molecular dynamics of n-alkanes. *Journal of Computational Physics* **23**, 327-341, doi: 10.1016/0021-9991(77)90098-5 (1977).

113 Andersen, H. C. Rattle: A "velocity" version of the shake algorithm for molecular dynamics calculations. *Journal of Computational Physics* **52**, 24-34, doi:Doi: 10.1016/0021-9991(83)90014-1 (1983).

114 Ewald, P. P. Die Berechnung optischer und elektrostatischer Gitterpotentiale. *Annalen der Physik* **369**, 253-287, doi:10.1002/andp.19213690304 (1921).

115 Darden, T., York, D. & Pedersen, L. Particle mesh Ewald: An N [center-dot] log(N) method for Ewald sums in large systems. *The Journal of Chemical Physics* **98**, 10089-10092 (1993).

116 Buehler, M. J. & Ackbarow, T. Fracture mechanics of protein materials. *Materials Today* **10**, 46-58 (2007).

117 Buehler, M. J., Keten, S. & Ackbarow, T. Theoretical and computational hierarchical nanomechanics of protein materials: Deformation and fracture. *Progress in Materials Science* **53**, 1101-1241, doi:10.1016/j.pmatsci.2008.06.002 (2008).

118 Keating, P. N. Effect of invariance requirements on the elastic strain energy of crystals with application to the diamond structure. *Physical Review* **145**, 637 (1966).

119 Keating, P. N. Theory of the third-order elastic constants of diamond-like crystals. *Physical Review* **149**, 674 (1966).

120 Gao, G., Cagin, T. C., Goddard III, W. A. Energetics, structure, thermodynamic and mechanical properties of nanotubes. *Nanotechnology* **9**, 183-191 (1998).

121 Pettitt, B. M., Cagin, T. C. Constants of nickel: Variations with temperature and pressure. *Physical Review B* **39**, 12484-12491 (1989).

122 Cagin, T. & Ray, J. R. Third-order elastic constants from molecular dynamics: Theory and an example calculation. *Physical Review B* **38**, 7940 (1988).

123 Kalay, M., Kart, H. H., Özdemir Kart, S. & ÇagIn, T. Elastic properties and pressure induced transitions of ZnO polymorphs from first-principle calculations. *Journal of Alloys and Compounds* **484**, 431-438, doi:10.1016/j.jallcom.2009.04.116 (2009).

124 Pham, H. & Cagin, T. Second and third-order elastic constants of Fe from first-principles. *Acta Mater.*(submitted)

125 Özdemir Kart, S., Uludogan, M., Karaman, I. & Cagın, T. DFT studies on structure, mechanics and phase behavior of magnetic shape memory alloys: Ni2MnGa. *Physica Status Solidi (a)* **205**, 1026-1035, doi:10.1002/pssa.200776453 (2008).

126 Zhao, J., Winey, J. M. & Gupta, Y. M. First-principles calculations of second- and third-order elastic constants for single crystals of arbitrary symmetry. *Physical Review B* **75**, 094105 (2007).

127 Andersen, H. C. Molecular dynamics simulations at constant pressure and/or temperature. *The Journal of Chemical Physics* **72**, 2384-2393, doi:10.1063/1.439486 (1980).

128 Parrinello, M. & Rahman, A. Crystal structure and pair potentials: A molecular-dynamics study. *Physical Review Letters* **45**, 1196 (1980).

129 Parrinello, M. & Rahman, A. Polymorphic transitions in single crystals: A new molecular dynamics method. *Journal of Applied Physics* **52**, 7182-7190, doi:10.1063/1.328693 (1981).

130 Ray, J. R. & Rahman, A. Statistical ensembles and molecular dynamics studies of anisotropic solids. *The Journal of Chemical Physics* **80**, 4423-4428 (1984).

131 Thurston, R. N. & Brugger, K. Third-Order elastic constants and the velocity of small amplitude elastic waves in homogeneously stressed media. *Physical Review* **133**, A1604 (1964).

132 Chakrabarty, A. & Cagin, T. Computational studies on mechanical and thermal properties of carbon nanotube based nanostructures. *Cmc-Computers Materials & Continua* **7**, 167-189 (2008).

133 Nielsen, O. H. Optical phonons and elasticity of diamond at megabar stresses. *Physical Review B* **34**, 5808 (1986).

134 Cagin, T. & Ray, J. R. Elastic constants of sodium from molecular dynamics. *Physical Review B* **37**, 699 (1988).

135 Cagin, T. & Ray, J. R. Fundamental treatment of molecular-dynamics ensembles. *Physical Review A* **37**, 247 (1988).

136 Wan, R., Li, J., Lu, H. & Fang, H. Controllable water channel gating of nanometer dimensions. *Journal of the American Chemical Society* **127**, 7166-7170, doi:10.1021/ja050044d (2005).

137 Hummer, G., Rasaiah, J. C. & Noworyta, J. P. Water conduction through the hydrophobic channel of a carbon nanotube. *Nature* **414**, 188-190 (2001).

138 Zheng, J., Lennon, E. M., Tsao, H.-K., Sheng, Y.-J. & Jiang, S. Transport of a liquid water and methanol mixture through carbon nanotubes under a chemical potential gradient. *The Journal of Chemical Physics* **122**, 214702-214707, doi:10.1063/1.1908619 (2005).

139 Tajkhorshid, E., Nollert, P., Jensen, M., Miercke, L., O'Connell, J., *et al.* Control of the selectivity of the aquaporin water channel family by global orientational tuning. *Science* **296**, 525-530, doi:10.1126/science.1067778 (2002).

140 Varnik, F., Baschnagel, J., Binder, K. & Mareschal, M. Confinement effects on the slow dynamics of a supercooled polymer melt: Rouse modes and the incoherent scattering function. *Eur. Phys. J. E* **12**, 167-171 (2003).

141 Lee, K.-H. & Sinnott, S. B. Computational studies of non-equilibrium molecular transport through carbon nanotubes. *The Journal of Physical Chemistry B* **108**, 9861-9870, doi:10.1021/jp036791j (2004).

142 Sun, L. & Crooks, R. M. Single carbon nanotube membranes: A well-defined model for studying mass transport through nanoporous materials. *Journal of the American Chemical Society* **122**, 12340-12345, doi:10.1021/ja002429w (2000).

143 Mao, Z. & Sinnott, S. B. Separation of organic molecular mixtures in carbon nanotubes and bundles: Molecular dynamics simulations. *The Journal of Physical Chemistry B* **105**, 6916-6924, doi:10.1021/jp0103272 (2001).

144 Cagin, T.C., Qi, Y., Zhou, Y., Demiralp, E., Gao, G., *et al*. Computational materials chemistry at the nanoscale. *Journal of Nanoparticle Research* **1**, 51-69 (1999).

145 Jirage, K. B., Hulteen, J. C. & Martin, C. R. Nanotubule-based molecular-filtration membranes. *Science* **278**, 655-658, doi:10.1126/science.278.5338.655 (1997).

146 Joo, S. H., Choi, S. J., Oh, I., Kwak, J., *et al.* Ordered nanoporous arrays of carbon supporting high dispersions of platinum nanoparticles. *Nature* **412**, 169-172 (2001).

147 Gogotsi, Y., Libera, J., Yazicioglu, A. & Megaridis, C. In situ multiphase fluid experiments in hydrothermal carbon nanotubes. *Applied Physics Letters* **79**, 1021-1023, doi:citeulike-article-id:3854813 (2001).

148 Zhu, F. & Schulten, K. Water and proton conduction through carbon nanotubes as models for biological channels. *Biophysical Journal* **85**, 236-244, doi: 10.1016/s0006-3495(03)74469-5 (2003).

149 Hummer, G., Rasaiah, J. C. & Noworyta, J. P. Water conduction through the hydrophobic channel of a carbon nanotube. *Nature* **414**, 188-190 (2001).

150 Mao, Z. & Sinnott, S. B. A Computational study of molecular diffusion and dynamic flow through carbon nanotubes. *The Journal of Physical Chemistry B* **104**, 4618-4624, doi:10.1021/jp9944280 (2000).

151 Walther, J. H., Jaffe, R., Halicioglu, T. & Koumoutsakos, P. Carbon nanotubes in water: Structural characteristics and energetics. *The Journal of Physical Chemistry B* **105**, 9980-9987, doi:10.1021/jp011344u (2001).

152 J.Marti & Gordillo, M. C. Temperature effects on the static and dynamic properties of liquid water inside nanotubes. *Physical Review E* **64**, 021504 (2001).

153 Kalra, A., Garde, S. & Hummer, G. Osmotic water transport through carbon nanotube membranes. *Proceedings of the National Academy of Sciences of the United States of America* **100**, 10175-10180, doi:10.1073/pnas.1633354100 (2003).

154 Berezhkovskii, A. & Hummer, G. Single-file transport of water molecules through a carbon nanotube. *Physical Review Letters* **89**, 064503 (2002).

155 Zhou, X., Li, C.-Q. & Iwamoto, M. Equilibrium and kinetics: Water confined in carbon nanotubes as one-dimensional lattice gas. *The Journal of Chemical Physics* **121**, 7996-8002 (2004).

156 Zhu, F. Q., Tajkhorshid, E. & Schulten, K. Collective diffusion model for water permeation through microscopic channels. *Physical Review Letters* **93**(2004).

157 Khazanovich, N., Granja, J. R., McRee, D. E., Milligan, R. A. & Ghadiri, M. R. Nanoscale tubular ensembles with specified internal diameters. design of a self-assembled nanotube with a 13-.ANG pore. *Journal of the American Chemical Society* **116**, 6011-6012, doi:10.1021/ja00092a079 (1994).

158 Motesharei, K. & Ghadiri, M. R. Diffusion-limited size-selective ion sensing based on sam-supported peptide nanotubes. *Journal of the American Chemical Society* **119**, 11306-11312, doi:10.1021/ja9727171 (1997).

159 Asthagiri, D. & Bashford, D. Continuum and atomistic modeling of ion partitioning into a peptide nanotube. *Biophysical Journal* **82**, 1176-1189 (2002).

160 Hwang, H., Schatz, G. C. & Ratner, M. A. Coarse-grained molecular dynamics study of cyclic peptide nanotube insertion into a lipid bilayer. *Journal of Physical Chemistry A* **113**, 4780-4787, doi:10.1021/jp8080657 (2009).

161 Sanchez-Quesada, J., Isler, M. P. & Ghadiri, M. R. Modulating ion channel properties of transmembrane peptide nanotubes through heteromeric supramolecular assemblies. *Journal of the American Chemical Society* **124**, 10004-10005, doi:10.1021/ja025983+ (2002).

162 Roux, B., Allen, T., Icirc, B., Che, S., Im, W., *et al.* Theoretical and computational models of biological ion channels. *Quarterly Reviews of Biophysics* **37**, 15-103 (2004).

163 Neher, E. & Sakmann, B. Single-channel currents recorded from membrane of denervated frog muscle fibres. *Nature* **260**, 799-802 (1976).

164 Doyle, D. A., Cabral, J. M. Pfuetzner, R., Kuo, A., Gulbis, J. M., *et al.* The structure of the potassium channel: Molecular basis of K+ conduction and selectivity. *Science* **280**, 69-77, doi:10.1126/science.280.5360.69 (1998).

165 Mackay, D. H., Berens, P. H., Wilson, K. R. & Hagler, A. T. Structure and dynamics of ion transport through gramicidin A. *Biophysical Journal* **46**, 229-248, doi: 10.1016/s0006-3495(84)84016-3 (1984).

166 Jordan, P. C. Microscopic approaches to ion transport through transmembrane channels: The model system gramicidin. *The Journal of Physical Chemistry* **91**, 6582-6591, doi:10.1021/j100311a006 (1987).

167 Duca, K. A. & Jordan, P. C. Comparison of selectively polarizable force fields for ion−water−peptide interactions: Ion translocation in a gramicidin-like channel. *The Journal of Physical Chemistry B* **102**, 9127-9138, doi:10.1021/jp981995z (1998).

168 Roux, B. & Karplus, M. Molecular dynamics simulations of the gramicidin channel. *Annual Review of Biophysics and Biomolecular Structure* **23**, 731-761, doi:doi:10.1146/annurev.bb.23.060194.003503 (1994).

169 Chiu, S. W., Novotny, J. A. & Jakobsson, E. The nature of ion and water barrier crossings in a simulated ion channel. *Biophysical Journal* **64**, 98-109, doi: 10.1016/s0006-3495(93)81344-4 (1993).

170 Fowler, P. W., Tai, K. & Sansom, M. S. P. The selectivity of K+ ion channels: Testing the hypotheses. *Biophysical Journal* **95**, 5062-5072, doi: 10.1529/biophysj.108.132035 (2008).

171 Noskov, S. Y., Bernèche, S. & Roux, B. Control of ion selectivity in potassium channels by electrostatic and dynamic properties of carbonyl ligands. *Nature* **431**, 830-834 (2004).

172 Noskov, S. Y. & Roux, B. Importance of hydration and dynamics on the selectivity of the KcsA and NaK channels. *The Journal of General Physiology* **129**, 135-143, doi:10.1085/jgp.200609633 (2007).

173 Cordero-Morales, J. F., Jogini, V., Lewis, A., Vasquez, V., Cortes, D. M., *et al.* Molecular driving forces determining potassium channel slow inactivation. *Nature Structural & Molecular Biology* **14**, 1062-1069 (2007).

174 Sands, Z. A. & Sansom, M. S. P. How does a voltage sensor interact with a lipid bilayer? Simulations of a potassium channel domain. *Structure* **15**, 235-244, doi: 10.1016/j.str.2007.01.004 (2007).

175 Jogini, V. & Roux, B. Dynamics of the Kv1.2 Voltage-gated k+ channel in a membrane environment. *Biophysical Journal* **93**, 3070-3082, doi:10.1529/biophysj.107.112540 (2007).

176 Nishizawa, M. & Nishizawa, K. Molecular dynamics simulation of kv channel voltage sensor helix in a lipid membrane with applied electric field. *Biophysical Journal* **95**, 1729-1744, doi: 10.1529/biophysj.108.130658 (2008).

177 Coalson, R. D. & Kurnikova, M. G. Poisson-Nernst-Planck theory approach to the calculation of current through biological ion channels. *IEEE Transactions on Nanobioscience* **4 ,** 81-93 (2005).

178 Muthukumar, M. & Kong, C. Y. Simulation of polymer translocation through protein channels. *Proceedings of the National Academy of Sciences of the United States of America* **103**, 5273-5278 (2006).

179 Daiguji, H. Ion transport in nanofluidic channels. *Chemical Society Reviews* **39**, 901-911 (2010).

180 Lynden-Bell, R. M. & Rasaiah, J. C. Mobility and solvation of ions in channels. *Journal of Chemical Physics* **105**, 9266 (1996).

181 Qiao, R. & Aluru, N. R. Atypical dependence of electroosmotic transport on surface charge in a single-wall carbon nanotube. *Nano Letters* **3**, 1013-1017, doi:10.1021/nl034236n (2003).

182 Tang, Y. W., Chan, K.-Y. & Szalai, I. Structural and transport properties of an spc/e electrolyte in a nanopore. *The Journal of Physical Chemistry B* **108**, 18204-18213, doi:10.1021/jp0465985 (2004).

183 Dzubiella, J., Allen, R. J. & Hansen, J.-P. Electric field-controlled water permeation coupled to ion transport through a nanopore. *The Journal of Chemical Physics* **120**, 5001-5004 (2004).

184 Dehez, F., Tarek, M. & Chipot, C. Energetics of ion transport in a peptide nanotube. *The Journal of Physical Chemistry B* **111**, 10633-10635, doi:10.1021/jp075308s (2007).

185 Grossfield, A., Ren, P. & Ponder, J. W. Ion solvation thermodynamics from simulation with a polarizable force field. *Journal of the American Chemical Society* **125**, 15671-15682 (2003).

186 Shao, Q., Huang, L., Zhou, J., Lu, L., Zhang, L., *et al.* Molecular simulation study of temperature effect on ionic hydration in carbon nanotubes. *Physical Chemistry Chemical Physics* **10**, 1896-1906 (2008).

187 Aksimentiev, A. & Schulten, K. Imaging the permeability of alpha-hemolysin with molecular dynamics. *Biophysical Journal* **88**, 584A-584A (2005).

188 Gazit, E. A possible role for π-stacking in the self-assembly of amyloid fibrils. *The FASEB Journal* **16**, 77-83, doi:10.1096/fj.01-0442hyp (2002).

189 Song, Y., Challa, S., Medforth, C., Qiu, Y., Watt, R., *et al.* Synthesis of peptide-nanotube platinum-nanoparticle composites. *Chemical Communications*, 1044-1045 (2004).

190 Sedman, V. L., Adler-Abramovich, L., Allen, S., Gazit, E. & Tendler, S. J. B. Direct observation of the release of phenylalanine from diphenylalanine nanotubes. *Journal of the American Chemical Society* **128**, 6903-6908, doi:10.1021/ja060358g (2006).

191 Ryu, J. & Park, C. B. High stability of self-assembled peptide nanowires against thermal, chemical, and proteolytic attacks. *Biotechnology and Bioengineering* **105**, 221-230, doi:10.1002/bit.22544 (2010).

192 Reches, M. & Gazit, E. Controlled patterning of aligned self-assembled peptide nanotubes. *Nature Nanotechnology* **1**, 195-200 (2006).

193 Hill, R. J., Sedman, V. L., Allen, S., William, P., Paoli, M., *et al.* Alignment of aromatic peptide tubes in strong magnetic fields. *Advanced Materials* **19**, 4474-4479, doi:10.1002/adma.200700590 (2007).

194 Tsai, C.-J., Zheng, J. & Nussinov, R. designing a nanotube using naturally occurring protein building blocks. *PLoS Computational Biology* **2**, e42 (2006).

195 Granja, J. R. & Ghadiri, M. R. Channel-mediated transport of glucose across lipid bilayers. *Journal of the American Chemical Society* **116**, 10785-10786, doi:10.1021/ja00102a054 (1994).

196 Liu, H., Chen, J., Shen, Q., Fu, W. & Wu, W. Molecular insights on the cyclic peptide nanotube-mediated transportation of antitumor drug 5-fluorouracil. *Molecular Pharmaceutics* **7**, 1985-1994, doi:10.1021/mp100274f (2010).

APPENDIX A

EDUCATIONAL SECTION: INTRODUCING MOLECULAR SIMULATION TO UNDERGRADUATES IN CHEMICAL ENGINEERING VIA INTERLINKED CURRICULUM COMPONENTS (ICCs)

A.1. Overview

As a part of a departmental curriculum reform project supported by the National Science Foundation, the Chemical Engineering Department at Texas A&M University is in the process of constructing web based interlinked curriculum components (ICCs) to strengthen unity and coherence of the curriculum and to introduce new content, reinforce the conceptual framework, and demonstrate the framework's application to emerging technological areas. These varied uses of ICCs can support broader reform efforts to make instruction more interactive and learner-centered.

Conventionally process analysis and design have played a substantial role in chemical engineering education and practice. Nowadays, due to emergence of new fields; such as nanotechnology, biotechnology and their applications, understanding the molecular level driving forces behind chemical, biological and materials processing have become important for chemical engineers of today and future; starting from fundamental theories of materials and chemicals in small scales has motivated to include molecular level theories and methods of modeling in education of chemical engineers. This chapter will describe efforts and progress in construction of a web-based molecular modeling and simulation module as an interlinked curriculum component (ICC) for chemical engineering. The updated version of the module can be found at *alcheme.tamu.edu* (ICC4).

While introducing the students to basic ingredients of molecular modeling and simulation, the Molecular Modeling and Simulation ICC, also addresses the connection to fundamental laws of conservation (energy, momentum and mass balances) and draws

attention to molecular level foundations of statistical thermodynamics, transport (mass, heat and flow) and chemical kinetics. Therefore it may be used in several chemical engineering courses from sophomore level to senior. Topics covered are relevant in traditional areas of chemical engineering as well as emerging fields such as the design of nanomaterials, sensors, drug delivery systems, membranes, novel catalysts, surface and interfaces, phase equilibria in nano-systems and flow in nano-scale confinement, among other problems. Through simple examples linked in the web based interactive materials, the expected outcome of this ICC is to provide a learning tool for chemical engineering students to gain basic knowledge of molecular level modeling and simulation methods.

Introduction of molecular simulation to the chemical engineering curriculum has been a recent topic of discussion in the academia[1]. In the past two decades several chemical engineering departments have introduced courses at the graduate level[2], including this department. In the light of Curriculum Reform project, it was undertaken a project aiming at development of Molecular Modeling and Simulation as one of the Interlinked Curriculum Components (ICCs).

During the last decades, the classical chemical engineering curricula has been focused on the design and study of the processes related to the basic conservation laws from micro/macro scales point of view. Recently, emerging chemical engineering areas recognize the need in the understanding at the molecular level of the phenomena and materials. Thus it has become important to include an introduction to physical-chemical related fundamental concepts at this level. By using an interactive web module, these concepts can be introduced in a practical point of view, directing the information to applications in chemical engineering fields.

Different institutions have been working on the integration of Molecular Simulation to the chemical engineering curriculum. In 1998 the CACHE Corporation founded a grant were seven co-PIs from different universities, experts in molecular simulation, started the design and implementation of web based modules for introducing molecular simulation to undergraduates in chemical engineering curriculum. They created a browser based module development environment for different modules

targeted at specific undergraduate courses[1]. Reports about educational aspects of molecular simulation for undergraduates and graduates students have been prepared previously[2, 3].

The initial ICC prototype focuses on conservation of mass (CoM)[4]. and has given the basis of the structure of the new modules as Molecular Simulation (MoS) module. The presented Molecular Simulation module is expected to:

- Provide concepts in chemical engineering undergraduate context about the molecular level mechanisms that are important for understanding experimentally observed/macroscale phenomena and material's properties.
- Enhance learning at the molecular level of materials using visualization and animations, providing an interactive environment to the student.
- Motivate active-learning and critical thinking in the area of Molecular Simulation using visually attractive material.
- Explain the basic concepts of Molecular Simulation in an understandable format.

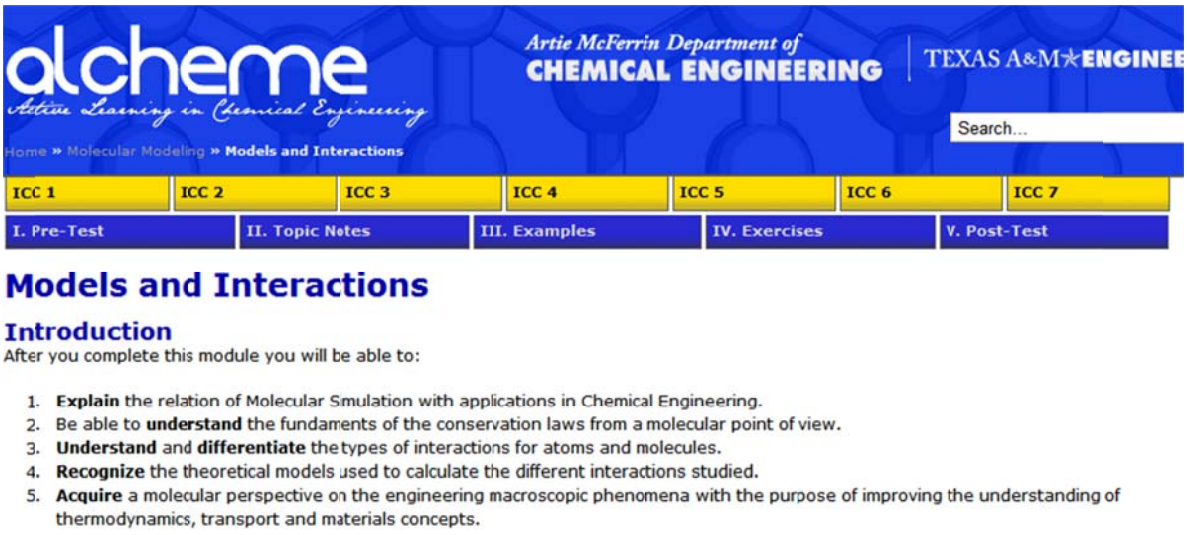

Fig. A-1. Main page, first section of Molecular Simulation Module

A.2. Interlinked Curriculum Web Module in Molecular Simulation

Below are described the skills expected after completion of the module, from students without previous knowledge on the topics.

Section a: Models and Interactions

- Couple Molecular Simulation to applications in chemical engineering.
- Recognize the mathematical models used to represent different molecular interactions.
- Understand the fundaments of conservation laws from a molecular point of view.
- Identify the types of interactions important in atoms and molecules.
- Acquire a molecular perspective on the engineering macroscopic phenomena with the purpose of improving the understanding of thermodynamics, transport and materials concepts.
- Introduce molecular simulation and provide the chemical engineering student with a better understanding of the molecular world through models.

Section b: Molecular Simulation Methods

- Differentiate the basic algorithms of molecular mechanics, Monte Carlo and Molecular Dynamics Simulations.
- Acquire criteria to select the appropriate molecular simulation method for the solution of a given problem.
- Evaluate different algorithms in terms of their applicability/limitations for specific problems.
- Understand the applications of molecular simulations through chemical engineering related examples.

Section c: Property Prediction

- Apply thermodynamic and statistic concepts for the calculation of properties from molecular simulations results.
- Be able to select the appropriate methodology for the calculation of specific properties.

The material was organized in five principal parts: Pretest, Topic Notes, Examples, Exercises and Post-Test for each section. An Introduction was added to the first section of the module. The topic notes were organized in a format that allows students to study the different concepts on their own. Depending on the level of understanding desired, the students can explore the concepts deeply by the use of the module's links.

Pre-Test and Post-Test

This session was designed with the intention of evaluating the knowledge of the students before and after the use of the module. Each sub-section evaluates the pre and post concepts of the students. The students will be able to compare and evaluate how familiarized they are with the concepts and how useful the material presented was. It is structured as a group of multiple-choice conceptual questions.

Examples and Exercises

The examples provided are designed as java based materials; the Lennard-Jones example allows the students to calculate and compare the LJ potential and force for different substances. In collaboration with the Dr. Kofke and the Etomica project[5], we have incorporated additional java applets studying problems of interest in chemical engineering.

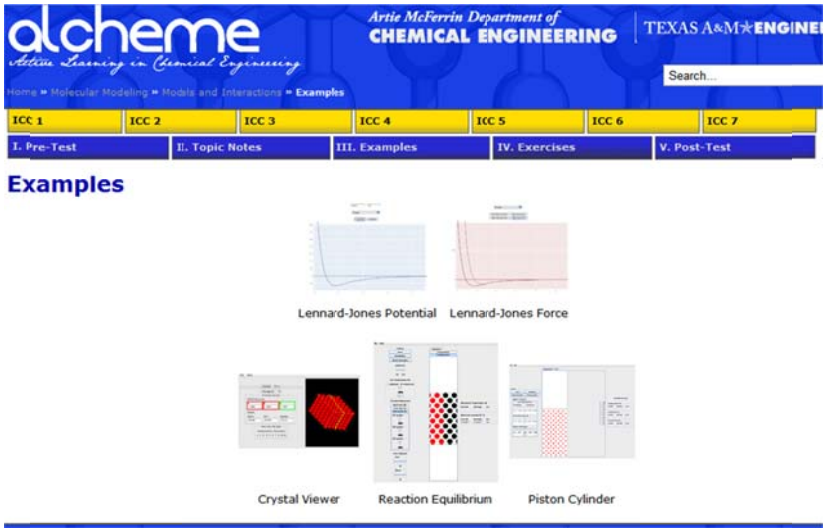

Fig. A-2. Snapshot of the Example web page (Models and Interactions)

These examples provide the user with an opportunity to apply the information learned through the module as they are studying the web based interactive course notes.

A.3 Classroom Assessment with undergraduate students at TAMU

The web-based molecular simulation module was presented to three undergraduate courses given at Texas A&M Univeristy; Chem. Engr. Materials (CHEN-313), Chem. Engr. Kinetics (CHEN-464) and Chem. Engr. Thermo II (CHEN-354). The students enjoyed the module and demonstrated interest in the topic. After exploring the molecular simulation module the students answered a questionnaire designed to assess the activity. The questions made and results obtained from the assessment are summarized below.

TableA-1. Assessments Questions

Question #	**This module**
1	… explained how molecular simulation can be used in Chemical Engr.
2	… was a good motivation to the topic
3	… was a good introduction to the topic
4	… would be a good study tool
5	… would be a good supplement for a text
6	… was user friendly
7	… was logical in the way it presented the content – made sense -
8	… motivated me to learn more about molecular simulation in Chem. Engr.

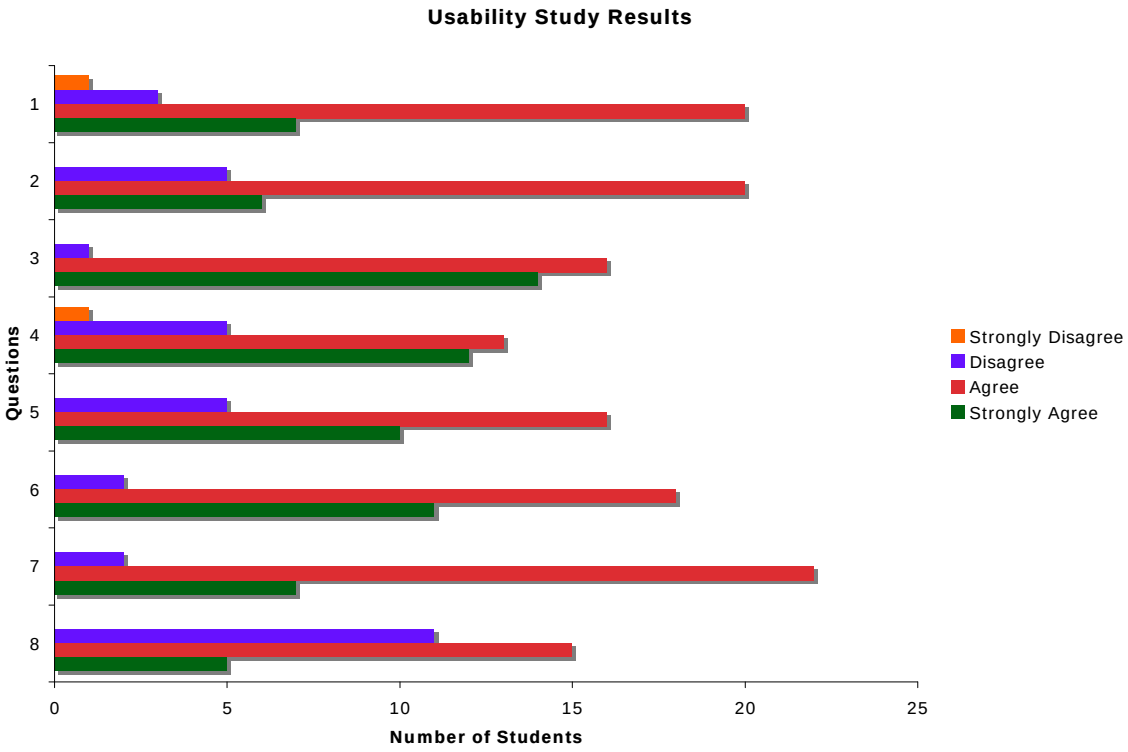

Fig.A-3. Usability Study results for CHEN-313, CHEN-354 and CHEN-464 courses.

A.4 Summary

A proto-type Molecular Simulation web-based module was designed as a part of a bigger Interlinked Curriculum Components (ICCs) project aimed at the renewal of the chemical engineering curriculum. This module will contribute to the education of the chemical engineering student with a focus of the basic phenomena on a molecular scale to achieve a better understanding of the interactions involved at that level. The students who participated in the assessment activities showed interest and curiosity to continue learning about the topic. The visual, audio, flash and java based material successfully motivated the students and keep their attention an interest open.

Incorporating this educational material by using the web–based modules provides the opportunity to introduce new concepts in the context of the traditional courses in chemical engineering.

A.5. References

1. Rowlew, R. World wide web-based Modules for Introduction of Molecular Simulation into the Chemical Engineering Curriculum. NSF Grant 9752243. Brigham Young University.

2. Wilcox, J. Incorporating Computational Chemistry into the ChE Curriculum. Chemical Engineering Education. Worcester Polytechnic Institute, Worcester, (2006).

3. Allen, M. Educational Aspect of molecular simulation. Molecular Physics, Vol. 105, Nos. 2-3, (2007).

4. Yurttas, L. Kraus, Z. Froyd J. Layne, J. El-Hawagi, M. Glover, C. A web-based complement to teaching conservation of mass in a chemical engineering curriculum. American Engineering for Engineering Education, (2007).

5. Koftke, David A. Molecular Simulation Modules. Department of Chemical Engineering and Biological Engineering, University at Buffalo, State University of New York Press.

6. Edgar, T.F. CACHE Corporation, "Computing Through the Curriculum: An Integrated Approach for Chemical Engineering". (2003).

7. Gaussian, Inc., Wallingford CT, (2004).

8. G. Kresse and J. Hafner, Phys. Rev. B 47 , 558 (1993); ibid. 49 , 14251 (1994).

9. D.M. Ivory, G.G. Miller, J.M. Sowa, L.W. Shacklette, R.R. Chance, R.L. Elsenbaumer and R.H. Baughman J Chem Soc Chem Commun (1980), p. 348.

10. S. J. Plimpton, Fast Parallel Algorithms for Short-Range Molecular Dynamics, J Comp Phys, 117, 1-19 (1995).

VITA

Name: Jennifer Andrea Carvajal Diaz

Education:
B.S., Chemical Engineering, Universidad Industrial de Santander, Colombia, 2006. Cum Laude.
Polymer Specialty Certificate, Texas A&M University, USA, 2010.
Ph.D., Chemical Engineering, Texas A&M University, USA, 2011.

Honors:
- Recognition from the Society of Plastic Engineers for time and dedication as President of Texas A&M Chapter (2010)
- Texas Engineering Experiment Station (TEES) Fellowship, Texas A&M (2009)
- International Student Education Scholarship (ISS), Texas A&M (2009)
- SPE (Society of Plastic Engineers) Scholarship, Polymer Technology Center, Texas A&M (2009).
- Second Place at the Student Research Week (SRW) Poster Competition, Texas A&M (2009)
- Outstanding Accomplishments in Interdisciplinary Research Award. SRW, Texas A&M (2008, 2009).
- Office of Graduate Studies Travel Grant, Texas A&M (2008).
- Cum Laude Distinction, UIS, Colombia (2006).
- UIS Outstanding Student Scholarship, Colombia (2001-2005).

Professional Affiliations:
- Sigma Xi "The Scientific Research Society"
- American Institute of Chemical Engineers (AICHE)
- American Chemical Society (ACS)
- American Physical Society (APS)
- Materials Research Society (MRS)
- Society of Plastic Engineers (SPE)

Contact: jennifercarvajal85@gmail.com
or through:
Dr. Tahir Cagin, Chemical Engineering,
Texas A&M University, TAMU-3122.
College Station, TX-77840